BOLU ABANT İZZET BAYSAL UNIVERSITY
INSTITUTE OF GRADUATE STUDIES
Department of Physics

FABRICATION AND APPLICATIONS OF BIOSENSOR FOR EARLY DIAGNOSIS OF LUNG CANCER AND CANCER METASTASIS

DOCTOR OF PHILOSOPHY

OZAN YILMAZ

ACADEMIC SUPERVISOR
Prof. Dr. ERCAN YILMAZ

BOLU, TEMMUZ - 2023

APPROVAL OF THE THESIS

Fabrication and Applications of Biosensor for Early Diagnosis of Lung Cancer and Cancer Metastasis submitted by **Ozan YILMAZ** and defended before the Examining Committe Members listed below in partial fulfillment of the requirements for the degree of **Doctor of Philosophy** in **Department of Physics, Institute of Graduate Studies of Bolu Abant Izzet Baysal University in 25.07.2023** by

Examining Committee Members	**Signature**
Supervisor Prof. Dr. Ercan YILMAZ BAİBU	.....
Member Prof. Dr. Ekrem GÜREL BAİBU	.....
Member Prof. Dr. Aliekber AKTAĞ BAİBU	.....
Member Prof. Dr. Ayşegül KAHRAMAN Bursa Uludağ University	.....
Member Prof. Dr. Kadir GÖKŞEN Düzce University	.....

Prof. Dr. İbrahim KÜRTÜL

Director of Instıtute of Graduate Studies

ETHICAL DECLARATION

In this thesis dissertation that was properly prepared according to the Thesis Writing Rules of Bolu Abant İzzet Baysal University of the Institute of Graduates Studies, I hereby declare that;

- All data, information, and documents presented in the thesis were obtained in accordance with the academic and ethical rules,
- All data, documents, assessments, and results were presented in accordance with the scientific ethical and moral rules,
- All works that were benefitted in the thesis were appropriately cited,
- No alteration was made in the data used,
- Study presented in this thesis is original,

Otherwise, I declare that I accept the loss of all my rights in case any contradiction that may arise against me.

The similarity rate obtained by using the Turnitin program, a plagiarism detection software, is within the limits approved by the University Senate.

_____

Ozan Yılmaz

ABSTRACT

FABRICATION AND APPLICATION OF BIOSENSORS FOR EARLY DIAGNOSIS OF LUNG CANCER AND CANCER METASTASIS
PHD THESIS
OZAN YILMAZ
BOLU ABANT IZZET BAYSAL UNIVERSITY
INSTITUTE OF GRADUATE STUDIES
DEPARTMENT OF PHYSICS
(SUPERVISOR: PROF. DR ERCAN YILMAZ)

BOLU, JULY 2023
xiv + 79

Lung cancer has one of the greatest mortality rates of all cancer varieties. This malignancy affects millions of people throughout the globe and in our country. Unfortunately, it is too late to diagnose the disease using traditional methods because they are insufficient. This necessitates the development of a method or device for early disease diagnosis. A biosensor to detect lung cancer and metastasis at an early stage has been investigated in this study. Biosensors based on GFET are preferred. Utilizing the Hummer procedure, graphite was converted into reduced graphene oxide. FTIR, Raman spectroscopy, transmission electron microscopy, and X-ray diffraction were used to examine the properties of graphene oxide (GO) and reduced graphene oxide (rGO). The outcomes demonstrated that the production met the intended standards. The rGO that has been synthesized has been deposited on the FET structure using a technique within the scope of this research. Micro RNAs were favored as biomarkers for malignancy. The biosensor's electrical properties were determined using the output characteristic and transfer characteristic method. The device's I_d-V_d measurements revealed that the rGO layer between the source and the drain formed a successful ohmic contact. In I_d-V_{gs} measurements, pH-dependent measurements of an ionic solution were taken first, with linear results. The consistency of subsequent measurements of the analyte linked to miRNA was comparable. The device was then evaluated with an analyte containing an incompatible miRNA to ascertain its selectivity. The test revealed that the device's sensitivity was limited to its own biomarker. Finally, the biosensor's sensitivity was evaluated. The solution of the analyte was diluted from 10M to 100 pM and then applied to the sensor. At 100 pM, the biosensor produced a significant response. At the conclusion of the study, a biosensor was created that, if implemented, could detect lung cancer at an early stage.

KEYWORDS: *GFET, Reduced Graphen Okside, Lung Canser, microRNA*

ÖZET

AKCİĞER KANSERİ VE KANSER METASTAZI ERKEN TANISI İÇİN BİYOSENSÖR ÜRETİMİ VE UYGULAMALARI
DOKTORA TEZİ
OZAN YILMAZ
BOLU ABANT İZZET BAYSAL ÜNİVERSİTESİ
LİSANSÜSTÜ EĞİTİM ENSTİTÜSÜ
FİZİK ANABİLİM DALI

(TEZ DANIŞMANI: PROF. DR. ERCAN YILMAZ)

BOLU, TEMMUZ - 2023
xiv + 79

Akciğer kanseri ölüm oranı en yüksek kanser türlerinden biridir. Dünyada ve ülkemiz de milyonlarca insan bu kansere yakalanmaktadır. Geleneksel yöntemler teşhis konusunda yetersiz olduğundan hastalığın tanısını koymakta maalesef geç kalınmaktadır. Bu nedenden dolayı hastalığın erken evrede taşhisini sağlayacak bir yöntem veya cihaza ihitiyaç vardır. Bu çalışmada, bu ihtiyaca binaen akciğer kanserini ve metastazını erken evrede teşhis edecek bir biyosensör üzerine çalışılınmıştır. GFET tabanlı biyosensör tercih edilmiştir. Çalışma ilk önce hummer methodu kullanılarak grafitten indigenmiş grafen oksit üretimi ile başlamıştır. Üretilen grafen oksit (GO) ve indirgenmiş grafen oksitin (rGO) karakteristik özellikleri FTIR, Raman spektroskopisi, TEM ve X ray diffraction analizleri ile incelenmiştir. Sonuçlar üretimin istenilen kalitede olduğunu göstermiştir. Sentezlenen rGO nun FET yapısına serilmesinde bu çalışma kapsamında bulunan bir yöntem ile yapılmıştır. Kansere özgü biyomarker olarak mikro RNAlar tercih edilmiştir. GFET biyosensörünün elektriksel özellikleri output karakteristik ve transfer karakteristik yaklaşımı ile yapılmıştır. Cihazın I_d-V_d ölçümleri kaynak ve akaç arasındaki rGO katmanının başarılı bir ohmic kontak yaptığını göstermiştir. Id-Vgs ölçümlerinde önce iyonik bir solüsyonun pH bağlı ölçümleri alınmıştır ve bu sonuçlar lineerilk göstermiştir. Sonrada miRNA ileveli analitin ölçümleride benzer şekilde tutarlılık göstermiştir. Sonrasında cihazın seçiciliğinin tespiti için uyumsuz bir miRNA ilaveli analit ile test edilmiştir. Test sonucunda cihazın sadece kendi biyobelirtecine duyarlı olduğu bulunmuştur. En son olarakta biyosensörün hassasiyeti test edilmiştir. Analit çözeltisi 10µM mertebesinden 100 pM mertebesine kadar seyreltilmiş ve sensöre uygulanmıştır. Sonuçta üretilen biyosensör 100 pM mertebesinde anlamlı bir respons vermiştir. Çalışmanın sonunda geliştirilmesi halinde akciğer kanserini erken evrede teşhis edebilecek bir biyosensör üretilmiştir.

ANAHTAR KELİMELER: *GFET, İndirgenmiş Grafen Oksit, Akciger Kanseri, mikroRNA*

TABLE OF CONTENTS

LIST OF FIGURES

Page

LIST OF TABLES

LIST OF ABBREVIATIONS AND SYMBOLS

QCM **:** Quartz Crystal Microbalance

SPR : Surface Plasmon Resonance

FET : Field Effect Transistor

CVD : Chemical Vapor Deposition

GO : Graphene Oxide

rGO : Reduced Graphene Oxide

POC : Point-of-Care

MOSFET : Metal-Oxide-Semiconductor Field Effect Transistor

GFET : Graphene Field Effect Transistor

rGO-FET : Reduced Graphene Oxide Field Effect Transistor

ISFET : Ion Sensitive Field-Effect Transistor

$\mathbf{I_{ds}}$: Drain-Source Current

$\mathbf{V_{ds}}$: Drain-Source Voltage

$\mathbf{V_{gs}}$: Gate-Source Voltage

$\mathbf{V_{Dirac}}$: Dirac Point Voltage

CNP : Charge Neutrality Point

DP : Dirac Point

$\mathbf{C_q}$: Quantum Capacitance

$\mathbf{C_{dl}}$: Double Layer Capacitance

$\boldsymbol{\varepsilon_r}$: Relative permittivity of electrolyte

$\boldsymbol{\varepsilon_o}$: Vacuum permittivity

$\boldsymbol{\lambda_D}$: Debye Length

WHO : World Healt Organization

NHL : Non-Hodgkin Lymphoma

DLBCL : Diffuse Large B-cell Lymphoma

CTC : Circulating Tumor Cells

DNA : Deoxyribonucleic Acid

RNA : Ribonucleic Acid

cf-DNA/RNA : Cell-free DNA/RNA

miRNA : Micro RNA

cf-miRNAs : Cell-free Micro RNA

LAA : L-Ascorbic Acid

XRD : X-Ray Diffraction Spectroscopy

FWHM : Full Width Half Maximum

FTIR : Fourier Transform Infrared Spectroscopy

TEM : Transmission Electron Microscopy

FET **:** Field Effect Transistor

LOD : Limit of Detection

PBS : Phosphate Buffered Saline

PBASE : 1-Pyrene butyric acid N-hydroxysuccinimide ester

PDMS : Polydimethlysiloxane

ACKNOWLEDGEMENTS

The author wishes to express his deepest gratitude to his supervisor Prof. Dr. Ercan Yılmaz for their guidance, advice, criticism, encouragements and insight throughout the research.

The author would also like to thank Prof. Dr. Aliekber Aktağ, Prof. Dr. Ekrem Gürel and Prof. Dr. Kadir Gökşen for their suggestions and comments throughout thesis study.

The author would also like to deeply thank Prof. Dr. Ayşegül Kahraman, Assoc. Prof. Dr. Erhan Budak and Assoc. Prof. Dr. Ercan Selçuk Ünlü for their guidance, advice and their help during experiments.

The author would also like to express his deepest gratitude to his dear brother Dr. Umutcan Gürer, with whom he has been a fateful partner throughout his thesis work.

The author would like to express his deepest thanks to his beloved wife Mrs. Dilek Haseki Yılmaz and his beloved daughter Miss. Nil İpek Yılmaz for their support throughout his doctoral studies.

The author would like to express his deepest appreciation to his beloved mother Mrs. Nurcan Yılmaz and his esteemed father Mr. Kemal Yılmaz, who have always supported him throughout his education life.

This research was supported by the Higher Education Council of the Republic of Turkey within the scope of YÖK 100/2000 Doctoral Scholarship program.

1. INTRODUCTION

Cancer is one of the most dangerous and deadly diseases of our time. Every year more than 8 million people, unfortunately, die for cancer-related causes (Bray et al., 2018; Chandra & Nee, n.d.; Siegel et al., 2019). Lung, stomach, and lymphoma cancers are among the leading types of cancer that cause death (Bray et al., 2018; Hacıkamiloğlu et al., 2017; Sung et al., 2021). Early diagnosis is vital in the treatment of cancer, while the standard diagnosis of cancer is made with a series of tests that take a long time and financially. Due to this situation, many biosensor studies have been carried out on the subject recently (Chandra & Nee, n.d.; Khanmohammadi et al., 2020; Khatri & Puri, 2022; P. Li et al., 2015; Y. Zeng et al., 2018).

Biosensors can be defined as devices that can use biological recognition elements in combination with a transduction element and are capable of providing information based on quantitative or semi-quantitative analysis (Bhalla et al., 2016; Leech, 1994; Mehrotra, 2016; Pandey & Malhotra, 2019; Rogers, 2000; Sezgintürk, 2020). A simple biosensor consists of a biological recognition element combined with a detector system. The bio-material part of biosensors may consist of enzymes, antibodies, nucleic acids, aptamers, whole cells, or tissues, while their transducer part may consist of electrochemical, optical, piezoelectric, thermal, or magnetic units. Biosensors are classified according to the type of diagnostic biomaterial and transducer used. The types of biosensors based on bioreceptors are enzyme-based, aptamer-based, antibody-based, whole cell, and DNA biosensors. On the other hand, electrochemical, optical, thermal, acoustic, gravimetric, and electronic biosensors are types of biosensors based on transducers (Bhalla et al., 2016; Haleem et al., 2021; Leech, 1994; Mehrotra, 2016; Pandey & Malhotra, 2019; Rogers, 2000; Sezgintürk, 2020; Turner, 2013).

Although biosensors have many different applications, such as environment (Kurosawa et al., 2006), water (Lagarde & Jaffrezic-Renault, 2011), soil and food quality monitoring (Baccar et al., 2010; Yoon & Kim, 2012), drug (Wei et al., 2011) and pathogen (Choi et al., 2019; Moldovan et al., 2008) discovery, toxin detection (Parker et al., 2009), plant studies, etc., there are a large number of studies on their use for disease diagnosis (Diba et al., 2015; Erdem et al., 2005; Jin et al., 2019; Kovalska et al., 2019; Lin & Ju, 2005; Martin & Patra, 2014; Schuck et al., 2020).

MicroRNAs (miRNAs), which play an important role in gene regulation, are single-stranded, 19-25 nucleotide long, non-coding RNA type molecules that can inhibit messenger RNA translation. In other words, although they are encoded by genes, they are not translated into proteins. While many miRNAs can bind to and control the same target, a single miRNA might include several target mRNAs. As a result, miRNAs have a function in a variety of biological processes, such as gene regulation, apoptosis, the development of the hemotological system, and the maintenance of cell differentiation. Diseases have a direct connection to miRNA, and their significance has grown since their discovery and our knowledge of what they do. Moreover, cancer, diabetes, vascular disorders, heart failure, Alzheimer's disease, and their influence on essential biological processes have all been related to miRNAs. Among other things, they are differently regulated in various types of cancer, such as ovarian, liver, stomach, pancreatic, colorectal, and breast lung cancers. In addition to this information, they are measurable in whole blood, plasma, serum, and sputum, making them suitable as potential marker. Because of these properties, miRNAs may also serve as biomarkers for lung cancer.

This thesis is about the production and development of a graphene-field effect transistor (GFET) based biosensor for use in the early diagnosis of lung cancer. In this study, miR-1268b and miR-6075 (Asakura et al., 2020) of microRNAs related to lung cancer were preferred as biomarkers to increase the sensitivity and selectivity of the biosensor. FETs with three different sizes (1.5*1.5 mm^2, 2*2 mm^2, and 2.5*2.5 mm^2) of sensory regions were fabricated. Reduced graphene oxide (rGO) was synthesized from graphite by following the Hummer method to be used in the acrive area of the biosensor. Then, the sensory region of the device was modified with reduced graphene oxide (rGO) to increase the electrical properties of the biosensor and its compatibility with the biomarker. As a result of these processes, GFET structures were produced. Afterwards, immobilization of anti-miRNA molecules to these GFET structures was performed. Finally, the fabricated biosensors' electrical performance was evaluated.

1.1 Biosensors

In the last hundred years, technological developments and inventions have enabled humanity to progress in many fields, such as the food industry, medicine, space applications, environmental monitoring, pharmacy, and military applications.

Sensor technology is key to this development. Sensors are found in almost every sector, and their usage areas are increasing day by day. Considering their intended use, there are various types of sensors with functions such as temperature and pressure measurement, imaging, environmental monitoring, and soil, water, and air quality measurement. Biosensors are a large familt of sensors that can perform such tasks. Biosensors are one of the important actors in these developments. According to the "International Union of Pure and Applied Chemistry" (IUPAC), biosensors are "integrated receptor–transducer devices that are able to provide selective quantitative or semi-quantitative analytical information using a biological recognition element." In simpler terms, biosensors are defined as analytical devices that merge a biologically sensitive element with a physical transducer. The elements of a biosensor are the analyte, bioreceptor, transducer, electronics, and display (**Figure 1.1**).

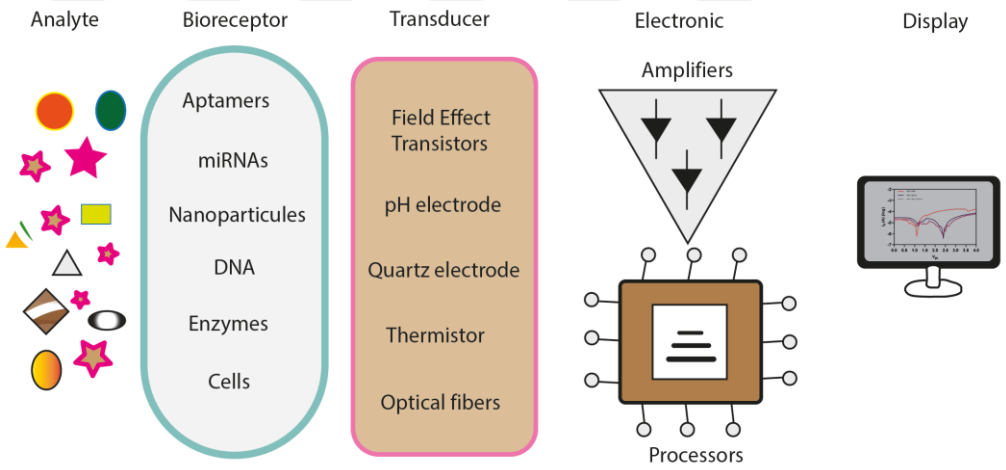

Figure 1.1 The drawing visualization of the components of a typical biosensor

Although Leland C. Clark, Jr. known the "father of biosensor" developed the first biosensor for oxygen detection in 1956, the historical adventure of the biosensor subject goes back to the pioneering studies of the early 1900s. The beginning of these studies is the study of M. Cremer in 1906. The study in which the electric potential difference in the two chambers separated by a glass membrane is proportional to the acid concentration. In 1922, W.S. Hughes developed an electrode to measure pH. Griffin and Nelson carried out studies of enzyme immobilization on materials such as aluminum hydroxide and charcoal between 1909 and 1922. Even though pioneering work dates back to the early 1900s, it was still Leland C. Clark who initiated the biosensor concept. In 1962, Clark developed

an amperometric enzyme electrode for the detection of glucose. Subsequently, in 1969, Guilbault and Montalvo invented the first potantiometric biosensor to detect urea. Afterwards, a private company introduced the first commercial biosensor in 1975. Today, the field has evolved into a multidisciplinary research area encompassing engineering, medicine, basic science, and micro/nanotechnology.

Biosensors have a huge range of applications aimed at enriching the standard of living. For this reason, their potential uses cover every conceivable analytical task, from medical diagnostics to drug discovery, soil, water, and air quality monitoring, space technology, food safety, defense, and security applications (**Figure 1.2**).

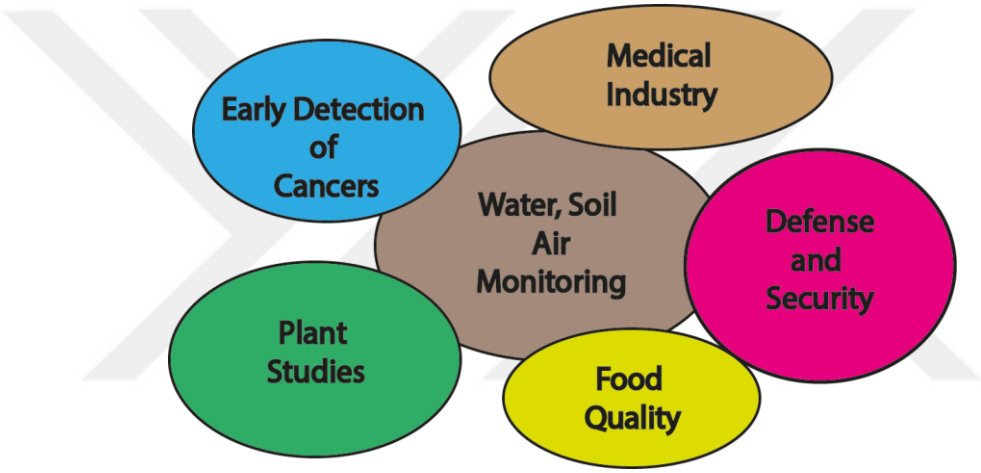

Figure 1.2 The application areas of Biosensors

In order to standardize biosensors, every one of them must have defined static and dynamic characteristics. Optimization of these properties affects the working performance of the biosensor. These features are the following;

Selectivity: it is the most important property of a biosensors, is the ability of a bioreceptor to detect a specific analyte in a sample containing other additives and contaminants. In other words, selectivity is the capability of a biosensor to produce a positive result only from interactions with rhe target bioanalytes. For example, the relationship of an antigen with an antibody or an enzyme with its substrate. This property is necessary and important so as to improve the performance of biosensors, especially because biological samples are complex and contain a large number of competing analytes (Bhalla et al., 2016; Coulet, 2005; Morales & Halpern, 2018).

Sensitiviy: it is actually the relationship between the amount of change in signal intensity due to changing analyte concentration in solution. In shorter terms, it is the lowest amount of analyte detected, i.e., the limit of detection (LOD). In addition, the maximum and minimum bioanalyte concentrations that can be measured consistently are important criteria in determining sensitivity (Bhalla et al., 2016). Studies to increase the possibility of treatment by diagnosing diseases at an early stage are the driving force behind technology. The desired sensitivity range of biosensors is generally in the femtomolar (fM, 10^{-15}) to nanomolar (nM, 10^{-6}) range (Coulet, 2005; Matsumoto et al., 2014; Morales & Halpern, 2018; Yan et al., 2017).

Stability: The inherent instability of biosensing molecules affects the sensitivity and accuracy of the biosensor. The degree of sensitivity of the biosensor to adverse changes in this sensing system is called stability. Ambient temperature, the degree of binding of the bioreceptor, and the degradation of the bioreceptor are factors that affect the stability of the biosensor. These factors should not be ignored to produce a consistent biosensor (Bhalla et al., 2016; Coulet, 2005).

Linearity: It can be described as the linearity of the response produced by the sensor depending on the relationship between the sensitivity of the biosensor and the concentration of the analyte. More preciesly it is the change in the response of the biosensor to a given change in analyte concentration at the same rate. Moreover, it is related to the solubility of the biosensor and the spectrum of analyte concentrations tested. A term related to the linearity is also called the "linear range," which is described as the interval of the analyte concentrations over which the biosensor answer varies linearly with concentration (Bhalla et al., 2016; Morales & Halpern, 2018).

Reproducibility: It is described as the capability to generate more than one identical biosensor that will reproduce a similar answer to a target bioassay. It is determined by the accuracy and sensitivity of the transducer and electronics in a biosensor. Furthermore, having an understanding of the biological recognition element's structure, behaviour, and fabrication process can enhance the reproducibility of the biosensor. As an important point, reproducible outputs provide high dependability and ruggedness for deductions made on the answer of a

biosensor. In order to increase the reproducibility, it is necessary to pay attention to various development processes, such as the construction of the recognition element, the attachment of the bio-recognition element to the surface, or variations in surface structure (Morales & Halpern, 2018).

The essential characteristics of a consistently working biosensor are described above. These properties should be taken into account for future studies.

1.1.1 The types of Biosensor

Another important issue in biosensor studies is choosing the right type of biosensor for the subject you are going to work on. Biosensors are basically divided into types according to biosensing material and transducer technology. At the beginning of biosensor technology, enzymes were first used as biosensing materials. The first type of biosensor was the enzyme-based biosensor. Enzyme biosensors have been developed with a focus on immobilization methods. That is, the ability of biological structures to form ionic bonds or covalent bonds has been taken into account. The most commonly used enzymes in these studies are oxidoreductases, polyphenol oxidases, peroxidases, and aminooxidases (Akter et al., 2013; Coulet, 2005; Moldovan et al., 2008). Following this, biosensors using aptamers emerged. This type of sensor is called aptamer-based biosensors. Aptamers are peptide molecules or oligonucleic acids that can bind to specific target molecules. Aptamers are a good example of functional molecules that are selected in vitro. In 1990, two groups separately established in vitro selection and amplification for the isolation of RNA sequences that can bind specific target molecules. They can compete with antibodies in a number of practical applications. They are tiny in size when compared to other biorecognition molecules such as antibodies or enzymes. These properties of aptamers allow for efficient immobilization. Hence, biosensors are easier to fabricate, miniaturize, integrate, and automate (Catanante et al., 2016; Charbgoo et al., 2016; Evtugyn & Hianik, 2016; Song et al., 2008; Strehlitz et al., 2008; Vasilescu & Marty, 2016). Later, following technological advances, biological elements such as cells, tissues, antibodies, and nanomolecules were used as sensing elements.

The types of transducers used in biosensor studies are optical, thermal, magnetic, electronic, and electrochemical (Figure 1.3). Devices that use a type of

transducer developed by utilizing the absorption, refraction, reflection, scattering, or brightness of light are called optical-based biosensors (Borisov & Wolfbeis, 2008; Ligler, 2009). The use of optical fibers is possible over long distances, so they do not need to be in close contact with the biosensor and can be easily minimized in in vivo studies (Leung et al., 2007; Ligler, 2009). Optical methods are one of the most widely used transducers in biomedical research, health care, pharmaceuticals, environmental monitoring, homeland security, and the battlefield (Karunakaran et al., 2015). Thermal biosensors take advantage of one of the fundamental properties of biological reactions-heat. More precisely, it is reflected as a change in temperature in the reaction medium. Its utilization in biosensors has prompted the development of various thermometric devices. These devices mostly target the change in temperature of the circulating fluid after the reaction of enzyme molecules with a suitable substrate (Mack et al., 1999; Ramanathan & Danielsson, 2001; Sivarajasekar et al., 2019; Xie et al., n.d.). Magnetic biosensors work by responding to a magnetic field (T. Wang et al., 2017). The magnetic particles used in this type of biosensor have significant advantages in terms of application. Sensing systems based on magnetic materials are characterized by analytical benchmarks such as improved sensitivity, a low limit of detection (LOD), a high signal-to-noise ratio, and shorter analysis time. For example, their magnetic dissociation and large active surface areas allow the biomaterial to be stabilized and purified under a magnetic field and, in addition, reduce the matrix effect. In addition to all these properties, they accelerate signal transmission and enhance target recognition, leading to improved detection sensitivity of the devices. Thanks to all these structural features, they offer advantages in biosensor applications, such as easy, reliable, and cost-effective detection for point-of-care diagnostics (Haun et al., 2010; Nabaei et al., 2018; Rocha-Santos, 2014; S. Wang et al., 2015; T. Wang et al., 2017; Xianyu et al., 2018). Electrochemical biosensors are devices that contain an electrode as a transducing element, which converts a biological event into an electrical signal. They are based on the measurement of different electrical properties such as resistance, current, potential, capacitance, impedance, etc., which occur in the presence of a biological event using methods such as potentiometry, conductometry, amperometry, or voltammetry (Ban et al., 2012; Karunakaran et al., 2015; Parker et al., 2009; Thévenot et al., 2001; J. Wang, 2005). The electrochemical biosensor type was preferred for this study.

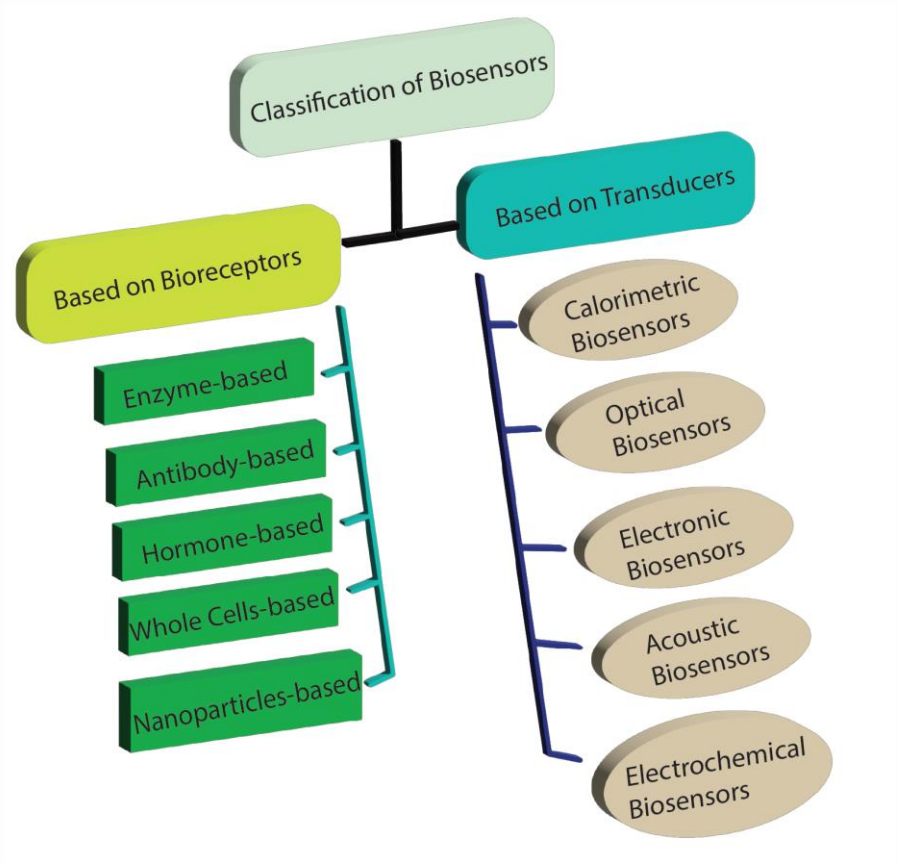

Figure 1.3 The Classification of Biosensors

1.1.2 The Electrochemical Biosensors

Electrochemical biosensors are instruments that contain an integrated electrode as a transduction component, which transforms a biological phenomenon into an electrical pulse (Frew et al., n.d.; Pohanka & Skládal, 2008). In simpler terms, they are sensors that measure the change in current (amperometric), potential (potentiometric), or conductivity (conductometric) in response to the change in analyte concentration with the help of an electrical converter (Grieshaber et al., 2008). Electrochemical biosensors have, in recent years, been the subject of intensive basic and applied research. This type of sensor has a wide range of applications, from food analysis to pathogen detection, from disease detection to different medical applications, from drug studies to pharmaceutical applications (Bahadir & Sezgintürk, 2015; Blair & Corrigan, 2019; Cesewski & Johnson, 2020; Karimi-Maleh et al., 2021; Masud et al., 2019; Negahdary & Angnes, 2022; Özbek et al., 2021a; Shabaninejad et al., 2019). They are divided into types that measure the change in analyte concentration using different measurement properties of

electricity such as current, resistance, impedance, capacitance, and potential. These types are called potentiometric, voltammetric, conductometric, impedimetric, and amperometric biosensors (Congur et al., 2015; Congur & Erdem, 2019; Frew et al., n.d.; Kour et al., 2020; Pohanka & Skládal, 2008; Singh et al., 2021).

In potentiometric biosensors, the biological sensing reaction causes an alteration of a redox potential, a transmembrane potential, or a modulation of the activity of an ion. That is, it is based on the relationship between the change in the measurement of the potential difference between the working electrode and the reference electrode in the sensor and the concentration of the analyte (Cuartero & Bakker, 2017; Ding & Qin, 2020; J. Wang et al., 2020; Yin & Qin, 2013). Potentiometric biosensors are therefore characterized by the measurement of the potential at one electrode relative to another electrode. This type of sensor consists of a counter, reference, and working electrodes. These electrodes are ion-selective electrodes (ISE) sensitive to anions or cations. Moreover, potassiometric biosensors have many different uses, such as pathogen detection, food safety, and early detection of diseases (Ding & Qin, 2020; Karimi-Maleh et al., 2021; Özbek et al., 2021b, 2021a; Yin & Qin, 2013).

The operation of biosensors using amperometric transducers is usually based on the measurement of the current strength at a given potential. In other words, this type of sensor is used to measure the currents arising from the electrochemical interaction of an electroactive element with a biorecognition element at a constant potential (voltage) applied to the working electrode (Bollella & Gorton, 2018; Emr & Yacynych, 1995; Frew et al., n.d.; Pohanka & Skládal, 2008). The resulting intensity at the sensor is expressed as a function of the concentration of the electroactive material oxidized or reduced at the working electrode. They usually consist of two electrodes. The second electrode in the line acts as a reference electrode (Frew et al., n.d.; Pohanka & Skládal, 2008). They have some important advantages compared to potentiometric biosensors. These are that the signal-generating species from the products are consumed on the electrode surface, and large-scale molecules and whole cells can be fixed on the working electrode. This type of sensor has different applications, such as toxicant determination and pathogen detection (Bollella & Gorton, 2018; Emr & Yacynych, 1995; Hayat et al., 2014).

Voltammetric biosensors are devices that detect analytes by measuring the current during a controlled change of potential applied to electrodes, allowing both potential and current to be measured and recorded. The position of the peaks in the graph obtained after measurement is chemically specific, while the peak intensity is related to the analyte concentration (Curulli, 2021; Grieshaber et al., 2008; Karunakaran et al., 2015). The most important advantages of this type of sensor are the ability to make highly sensitive measurements and, in addition, the ability to detect a large number of analytes simultaneously. This technique is subcategorized into cyclic voltammetry (CV), linear scanning voltammetry, hydrodynamic voltammetry, differential pulse voltammetry, ac voltammetry, polarography, and stripping voltammetry (Curulli, 2021; Karunakaran et al., 2015). This group of biosensors has many different applications (Alinejadian et al., 2023; Antiochia, 2022; Lakard, 2020; Oprea et al., 2022).

Impedimetric biosensors are devices that measure the electrical impedance that occurs at the electrode-electrolyte interface when an excitation signal is applied to electrodes functionalized with biomaterial. In more understandable terms, immobilization of bioreceptors to electrodes results in differences in the capacitance and electron transfer resistance of the electrodes. In this case, changes occur in the impedance of the device (Curulli, 2021; Grieshaber et al., 2008; Karunakaran et al., 2015; Pohanka & Skládal, 2008). This type of transducer is mostly used for the label-free detection of analytes due to interfacial changes produced by biological recognition processes. These devices have lower detection limits for label-free detection compared to amperometry or potentiometry devices (Guan et al., 2004). Nevertheless, there are many different uses for this type of biosensor (Bonanni et al., 2012; Erdem et al., 2014; Guan et al., 2004; Gupta et al., 2013; Kirchhain et al., 2020; J. Zeng et al., 2022).

Conductometric biosensors are devices that detect by measuring the change in conductivity between electrodes caused by an electrochemical reaction (Curulli, 2021). In fact, the working principle of the sensor is based on ion mobility between electrodes. To elaborate, by applying a potential difference to the ionic conducting liquid medium between the electrodes, an electric field is generated in the electrolyte, and the random ion movement is then influenced by the regular, oppositely directed movement of ions, i.e. negatively charged ions move towards

the anodes, while positively charged ions move towards the cathodes (Adley & Ryan, 2015; Dzyadevych & Jaffrezic-Renault, 2014). This results in a variation in the lithiquity of the device. This type of transducer has significant advantages over others, such as no need for a reference electrode, being insensitive to light, using low-cost thin-film technology, being very amenable to miniaturization and integration, and being suitable for monitoring metabolic processes in living biological systems (Adley & Ryan, 2015; Dzyadevych & Jaffrezic-Renault, 2014; Shul'gao et al., 1994; Zhylyak et al., 1995). Nowadays, there are many different applications for this sensor.

In electrochemical biosensors, different companions such as field-effect transistors (FETs), chemorefluoresistors, chemoresistors, chemical diodes, pH electrodes, etc. have been used as inverting substrates, mainly because they try to detect the change in analyte concentration using the change in the electrical signal. Each of these inverter types has advantages and disadvantages compared the others. In fact, all of them offer options for researchers or users to choose from, depending on the needs of the application, available facilities, and many other factors. Among these transducer substrates, Field Effect Transistors (FETs), the subject of this study, have been the subject of considerable study in the field of biosensing over the last few decades due to their remarkable characteristics such as label-free sensing, high sensitivity, fast response, real-time measurement capability, low operating power, and miniaturization into a portable device.

1.1.3 Field Effect Transistors (FETs)

A field-effect transistor (FET) is a type of transistor that uses an electric field to control current. Its structure consists of conductor, Semiconductor, and insulator parts (S. Zhang, 2020) (Figure 1.4). FETs basically have a three-terminal structure. These terminals are called source, drain, and gate (Dacey & Ross, 1955; Lundstrom, 2008). The principle of operation is based on changing the voltage between the conductor and the semiconductor and changing the density and sign of the charges in the semiconductor layer under the insulator layer (Prew, 1975). The current between source and drain is controlled by the voltage applied to the gate (Syu et al., 2018). While the gate terminal is related to the conductive material, the source and drain terminals must be junctions. That is, there must be a physical

connection between the two terminals (Dacey & Ross, 1955; Hayes, n.d.; Introduction, 1997).

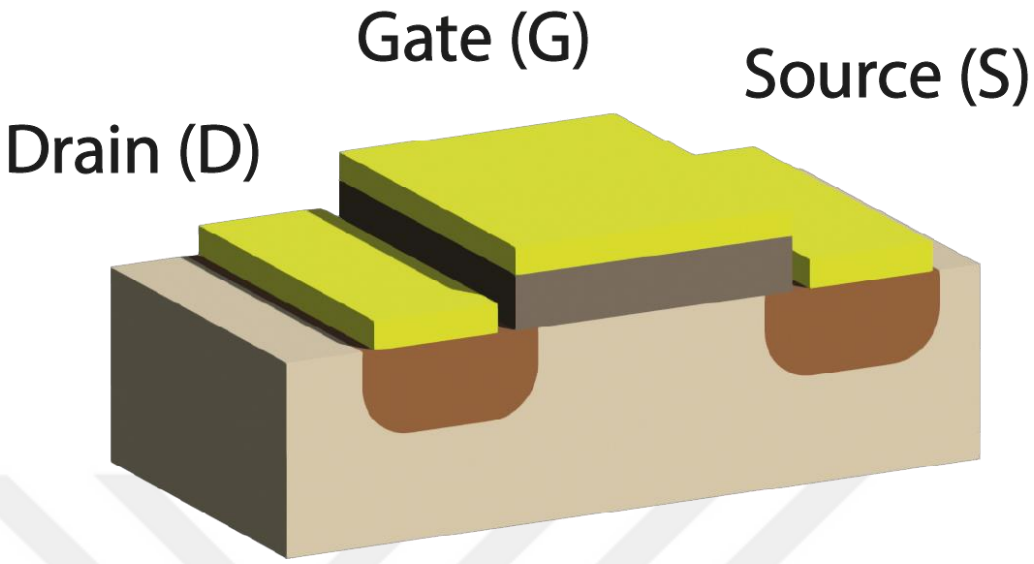

Figure 1.4 The 3D drawing of Field Effect Transistor (FET) structure.

The first studies on FETs date back to the patent of J. E. Lilienfeld in 1925 (Nishizawa et al., 1975). In 1952, Shockley provided a theoretical description of the FET, enabling the development of a basic electronic device that could fulfill all the functions of a simple electrical circuit. This description also enabled the evolution of transistor technology from a unipolar to a multipolar structure (Shockleyt, 1948).

FETs can be divided into two groups: junction FETs and MOSFETs. While both JFETs and MOSFETs have both n and p channels, JFETs are depletion mode devices (Zolper, n.d.). But MOSFETs have both boost and depletion modes. JFETs are made of a slightly high-resistance semiconductor material (mostly silicon) that forms a channel for the carrier flow. The magnitude of this current is controlled with the help of voltage interference at the gate, which is a reverse biased p-n junction formed across the channel. This device is a reverse biased transistor with high gate resistance. If the device is doped with a donor material to form the channel between the source and drain, an n-type structure is formed (i.e. the channel current consists of electrons), while if it is doped with an acceptor material, a p-type structure is formed (the channel current consists of holes)(Zolper, n.d.). The basic structure of MOSFETs consists of an oxide layer under the gate region and a p-type

substrate underneath, which is the same MOS capacitor structure and hence the name of the device (Colinge, 2004; Ferain et al., 2011; S. Zhang, 2020). In addition to this structure, there are source and drain terminals through which current flows, and there is an n-type layer underneath them. The current flows between these two terminals through the channel region close to the interface between the oxide and the semiconductor. The current flow is controlled by the voltage applied to the gate terminal. The physical implementation of MOSFETs was realized in the 1970s (Nishizawa et al., 1975). They were preferred for use in digital circuits because they could be designed and manufactured to be very small. In addition, the fact that they do not need resistors or diodes has paved the way for their use in the construction of memories and microprocessors. MOSFETs are used in many different digital circuits (Afzalian et al., 2011; Colinge, 2004; Cooper et al., 2002; Del Alamo et al., 2016; Dennard et al., 1974; Ferain et al., 2011; J. Y. Kim et al., 2021; Lundstrom & Ren, 2002; Moselund et al., 2008).

Field effect transistors (FETs) serve as transducers in biosensor applications (Abdi & Kumar, 2015; Y. Chen et al., 2017). They are advantageous over other types of transducers due to their unlimited design possibilities for multi-analyte measurement, their cost-effectiveness in terms of production, and their ability to be manufactured in large numbers on a production line (Fathil et al., 2017; J. Y. Kim et al., 2012; Mansouri Majd & Salimi, 2018; Sheliakina et al., 2014; Syu et al., 2018). In addition, they have significant advantages in terms of compatibility with the materials to be applied in the sensitive region (Abdi & Kumar, 2015; Ben Halima et al., 2021; Castellarnau et al., 2007, 2008; H. C. Chen et al., 2015; Y. Chen et al., 2017; Fathil et al., 2017; J. Y. Kim et al., 2012; S. Kim et al., 2018; Kulkarni et al., 2022; Mansouri Majd & Salimi, 2018; Mirzaii Babolghani & Mohammadi-Manesh, 2019; Poghossian, 1997; Sasipongpana et al., 2017). All these properties have led to their increased use in biosensor technologies. In this study, a reduced graphene oxide layered FET structure was preferred as the translator part of the biosensor. Detailed information about the structure is given in the next section.

1.1.4 Graphene based Field Effect Transistor (GFET)

Many types of transducers have been used in biosensor studies and applications, depending on the requirements of the application, available resources, and other relevant factors. Among these, GFETs are preferred as the transducer element of biosensors due to their high sensitivity and fast response (Burghard et al., 2009; de Moraes & Kubota, 2016a; Fu et al., 2017; H. E. Kim et al., 2019; Yan et al., 2017). The unique electronic properties of graphene or its derivatives used in this type of transducer offer significant advantages in the detection and identification of biological molecules. Structurally, these transistors are similar to MOSFETs in that they have a three-electrode structure (source, drain, and gate) (H. E. Kim et al., 2019) (Figure 1.5). The main difference is that in GFETs, the source and gate electrodes are connected by a layer of graphene or its derivatives, which is absent in MOSFETs. Instead, MOSFETs have a semiconductor material (traditionally silicon oxide) in the gate region. There are basically two types of GFETs, the back-gated GFET and the liquid-gated GFET (Fu et al., 2017; Hwang et al., 2020; H. E. Kim et al., 2019; Kwong & Tsang, n.d.). A back-gated GFET consists of source and drain electrodes of metallic material (gold, aluminum) connected by graphene or graphene derivatives on the top trace, a layer of semiconductor material (SiO_2, Al_2O_3, and so on) below them, and a gate electrode of metallic material at the bottom. Similarly, liquid-gated GFETs consist of the source and drain electrodes connected to each other with graphene material, a small liquid pool covering this region, and at the top either a rod-shaped immersion gate electrode (Ag/AgCl (Fu et al., 2017) or platinum wire (Jacobs et al., 2010)) or a gate electrode of the same material as the other electrodes suitable for the architecture (Hwang et al., 2020).

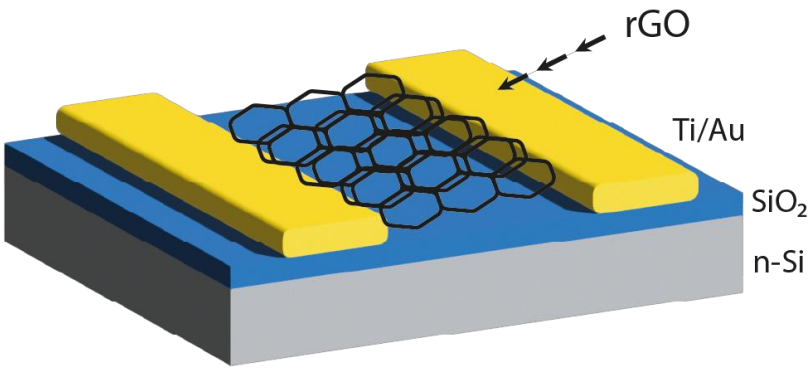

Figure 1.5 The 3D drawing of GFET structure.

The working principle of GFET-based biosensors is based on the detection of electrical differences caused by the interaction of the graphene layer with biological agents in the analyte (Béraud et al., 2021; N. Gao et al., 2016; Matsumoto et al., 2014; X. Wu et al., 2018). To explain, the graphene layer is usually placed on an insulating material and must be balanced with the gate electrode. The insulating layer creates a barrier between the graphene and the biomolecules in the analyte. With the help of the voltage applied through the gate electrode, the electrical properties of graphene can be changed. When biomolecules bind to the graphene layer, the movement of electrical charges and carriers on the surface changes. This interaction causes a change in the conductivity and resistance of graphene (Dong et al., 2010; Liu et al., 2019; Syu et al., 2018; Zhan et al., 2014). GFET biosensors have two different working approaches: direct sensing and indirect sensing (Béraud et al., 2021; N. Gao et al., 2016; Khatayevich et al., 2014; Matsumoto et al., 2014; Syu et al., 2018). In the first, direct sensing, biomolecules bind directly to the graphene layer and change its electrical properties. The changes can be electrically calibrated and provide information about the presence and quantity of the molecule. In the second approach, the biomolecule binds to the graphene surface, and the conductivity of graphene is changed by the voltage applied through the gate electrode. This change alters the intensity of the current flowing through the gate electrode. The change in current is used to detect the presence and interaction of the biomolecule (Jacobs et al., 2010; Jahromi et al., 2022).

Electrical measurement methods such as resistance measurement, conductivity measurement, current-voltage (I-V) measurements, and gate voltage measurements (de Moraes & Kubota, 2016b; Fu et al., 2017) are most commonly used in these biosensor applications.

Resistance measurement: The resistance of the GFET layer changes when it interacts with biomolecules. Therefore, measuring the resistance of the GFET layer is a fundamental method used to detect biomolecule sensing and interaction. The change in the resistance of the graphene sheet upon biomolecule binding can be detected by electrical measurement devices.

Conductivity measurement: The conductivity of the GFET layer can change as a result of interaction with biomolecules. Conductivity measurement is used to detect the change in the conductivity value of the GFET. Conductivity measurement is widely used in analyses such as biomolecule detection and concentration determination.

I-V measurements: Depending on the voltage applied across the GFET layer, current-voltage (I-V) characteristics can be obtained. These measurements are used to detect changes in electron mobility and conduction properties in the graphene layer as a result of the presence or interaction of biomolecules.

Gate voltage measurement: The gate voltage applied from the control electrode in the GFET layer can change the conductive properties of graphene. Therefore, gate voltage measurement is a method used to detect the presence and interaction of biomolecules. Gate voltage measurement can improve the sensitivity of the biosensor based on the working principle of the GFET.

In this study, a liquid gate GFET structure was preferred as the biosensor transducer part. Because this structure is more advantageous than other transducer types due to its high sensitivity, fast response time, low cost, and design flexibility. Moreover, its operating principle is well suited for the methodology of this study. For example, the working principle of liquid gate GFETs is based on the change of charges on the surface of graphene in the presence of biological analytes (e.g. DNA, RNA, protein, viruses, or cells) in the electrolyte solution. That is, the bio-analytes interact with the electrolyte solution, causing the charges on the surface to change and thus affecting the electrical conductivity of graphene. These changes are measured by the voltage applied through the gate electrode. This is reflected in changes in the current-voltage curves of the inverter transistor. As a result, the presence of the bioanalytes is signaled by current or voltage measurements, enabling the bioanalytes to be detected and quantified. Liquid gated GFET biosensors have been used in many fields, such as medical diagnostics (H. C. Chen et al., 2015; Khatri & Puri, 2022; Seo et al., 2020), environmental analysis (Lamberti et al., 2021; Tu et al., 2018), food safety (Ordonez et al., 2017; Son et al., 2016), DNA sequencing (Syu et al., 2018) and biomedical applications (Syu et al., 2018) fields.

1.2 Information of Reduced Graphene Oxide (rGO)

The carbon atom is one of the most common elements in the world. It is one of the cornerstones of life. Therefore, carbon-based materials such as graphite, graphene, graphene oxide, carbon nanotubes, and reduced graphene oxide are known to be more environmentally and biologically friendly than other inorganic materials. These properties have formed the basis for studies on their use in many sectors and fields. Among these, graphene and its derivatives have started to be preferred in biosensor studies. Graphene is a 2-dimensional material consisting of conjugated sp^2 carbon atoms covalently bonded to each other with a hexagonal structure like a honeycomb (Carvalho et al., 2022; Ghany et al., 2017; Phiri et al., 2017; Randviir et al., 2014; Soldano et al., 2010; Y. Zhong et al., 2017) (Figure 1.6). Graphene and its derivatives have been studied in a wide range of different fields thanks to their unique properties, such as specific surface area (2620 $m^2 g^{-1}$), mechanical properties (Young's modulus of 1 TPa and intrinsic strength of 130 GPa), high electronic conductivity (room temperature electron mobility of 2.5 × 105 cm2 $V^{-1} s^{-1}$), and high thermal conductivity (over 3000 W m K^{-1}) (Carvalho et al., 2022; Kumar et al., 2013; Soldano et al., 2010). These include drug delivery, hydrogen storage, fuel cells, supercapacitors, batteries, solar cells, electromagnetic shielding, polymers, conductive paints, and inks, to name a few (W. Gao, n.d.; Park et al., 2021; Ryon et al., 2016). Among these sectors, the properties of interest for the biomedical field are its aqueous processability, amphiphilicity, surface functionalizability, very high biocompatibility, and fluorescence quenching ability (Soldano et al., 2010; Y. Zhong et al., 2017).

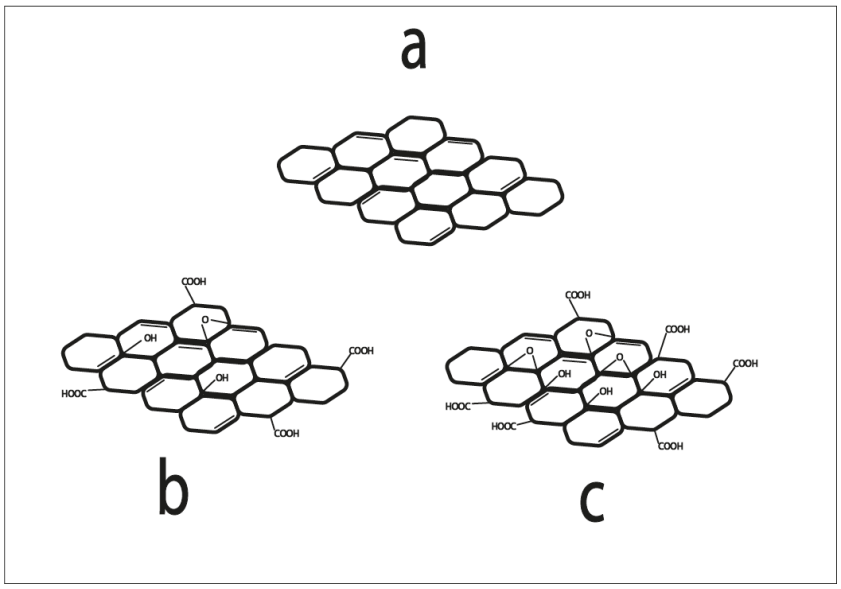

Figure 1.6 The drawings format of (a) Gaphene, (b) Reduced Graphene Oxide, (c) Graphene Oxide

There are basically two approaches to the production of graphene material: bottom-up and top-down. The first one, the bottom-up approach, is based on layer formation starting from simple carbon molecules. Laser induction, SiC graphitization by heating, and chemical vapor deposition (CVD) are the most commonly used methods. The second, top-down approach is based on obtaining graphite using chemical (Shengtao et al., 2011; Y. L. Zhong et al., 2015) and mechanical methods. Different methods, such as mechanical exfoliation, ultrasonication, and electrochemical exfoliation, are included in this approach. Production by chemical oxidation and reduction is highly beneficial in terms of high yield and low cost (Ghany et al., 2017; Y. Zhong et al., 2017).

The use of graphene and its derivatives in biosensor technology has opened new frontiers. Graphene has exceptional chemical and physical properties due to its structure. Graphene and its derivatives are known to be integrated with different materials, such as nanoparticles and nanowires, to fabricate or modify the electrodes in biosensors (Chiu et al., 2017; Hwang et al., 2016; Jiang et al., 2014; M. Li et al., 2012; Marrani et al., 2018; Ryon et al., 2016; Valera et al., 2007; M. Yang et al., 2010; Q. Zhang et al., 2018). Biosensors produced with this technology have a very low detection limit and sensitivity to detect a single molecule. Moreover, there is a considerable number of studies in the literature on this subject, and they are increasing day by day (Béraud et al., 2021; H. C. Chen et al., 2015; He et al., 2012;

Khatri & Puri, 2022; Kybert et al., 2014; Matsumoto et al., 2014; Seo et al., 2020; X. Wu et al., 2018).

Graphene and its derivatives have very important properties, such as a larger specific surface area, very good conductivity, very efficient mechanical performance, and most importantly, the functional groups required for the immobilization of biomarkers (Abdolhosseinzadeh et al., 2015; Chiu et al., 2017; Marrani et al., 2018; M. Yang et al., 2010; Zare et al., 2021). Normally, graphene lacks functional groups such as hydroxyl, carboxyl, etc. which are necessary for biosensor application (Chua & Pumera, 2014; Eigler et al., 2013; Thakur & Karak, 2015; Zunic & Peter, 2018). The use of rGO facilitates the production of biosensors without the need for this process and its cost. In addition to these features, chemical synthesis (Hummer method) is very good in terms of cost and time and was preferred in this study. Detailed information about the synthesis of rGO is given in the material and method section.

1.3 Cancer: Lung cancer

Cancer, the plague of our age, can be defined in the most basic way as the uncontrolled growth and proliferation of abnormal cells in the body. This uncontrolled growth spreads unlimitedly throughout the body, causing organs and tissues to lose their functions and leading to the death of the living being. It is an extremely painful and agonizing process for cancer patients. Recent studies show that six people are diagnosed with this disease every minute and eight million people worldwide die from it every year. It is the leading cause of death in our country and worldwide (Hacıkamiloğlu et al., 2017; Siegel et al., 2019). More than 200 types of cancer have been identified so far. Among these cancers, lung, breast, colorectal, stomach, liver, cervical, head and neck, blood cell, etc. cancers are the most common (Bray et al., 2018; Chandra & Nee, n.d.; Hacıkamiloğlu et al., 2017; Ho et al., 2010; H. Kim et al., 2021; Marrinucci et al., 2007; Schabath & Cote, 2019; Siegel et al., 2019; Sung et al., 2021; Susman, 2005).

Lung cancer can be defined as the uncontrolled growth of abnormal cells in the lung tissues. These abnormal cells cause normal cells to lose their function and

cause the organ to be unable to perform its basic function. As a result, it leads to organ failure and death (Carlsen et al., 2005; Collins et al., 2007; Molassiotis et al., 2015; Siegel et al., 2019). This type of cancer is one of the most common types of cancer worldwide. Today, the survival rate for lung cancer is very low. For example, although new chemotherapy agents and radiotherapy have slightly improved the quality of life of patients, only 15% of patients survive for 5 years after diagnosis (Minna et al., 2002; Nooreldeen & Bach, 2021; Schmekel et al., 2014; Wadowska et al., 2020). Drastic changes in lifestyle with modernization have led to an exponential increase in cancer cases. In support of this, it is known that approximately 90-95% of all cancers are caused by environmental and lifestyle factors. For example, smoking and tobacco use, poor dietary habits, increased alcohol consumption, constant exposure to environmental pollutants, infections, stress, obesity, and physical inactivity are some of the known risk factors for many common cancers (Chandra & Nee, n.d.).

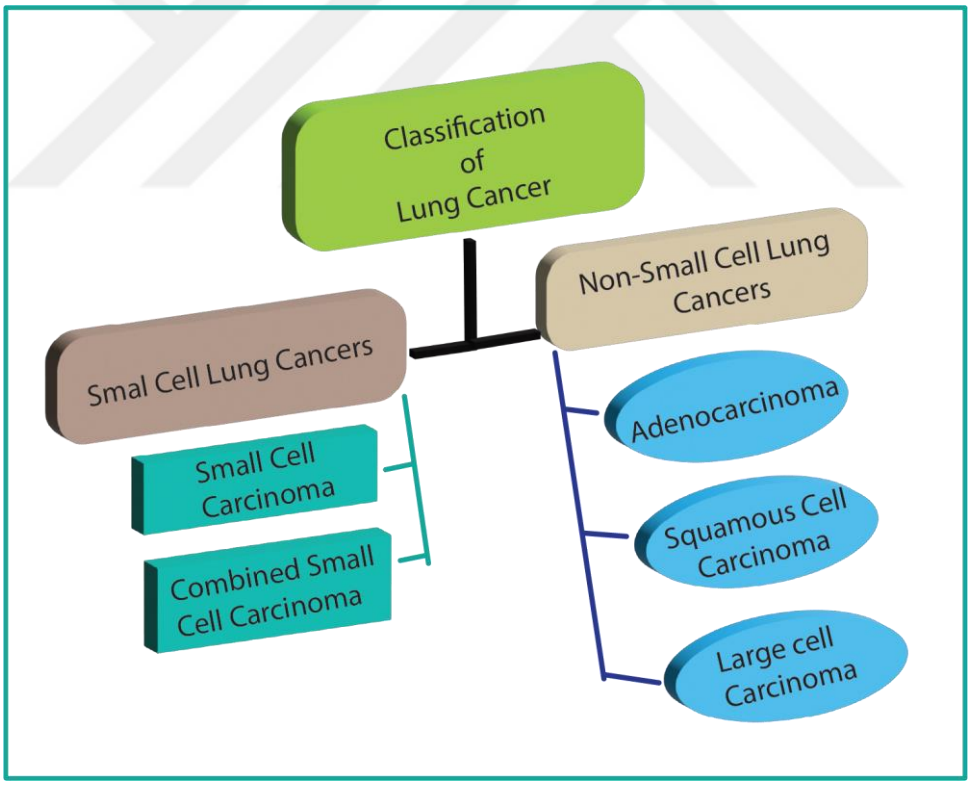

Figure 1.7 The shematic illustration of Lung Cancer types

For lung cancer, five different cancer types have been reported under two main types (Figure 1.7). These are small cell carcinoma (Oat Cell Cancer) and combined small cell carcinoma types of small cell lung cancer (SCLC) and

adenocarcinoma, squamous cell carcinoma, and large cell carcinoma types of non-smal cell lung cancer (NSCLC) (Minna et al., 2002; Nooreldeen & Bach, 2021; Tanoue et al., 2015). Of these cancer types, non-small cell types are the most common and account for more than 80% of cases. The diagnosis of these cancers in their early stages (stage 1) is purely coincidental, as they usually do not show any symptoms. However, since about 75 percent of them show symptoms in the late stages, the percentage of patient survival after treatment (37 percent) is very low (Chandra & Nee, n.d.; Marrinucci et al., 2007; Schabath & Cote, 2019; G. Yang et al., 2019). Even during treatment, the risk of cancer recurrence and metastasis is high. For all these reasons, it is vital to detect cancer at an early stage.

Currently, imaging techniques (Computed Tomography (CT) scan, Magnetic Resonance Imaging (MRI), positron emission tomography (PET) scan), endoscopic techniques (Bronchoscopy, sputum cytology, needle biopsy), and different blood and serum tests are mostly used to diagnose the disease (Chandra & Nee, n.d.). Although imaging (based on tumor phenotype) and endoscopic (invasive) techniques are highly successful in making a definitive diagnosis, as mentioned above, it is both procedurally and economically infeasible to perform them without any symptoms, i.e. before the disease has tumorized. Moreover, the symptom-based application of these techniques leads to a delay in the diagnosis of the disease. In terms of blood and serum tests, there are no effective parameters and biomarkers. Today, genetic (COX2, K-ras mutant, FHIT, DAPK, RASSFIA, etc.) (Wadowska et al., 2020) and protein (CEA, TPA, tumor M2-pyruvate kinase, KLKB1, etc.) (Khanmohammadi et al., 2020; G. Yang et al., 2019) biomarkers are used for detection. However, they are still not at the desired level to detect lung cancer at an early stage. Recent studies have revealed the relationship between microRNAs and cancer types. This has paved the way for the use of miRNAs as biomarkers. Therefore, in this study, miRNA (Asakura et al., 2020) was preferred as a biomarker in the biosensor developed for early detection of lung cancer. Detailed information about miRNAs will be given in the next section.

1.4 Micro RNA as a biomarker

Biomarkers play a key role in detection in biosensor studies. Biomarkers can be defined as molecular structures that enable us to distinguish between normal

and cancerous conditions. In other terms, biomarkers are biological molecules (enzymes, antibodies, nucleic acids, and proteins) or biological systems (tissues, microorganisms, and cells)(Sezgintürk, 2020) that interact with the specific analyte of interest. Biomarkers can also be used to assess the body's response to a particular treatment for a disease. They are secreted from cancerous tissues in the body into body fluids such as serum or plasma, urine, saliva, sputum, and tears (Jansson & Lund, 2012; Kulkarni et al., 2022; T. X. Lu & Rothenberg, 2018). Biomarkers that undergo significant changes in quantity can be divided into three categories for cancer detection and monitoring. Firstly, diagnostic biomarkers, which are related to the detection of disease, secondly, prognostic biomarkers, which are related to the likelihood of recurrence, and finally, predictive biomarkers, which are related to the response of cancer to treatment (Jayanthi et al., 2017).

MicroRNAs have their origins in the evolution of a large number of small RNA species to suppress unwanted genetic material and transcripts in eukaryotic organisms. These RNA molecules are small in size and range in length from 20 to 30 nucleotides (Griffiths-Jones, 2010; Ha & Kim, 2014). Within living organisms, three types have been identified in the animal class: microRNA (miRNA), siRNA and PIWI-interacting RNA (piRNA)(Ha & Kim, 2014). Of these, miRNAs are a class of short RNAs between 19 and 25 nucleotides in size that regulate posttranscriptional silencing of target genes and are predominant in most somatic tissues. They result from the activity of two RNase III proteins, Drosha and Dicer (Mohr & Mott, 2015). Specifically, they cause mRNA degradation by inhibiting messenger RNA (mRNA) translation and binding to complementary regions of target mRNAs through base pairing. Through this mechanism, a miRNA targets a large number of miRNAs and post-transcriptionally alters the expression of many functional genes (MaClellan et al., 2014; K. L. Wu et al., 2019). In 1993, the first miRNA was identified and named *lin-4* as a result of a genetic study on *Caenorhabditis elegans,* a free-living nematode species of roundworms (K. L. Wu et al., 2019). Although miRNAs were not identified as a separate regulatory genetic molecule in subsequent studies, this situation has changed as a result of intensive studies since the 2000s. A database of microRNAs called miRBase (managed by the Griffiths-Jones laboratory in the School of Biology, Medicine, and Health at the University of Manchester) has been established, and more than 2500 different

miRNAs have been identified (Griffiths-Jones, n.d.; Vishnoi & Rani, 2017; K. L. Wu et al., 2019).

The recent increase in the use of miRNAs as biomarkers has been driven by the understanding of their role in many cellular activities such as gene regulation, apoptosis, hematopoietic development, and maintenance of cell differentiation (Griffiths-Jones, 2010; Ha & Kim, 2014; Mohr & Mott, 2015; Vishnoi & Rani, 2017). In fact, it is estimated that they are involved in the regulation of almost one-third of human genes (K. L. Wu et al., 2019). In other words, miRNAs are active actors in genomic and epigenomic interactions. In addition to these features, their presence in body fluids allows them to be used as biomarkers (MaClellan et al., 2014). Many miRNAs have been studied to test different cancer types (Asakura et al., 2020; Hashemi et al., 2017; Joshi et al., 2014; J. Lu et al., 2020; Y. Wang et al., 2014; Xia et al., 2015; Ying et al., 2020; X. Zeng et al., 2016). In the study conducted by Asakura et al. (Asakura et al., 2020), which is the reference article for the biomarkers of this study, two miRNAs (miR-1268b and miR-6075) were detected with 99 percent sensitivity and selectivity as a result of molecular studies to identify miRNAs related to lung cancer (Asakura et al., 2020). These RNA molecules were preferred as biomarkers in our study, and the studies were performed in vitro. Detailed results are presented in the following sections of the study.

2. AIM AND SCOPE OF THE STUDY

The main aim of this study is to fabricate and develop a reduced graphene oxide layered field effect transistor based biosensor that can detect lung cancer at an early stage. Because lung cancer is one of the types of diseases that cause the greatest losses to human beings both in our country and worldwide. In addition, it is in the top three in terms of mortality rate among cancer types. However, if it is detected at an early stage, in the first stage of cancer, the cure rate is very high. Therefore, it is important to develop biosensors to detect this disease at an early stage. Moreover, this is the main motivation for this study and future studies.

In order to achieve the main objective of this study, an important literature review was carried out to identify the transducer and biosensing elements of the biosensor. As a consequence of this review, FET structure was identified as the transducer element and cancer-specific microRNAs as the biosensing agent. The FET structure was designed and fabricated in line with the existing facilities. In order to make the FET structure compatible for immobilization of the biosensing agent and to increase the measurement sensitivity of the device, reduced graphene oxide (rGO) material was preferred as the active region (between source and drain) layer. The rGO was synthesized from graphite powder following the procedure of Hummer method. Subsequently, a method that is not available in the literature and was developed for the first time during this study was applied for the placement of the FET structure of the rGO material between the welding and flux electrodes with the desired properties. For this method, an application was made to the Turkish Patent and Trademark Office to patent the invention. As a result of this process, GFET production, one of the sub-objectives, was realized. Afterwards, immobilization of miRNAs selected as biomarkers on the rGO layer of GFET was performed. In this study, biomarker immobilization was carried out in the most economical way (to reduce the cost) without using immobilization agents in the literature. As the last step of the study, electrical characterization of the biosensor in vitro and limit of detection (LOD) studies were performed.

As a result, a biosensor candidate has emerged that is open to further development for future studies and provides promising results in detecting lung cancer at an early stage.

3. MATERIALS AND METHODS

3.1 Materials

The production and electrical measurements of the Graphene-based Field Effect Transistor (GFET) structure and the synthesis of reduced graphene oxide (rGO) were carried out in the laboratories of the Nuclear Radiation Detectors Application and Research Center (NURDAM), affiliated to Bolu Abant İzzet Baysal University (BAİBU).

The chemicals that were used in the synthesis of rGO, are listed below.

- Graphite powder (<20 μm, synthetic, Sigma-Aldrich)
- Sulfuric Acid (96%, Suprapure, Merck)
- Potassium permanganete (>99%, Sigma Aldrich)
- Hydrogen peroxide (30%, Suprapure, Merck)
- L-ascorbic acid (ACS reagent)

The list of devices used in the production of GFET is given below.

- ✓ Diffusion Furnaces (CVD, Wet/Dry Oxidation, B/P Doping)
- ✓ Mask Aligner System
- ✓ Electron Beam System (thermal and e-beam evaporation)
- ✓ NP Cleaning Wet Bench System
- ✓ Spin Coating System
- ✓ Hot plate
- ✓ Dicing Saw System
- ✓ Spectroscopic Reflectometer
- ✓ Ultrasonic bath

Micro-RNAs (hsa-miR-6075 and hsa-miR-1268b) and their complementary that acting as bioreceptors, were synthesized by Oligomer Biyoteknoloji A.Ş. Company. The Phosphate Buffered Saline (PBS) solution was prepared as 10 mM with 7.4 pH. 2 mL eppendorf tubes were used to store the oligonucleotide samples. In addition, micropipet with 2-20 μL working range and sterilized pipette tips were used for dropping.

3.2 The Synthesis of Reduced Graphene Oxide (rGO)

To synthesize reduced graphene oxide (rGO), graphene oxide (GO) was first synthesized from graphite powder (<20 μm 99% Sigma Aldrich). For this, the

Hummer method, which is well-known method in the literature, was used (Surekha et al., 2020; Thakur & Karak, 2015). Firstly, 50 ml of sulfuric acid (98%, Merck) was poured into the beaker with a volume of 250 ml, and the beaker was placed in a bowl filled with ice on the magnetic stirrer (**Figure 3.1.a**). Then 1 g of graphite powder was added and mixed with the help of magnetic fish at 600 rpm for 10 minutes (**Figure 3.1.b**). At the end of the 10 minutes, it was observed that the graphite powder was homogeneously dispersed in the liquid, and then 3 grams of Potassium permanganate (>99%, Sigma Aldrich) were carefully added into the mixture little by little (**Figure 3.1.c**). The mixture was stirred at 600 rpm for 3 hours. Since it is important for the quality and efficiency of the GO to be obtained that the temperature of the mixture remains below 10 °C from this process, the temperature of the mixture was continuously measured with the help of a thermometer. Afterwards, 50 ml of DI water was carefully added little by little to the mixture (**Figure 3.1.d**). During this process, the color of the mixture changed from black to brownish, and then, it was continued to stir at 600 rpm for 1 hour. Next to this step, another 100 ml of DI water was carefully poured into the mixture and stirring was continued for 1 hour. Thereafter, in order to stop the chemical reaction in the mixture, 5 ml of Hydrogen peroxide was added dropwise into the beaker. During this step of the process, bubbles formed on the surface of the mixture. And the end of the bubbles means that the reaction is finished. At the end of these processes, GO was obtained. The GO mixture was washed five times using DI water so as to get rid of GO from chemical residues. After the washing step, to remove excess water from the GO solution, it was filtered with the help of blue band filter paper, and then this slurry of GO was left at room temperature for a day to dry (**Figure 3.1.e**). Last of all, the flake form of GO was obtained (**Figure 3.1.f**).

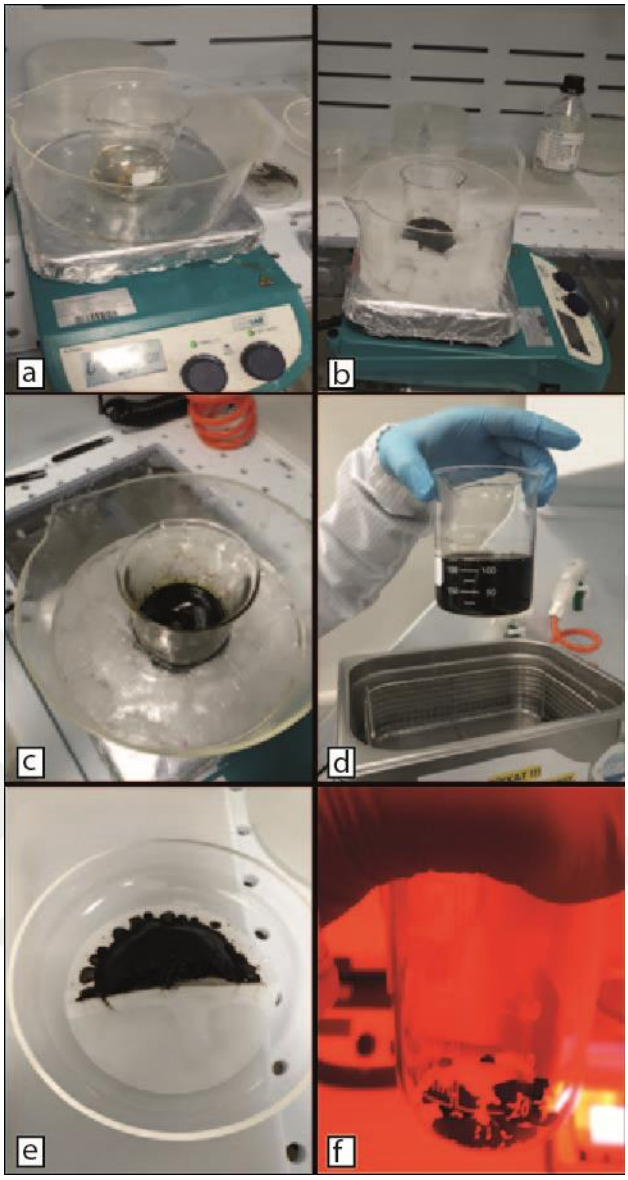

Figure 3.1 The steps of GO synthesizing process

Because L-ascorbic acid is a cheaper and more accessible alternative chemical reduction agent of GO to others (e.g. sodium borohydride, pyrogallol, and hydrazine), it was used as the reduction agent to obtain rGO from GO. In the first instance, 50 ml of DI water was poured into the beaker, which had a volume of 250 ml, and the beaker was placed on the magnetic stirrer. Thereafter, 1 mg GO and 2 mg L-ascorbic acid were added into the beaker, and they were stirred with the help of the magnetic fish for 24 hours at 900 rpm (**Figure 3.2.a**). Then, the rGO mixture was washed five times using DI water in order to purify it from chemical residues. In the next step, the rGO mixture was filtered using blue-band filter paper (**Figure 3.2.b**). And then, it was left to dry at room temperature for a day (**Figure 3.2.c**). In

conclution, at the end of these processes, flakes of rGO were acquired (**Figure 3.2.d**).

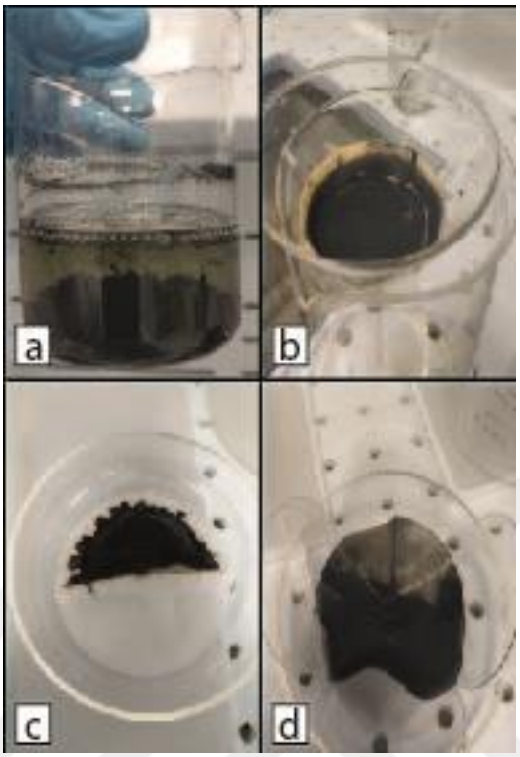

Figure 3.2 The steps of rGO synthesizing process

The chemical and morphological characteristics of graphite, graphene oxide, and reduced graphene were researched using Raman spectroscopy (Dispersive Raman spectrometer, Central Lab., METU) X-Ray Diffaction spectroscopy (XRD, Rigaku, BAİBU), Fourier Transform Infrared spectroscopy (ATR-FTIR spectrometer, BAİBU), High Resolution-Transmission Emission Microscopy (Jeol 2100F HRTEM, Central Lab., METU).

3.3 Fabrication of Graphene based Field Effect Transistor (GFET)

Recently, field effect transistors (FET) have been more preferred as infrastructure in biosensor studies because they have some important advantages such as miniaturization of the device, low noise, low power consumption, wide dynamic rage, simple device configuration, easy integration, a wide safe operating range, and real-time detection (H. C. Chen et al., 2015; Y. Chen et al., 2017; He et al., 2012; Trung et al., 2014; Zhan et al., 2014). Because of this reason, FET was preferred as a biosensor infrastructure in this study.

3.3.1 Design of Graphene Based Field Effect Tansistor (GFET)

Field Effect Transistors (FETs) are semicoductor devices that change the channel current and conductivity with the help of charge carriers. Moreover, FETs classically consist of three elements such as Source (S), Drain (D), and Gate (G) (Dacey & Ross, 1955; Hayes, n.d.) (**Figure 3.3**). These elements are called electrodes. In this study, firstly, the GFET structure, which is seen in Figure 3.3, is designed in a vector-based graphics software to be similar to a basic FET device. The most important part of the GFET design is the sensory area. Because reduced graphene oxide is placed in this area and biomarkers are immobilized on it. Moreover, whether the biosensors works or not and their working performance depend on this area. Therefore, three GFETs with different sizes of sensor areas were designed. The dimensions and definitions of the GFET design are given below.

- Distance from gate electrode to sensory area (d): 1.5 mm
- Length (L) x Width (W) of sensory area: 2 x 2.5 mm, 2 x 2 mm, 2 x 1.5 mm, for three different GFET designs respectively

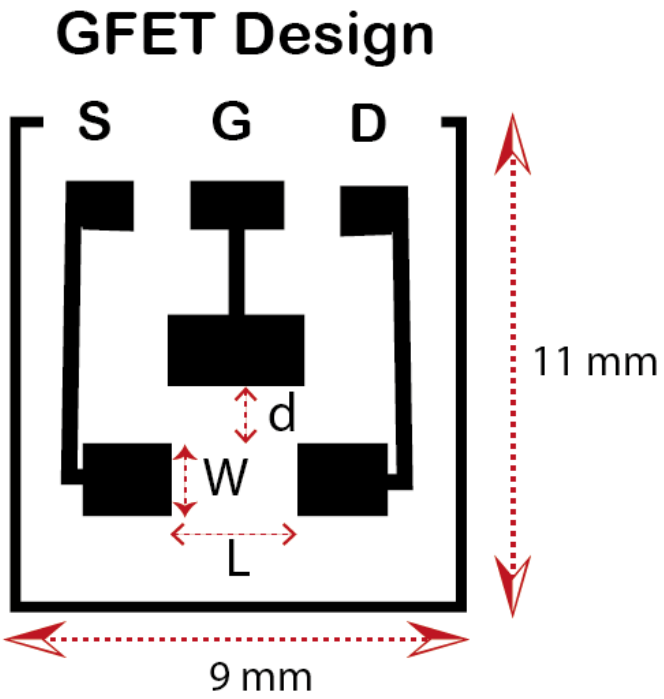

Figure 3.3 The design of GFET as a biosensor infrastructure. (Symbols: S, Source; G, Gate; D, Drain; d, distance from gate electrode to active area; W, width of active area; L, length of active area)

Finally, this GFET design has been converted to a photomask design for a 6- inch substrate. There are more than 150 GFETs in this photomask design (**Figure 3.4**).

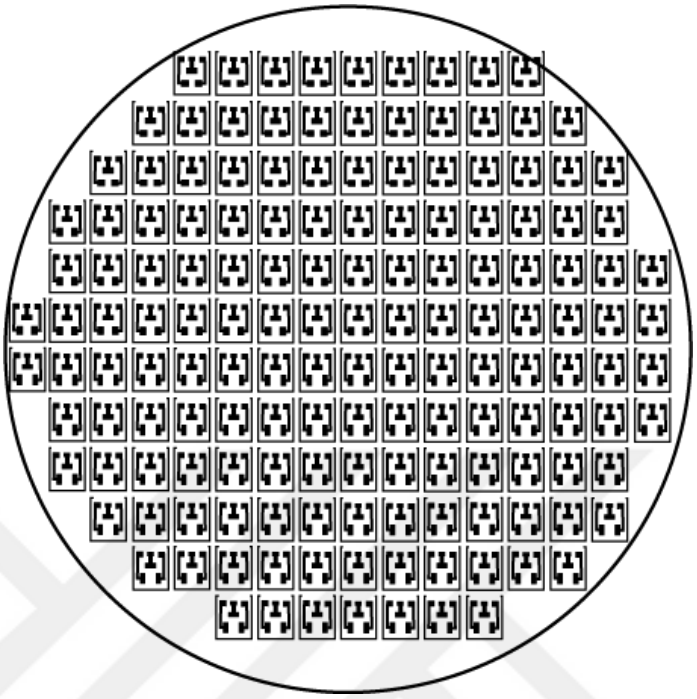

Figure 3.4 The designed photomask of the GFET structures for 6-inch wafer.

3.3.2 Cleaning of Silicon (Si) Wafers

Silicon (Si) wafer (n-type (100), 2-4 Ω resistance, 500 μm) was preferred as a substrate in the production of GFETs, as it was cost-effective and suitable for the infrastructure of the laboratory where this study was conducted. First of all, Si wafers were cleaned by applying the Radio Corporation of America (RCA) procedure in order to be free of contamination. Because the contamination adversely affects the performance of semiconductor devices. Therefore, the cleaning process is the first and most critical step in the production process. The RCA cleaning procedure includes three stages, and the details are below.

- ✓ **Organic cleaning:** this step is applied to purify the wafers from organic contaminants. The solution consists of ammonium solution (NH_4OH), hydrogen peroxide (H_2O_2), and DI water (DIW) (H_2O) in a ratio of 5:1:1, H_2O: H2O2:NH4OH. The mixture is heated to 55°C, and the wafers are kept in this solution for 15 minutes. Then it is rinsed with DI water 10 times.

- ✓ **Ionic cleaning:** the target of this step is cleansed from hevy ions by using a solution that includes hydrochloric acid (HCl), hydrogen peroxide (H_2O_2) and DI water (DIW) (H_2O) in a ratio of 6:1:1, H_2O: HCl:H_2O_2. The solution is heated to 60°C and the wafers are kept in it for 15 minutes. Then they are rinsed with DI water 10 times.
- ✓ **Native oxide cleaning:** this stage, the last step of the RCA procedure, is used to remove the native oxide (SiO_2) formed on the surface of the wafers. A dilute HF solution is obtained by mixing hydrofroluoric acid (HF), and DIW in a ratio of 50:1, DIW: HF. Afterwards, the wafers are kept in this solution for 20 seconds. Then they were rinsed with DI water 10 times. Lastly, the wafers were dried using pure nitrogen gas (N_2).

3.3.3 Growth of Insulating Layer

After the RCA cleaning step, silicon oxide (SiO_2) as an insulating layer (IL) was grown onto the Si wafer using the diffusion furnace. The dry oxidation technique (at 1100°C, using N_2 and O_2 gases) was applied to deposit the insulating layer onto the Si wafer (**Figure 3.5**).

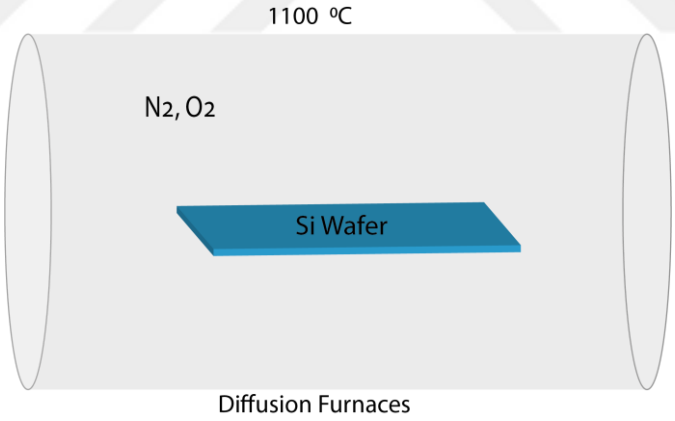

Figure 3.5. Schematic diagram of Diffusion Furnace (Dry oxidation)

The thickness of the SiO_2 layer was measured at approximately 300 nanometers (nm) using the spectroscopic reflectometer (**Figure 3.6**). In order to avoid short circuits and leakage current, the thickness of this layer must be greater than 200 nm. The schematic of the SiO_2/n-Si structure is given in Figure 3.6.

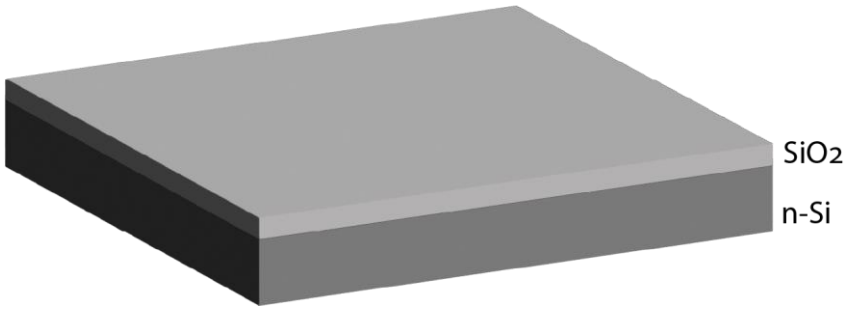

Figure 3.6. The schematic diagram of Insulating layer (SiO_2) onto Si wafer.

3.3.4 The Lithography and Metalization Processes

Firstly, before the contact electrodes (drain, source and gate) of the biosensor are made, the design made in the computer environment must be turned into a photomask. For this purpose, the mask draft shown in Figure 3.4 was printed on the transparent acetate sheet (200 μm thickness, size 210*297 mm A4) using a laser printer. Then this acetate sheet was cut and glued to a piece of glass in the dimensions of the photomask suitable for the Mask Aligner device. As a result, the photomask of the FET structure was made.

The lift-off technique was used to produce the electrodes of the FET structure. In this method, photoresist is first applied, and then the target metal is coated on the surface of the substrate. Then, using the appropriate solvent (remover), the photoresist is removed from the surface of the substrate, and the desired pattern is obtained. The lift-off method is more advantageous than the conventional etching method because it does not use an extra metal etching process. In the FET structure, gold (Au) with very good electrical conductivity was preferred as the contact electrode metal. In addition, titanium (Ti) was used to increase the adhesion of the gold (Au) and silicon oxide (SiO_2) layers. The production processes of the FET structure are described in detail below.

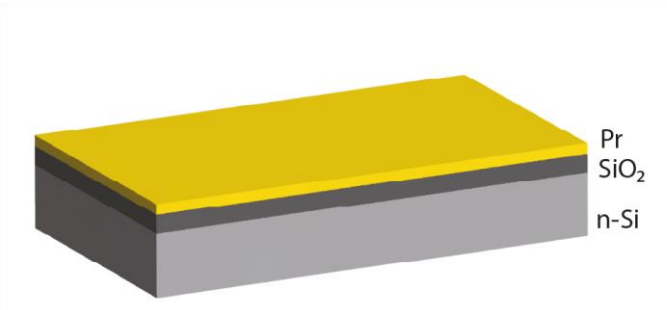

Figure 3.7 The 3D drawing visual of SiO_2/n-Si wafer with 1 μm photoresist (Pr).

In the litography process, to begin with, the wafer surface was coated with negative photoresist (1µm, ma-N 1410, Micro Resist Technology) using a spin coater device (3000 rpm, 30 seconds) (Figure 3.7). The wafer was then placed on the hotplate at 100° C for 90 seconds to prebake stage, and then the handcrafted photomask was applied to the wafer in the mask aligner device (exposure dose; 450 mj/cm^2) (Figure 3.8).

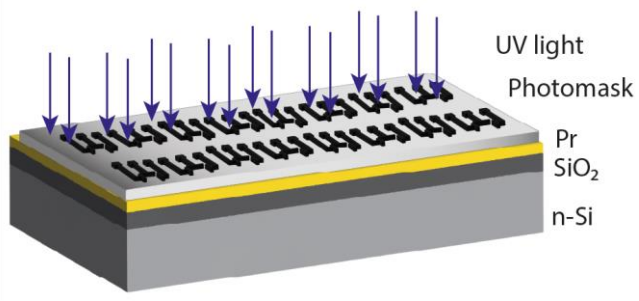

Figure 3.8 The 3D drawing visualization of the photolithography application.

Following the photomask stage for the FET structure, the wafer was exposed to developer solution for 50 seconds to remove the unwanted parts of the photoresist that had been decomposed by UV light from the surface of the wafer (Figure 3.9a). And then, the wafer was washed with DI water and dried with N_2 gas. After that, for the hard-bake step, the wafer was placed on the hotplate at 100°C for 180 seconds.

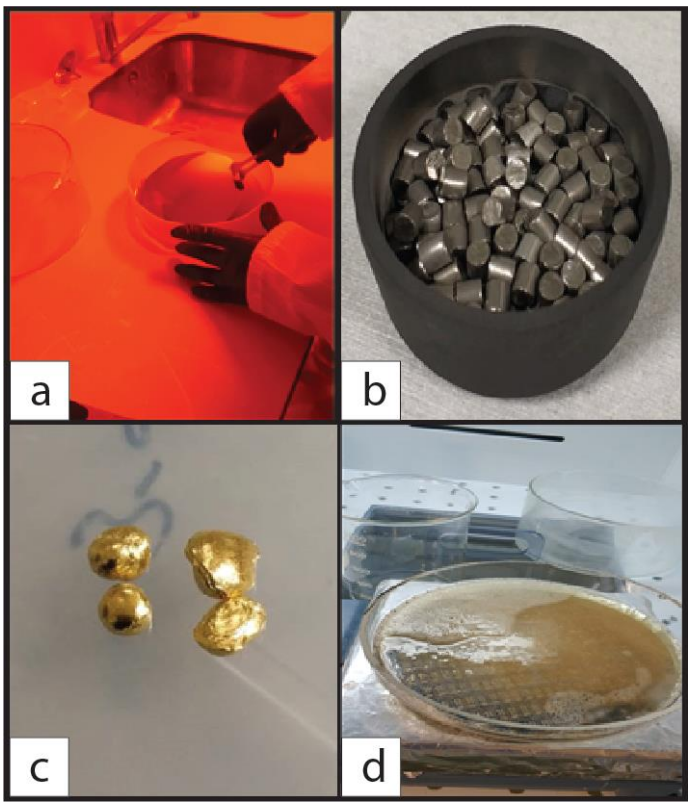

Figure 3.9 Photographs of the photolithography and metalization processes of the FET structure fabrication. (a; Developer step, b; Titanium pellets, c; Gold pellets, d; Remover step).

To create the metal electrodes of the structure, the E-beam device was used. First, 5 nm of titanium (Ti) was coated, and then 50 nm of gold (Au) was coated using the thermal evaporation technique (Figure 3.9 b,c). The coated wafer was then soaked in a remover solution for 120 seconds to remove photoresist. Afterwards, the wafer was taken out of this solution, washed with DI water, and dried using N_2 gas (Figure 3.9 d).

Finally, the FET structures on the wafer were cut out with the help of a dicing saw device (Figure 3.10).

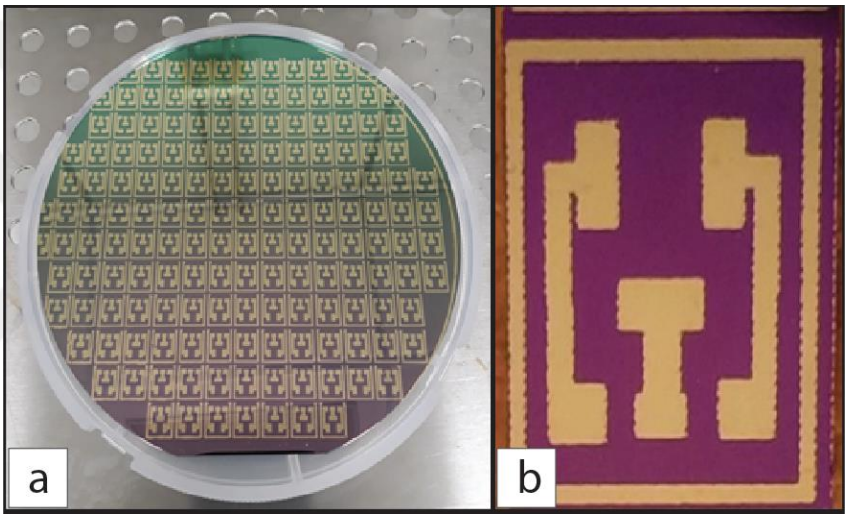

Figure 3.10 Photos of (a) whole wafer and (b) a FET structure after the metalization step.

3.3.5 The Coating of Reduced Graphene Oxide on FET Structure

In order to transform the FET structure into a GFET structure, at this stage of the study, the synthesized reduced graphene oxide was coated as a thin layer between the source and drain (where the sensitive area of the GFET is) of the FET structure. Although there are many methods to form the rGO layer, a method that was found in this study and not in the literature was applied. A patent application (Patent Application Number:2021/008695) was filed for this method, which was presented at an international symposium and published as a full paper (Gürer et al., 2022).

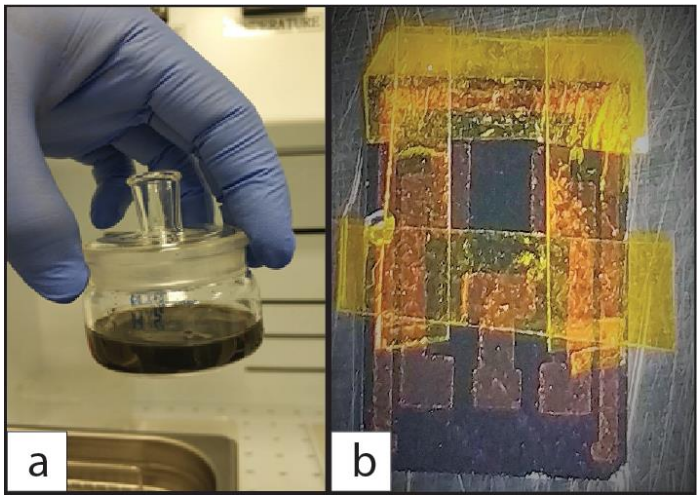

Figure 3.11 a) The dispersed suspension of rGO/DIW (10 mg/ml), b) A FET chip covered with polyimide capton tape.

Before starting the rGO coating process on the sensitive region of the FET structure, a 10 mg/ml suspension of rGO/DI water was prepared. This suspension was treated in an ultrasonic bath for 24 hours to obtain a homogeneous dispersion (**Figure 3.11a**). As another preliminary preparation, the sensitive areas of the FET chips were covered with polyimide capton tape, as shown in Figure 3.11b. Unlike the literature, an ultrasonic device was used in this coating process to ensure a homogeneous coating.

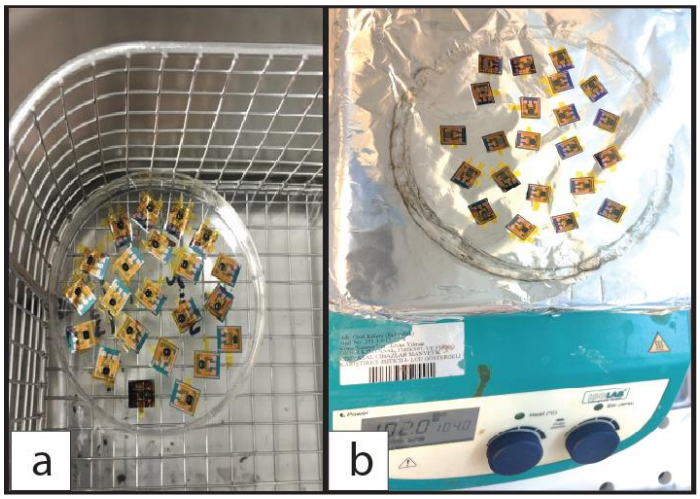

Figure 3.12 a) The FET chips with rGO in the ultrasonic bath, b) The FET chips on the hotplate.

First, the chips were placed in a petri dish and placed in the ultrasonic bath while the device was working. Afterwards, using a micropipette, 5 µl of the homogeneously dispersed rGO suspension was taken and dripped onto the sensitive areas of the chips. The water in the dripped suspension was allowed to dry (about 5

minutes), and the these chips were removed from the ultrasonic bath (**Figure 3.12a**). Immediately afterwards, the polyimide capton tapes on the chips were carefully removed. The chips were then placed on the hotplate at 50°C and annealed at 100°C by gradually increasing the temperature by 10°C every 5 minutes (30 minutes in total) in order to dry the rGO layer on the sensitive area of the chips and to ensure a good adhesion with the SiO_2 layer (**Figure 3.12b**). After annealing, the GFET structure emerged (**Figure 3.13a, b**).

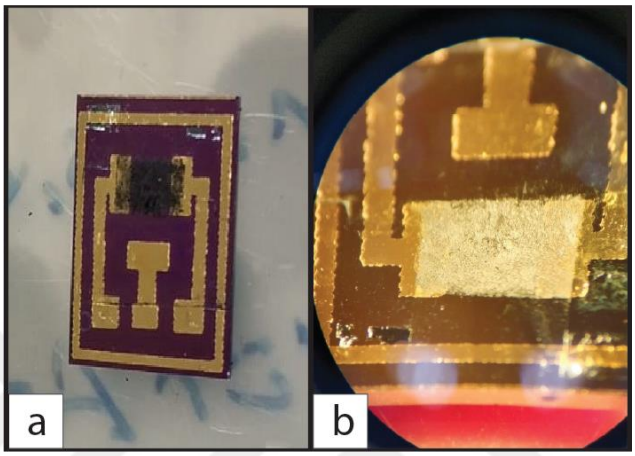

Figure 3.13 a) A photograph of GFET chip, b) An image of the rGO layer on GFET chip under microscope.

Finally, the GFET chips were soaked in piranha solution (3:1, H_2SO_4:H_2O_2 at 50°C) for 5 seconds to remove the non-adherent rGO particles on the surface of the sensitive region and also to remove the residues of polyimide capton tape (**Figure 3.14a, b**). And then they were immediately washed with DI water and dried with N_2 gas. As a result, the GFET structure of the biosensors was produced.

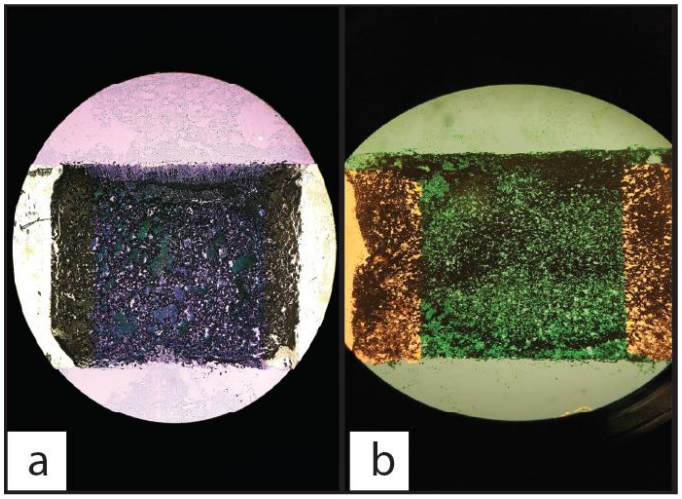

Figure 3.14 The images of rGO layer before (a) and after (b) application of piranha solution.

3.4 Immobilization Process of Biomarkers on GFETs

In this study, the oligonucleotide sequences of microRNAs (miR-1268 and miR-6075 (Asakura et al., 2020) and miR-99a-5p as non-complementary probes) synthesized by Oligomer Biotechnology Inc. were used as biomarkers and probes. The sequences of oligonucleotides are given in **Table 3-1**.

Table 3.1. The squences of micro RNA's (miR-1268b, miR-6075 and their complementary)

Oligonucleotides	*Sequences (5′→3′)*
miR-1268b target	CGGGCGTGGTGGTGGGGGTG
miR-1268b Complementary probe	CACCCCCACCACCACGCCCG
miR-6075 target	ACGGCCCAGGCGGCATTGGTG
miR-6075 Complementary probe	CACCAATGCCGCCTGGGCCGT
miR- 99a-5a Non- complementary	AACCCGTAGATCCGATCTTGTG

The immobilization process of antibodies is critical for biosensor studies (Bahri et al., 2021; Xu et al., 2018; Q. Zhang et al., 2018). Because the sensitivity, selectivity, and consistency of the biosensor, that is, its correct operation-depend on the success of this process. For this reason, biological materials need to be stored in appropriate conditions. Therefore, the samples were stored at -20 ºC before use (Pei-Wen et al., 2014). Before starting immobilization, 10 μM in buffer solution (Phospahte Buffered Saline) complementary DNA probes were prepared (Béraud et al., 2021; Hwang et al., 2020; Islam, 2020; A. Kim et al., 2010; J. W. Kim et al., 2018; Mohamed et al., 2022; Pei-Wen et al., 2014; Rodrigues et al., 2023; Torrisi et al., 2022).

First, the immobilization process started by placing the GFET sensors on a hotplate. Then, 5 μL of probe DNA were dropped onto the rGO layer in the GFETs. Afterward, the GFETs were immediately heated to 50 ºC and allowed to incubate the probe on the rGO layer for 30 minutes (Figure 3.15). Finally, the rGO layer was washed with DI water to remove unbound fragments. This process was repeated three times to ensure the binding of all functional groups in the rGO layer of the GFET with the probe (H. E. Kim et al., 2019).

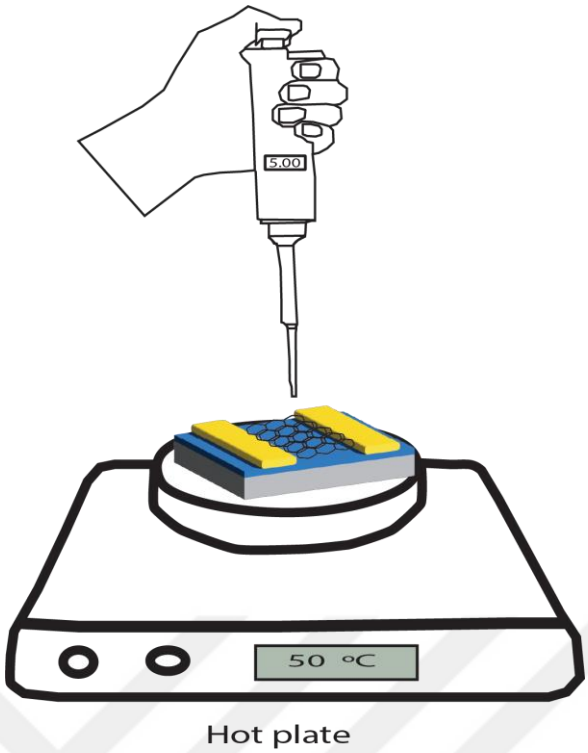

Figure 3.15 The drawing image of the Immobilizaiton process.

3.5 Establishment and Implementation of Electrical Measurement System

The electrical characteristics of a GFET based biosensor were measured using a probe station-integrated Keithley 4200 SCS system (Figure 3.16).

The output characteristics of the GFET biosensor were measured to investigate whether the reduced graphene oxide layer between the source and drain terminals is a successful contact. In this measurement, a sweep voltage between -0.5 V and 0.5 V was applied to the source and flux contacts, while no voltage was applied to the gate electrode.

To measure the transfer characteristics of the GFET device;

- In pH solutions prepared from pH 1 to pH 4, the gate electrode was applied a sweeping voltage between-0.5V and 2V while the flux voltage was kept constant at 0.1 V and the source electrode was grounded.

- For miRNA analyte solutions, sweeping voltages ranging from 0V to 5V were applied to the gate electrode while the flux voltage was kept constant at 0.1 V and the source electrode was grounded.

The transfer characteristics and output characteristics of the GFET biosensor were measured with solutions that contain oligonucleotides that were prepared with 1×PBS solution at different concentrations.

Target oligonucleotides (miR-1268b and miR-6075) were diluted with 1X PBS (pH 7.4) in the range from 100 pM to 1 µM for the limit of detection (LOD) measurement.

Three GFETs were utilized for each electrical measurement. The outcomes are interpreted based on the mean of these three processors.

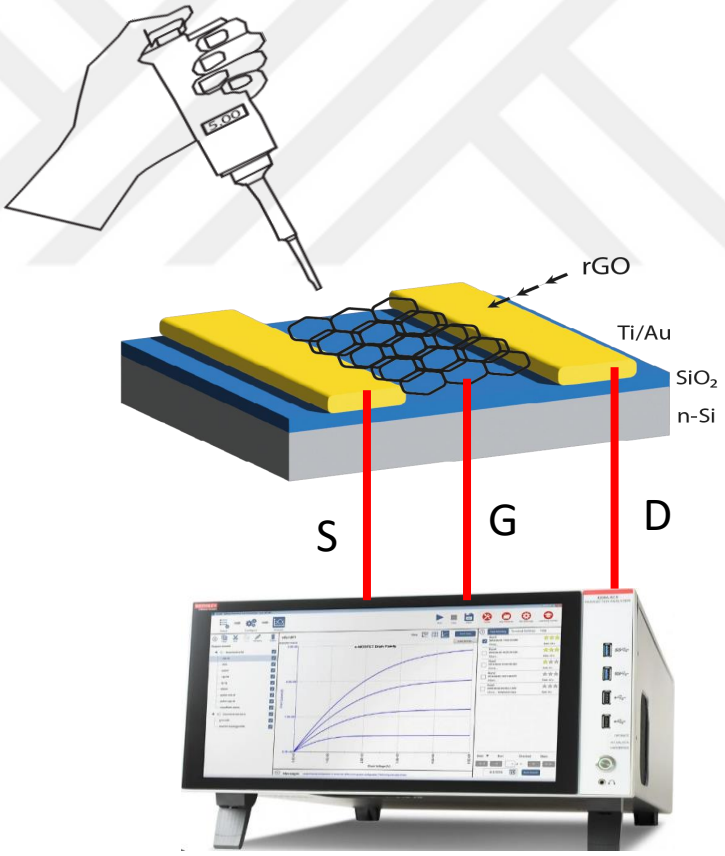

Figure 3.16 The electrical measurement system of GFET based Biosensors

4. RESULTS AND DISCUSSION

In this part of the study, firstly, the structural and chemical properties of GO and rGO that were synthesized from graphite powder were investigated using analysis methods such as XRD, FTIR, Raman spectroscopy, and TEM images. The results of these analyses were discussed and compared with similar studies in the literature. Then the electrical response of the fabricated GFET based biosensor was investigated. The results were discussed and explained in detail in the following section.

4.1 The Structural and Chemical Characterization of Reduced Graphene Oxide (rGO)

4.1.1 X-ray Diffraction (XRD) Analysis

In this study, XRD analysis was used to survey the crystal structures of graphite (Gr), graphene oxide (GO), and reduced graphene oxide (rGO). XRD characterization of Gr, GO, and rGO was carried out by the X-ray Diffrectometer System (Rigaku DMAX 2000/PC using CuKα radiation (λ=1.54 Å)) in Bolu Abant Izzet Baysal University.

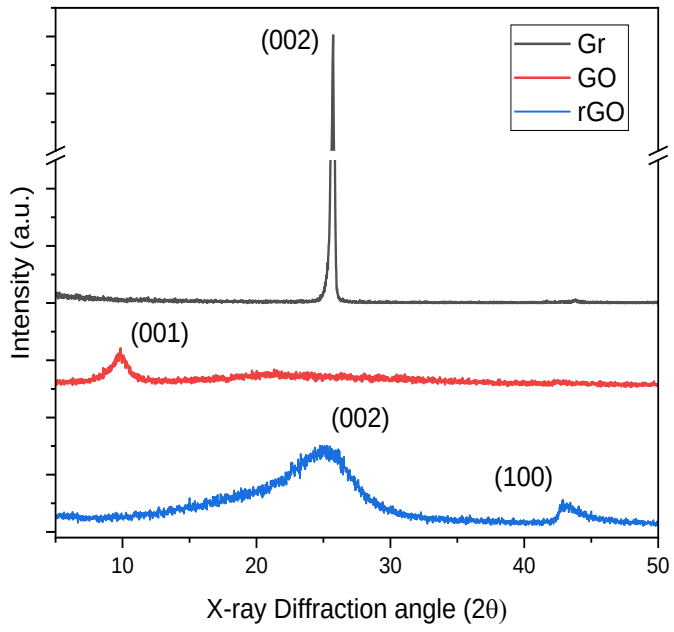

Figure 4.1 XRD patterns of Graphite (Gr), Graphene Oxide (GO) and Reduced Graphene Oxide (rGO).

According to the literature, since graphite has a multilayer structure, the main characteristic peak of graphite is a sharp and strong diffraction peak corresponding to between 25 and 27 degrees (Abid et al., 2018; Chong et al., 2015; Kant Upadhyay et al., n.d.; Krishnamoorthy et al., 2013; Lesiak et al., 2021; Sieradzka et al., 2020; Surekha et al., 2020). When the XRD pattern of Gr in **Figure 4.1** is examined, it is seen that the characteristic peak is in a degree ($2\theta=25.7^{o}$) compatible with the range in the literature, and the interlayer distance (d) is 0.34 nm with indices (002). However, the XRD spectrum of the synthesized GO shows that the main peak is shifted 9.82 degrees with a d-spacing of 0.9 nm with indices (001). This is due to the introduction of oxygen-containing functional groups between the graphite layers by using the Hummer method. This finding is also an indication of the successful application of the method. The primary peak of rGO moved back to 24.93 degrees, and the separation between the layers sank to 0.35 nm with indices (002) (Abid et al., 2018; Chong et al., 2015; Sieradzka et al., 2020), in accordance with the XRD analysis performed after the reduction process of GO (**Figure 4.1**). This outcome demonstrates that the oxygen-containing functional groups between the layers have dispersed from the GO structure. In other words, the reduction procedure successfully worked, and reduced graphene oxide was produced. Lastly, when compared with other studies in the literature (Abid et al., 2018; Chong et al., 2015; Chung et al., 2012; Kant Upadhyay et al., n.d.; Krishnamoorthy et al., 2013; Lesiak et al., 2021; Sieradzka et al., 2020; Surekha et al., 2020; Thakur & Karak, 2015), the XRD analysis results of GO and rGO structures obtained as a result of chemical oxidation such as the Hummer method and subsequent reduction using chemical agents (such as L-ascorbic acid and hydrazine) are similar to those in this study.

Table 4.1. Some calculations based on the XRD analysis of Gr, GO and rGO. (Abbrevation; FWHM: Full Width Half Maximum)

	Diffraction Peak (2θ)	**FWHM**	**Particle Size (nm)**	**D-Spacing (nm)**	**No of Layer**
Gr	25.7	0.272	30.41	0.34	88.89
GO	9.82	1.94	20.76	0.9	22.14
rGO	24.93	8.21	0.97	0.35	3.73

The values of the full width half maximum (FWHM), particle size, d-spacing, and number of layers found by Bragg's (4.1, 4.2) and Scherrer's (4.3) equations are given in Table 4.1. the d-spacing values of Gr, GO, and rGO samples were determined using Bragg's equation (Sieradzka et al., 2020);

$$n\lambda = 2dsin\theta \tag{4.1}$$

where n is an integer; λ, the wavelength; d, the interlayer spacing and θ, the scattering angle. In addition, the following equation was used to calculate the layer numbers of Gr, GO, and rGO samples.

$$N = \frac{D}{d} + 1 \tag{4.2}$$

where D is size of crystallites, d is the interlayer distance and N is an average number of the layer. The crystallite size of the samples was found by using Scherrer's equation;

$$D = \frac{K\lambda}{\beta cos\theta} \tag{4.3}$$

where D, an average crystallite size; *K*, constant; λ (0.154 nm), the wavelength of incident X-Rays; β, the Full Width Half Maximum (FWHM) in Radius; θ, the Bragg angle in Radius.

Examining the numbers for particle sizes and layer counts in **Table 4.1** reveals that they drop when the graphite form transforms into a reduced graphene oxide structure. This decrease is normal in terms of the method used and is desired for this study (Gürer et al., 2022). Because the few layers of the rGO structure allow the electrical conductivity to be high and the designed device to work more sensitively. On the other hand, the small particle size increases the surface area in the sensitive part of the GFET, and because of this increase the the retention rate of bioreagent (Cai et al., 2022; Ciou et al., 2023; Kireev et al., 2017; Lerner et al., 2017; Liang et al., 2015; Trung et al., 2014; M. Yang et al., 2010). As a conclude, the Hummer method was successfully applied, and rGO with the desired size and number of layers was produced.

4.1.2 Fourier Transformation Infrared Spectroscopy (FTIR) Analysis

The Fourier Transform Infrared Spectroscopy (FTIR) results of Gr, GO, and rGO samples were obtained with the Perkin Elmer Spectrum Two FTIR-ATR spectrophotometer in BAIBU. The FTIR peaks of the samples are given in **Figure 4.2**. The spectrum of pristine graphite does not show any obvious vibration peaks (Chang et al., 2013; Shengtao et al., 2011; Ţucureanu et al., 2016). This is because the crystal structure of graphite has a 2-dimensional structure with layers of hexagonal rings of carbon atoms with sp^2 hybridization and no functional groups between these layers (Ţucureanu et al., 2016).

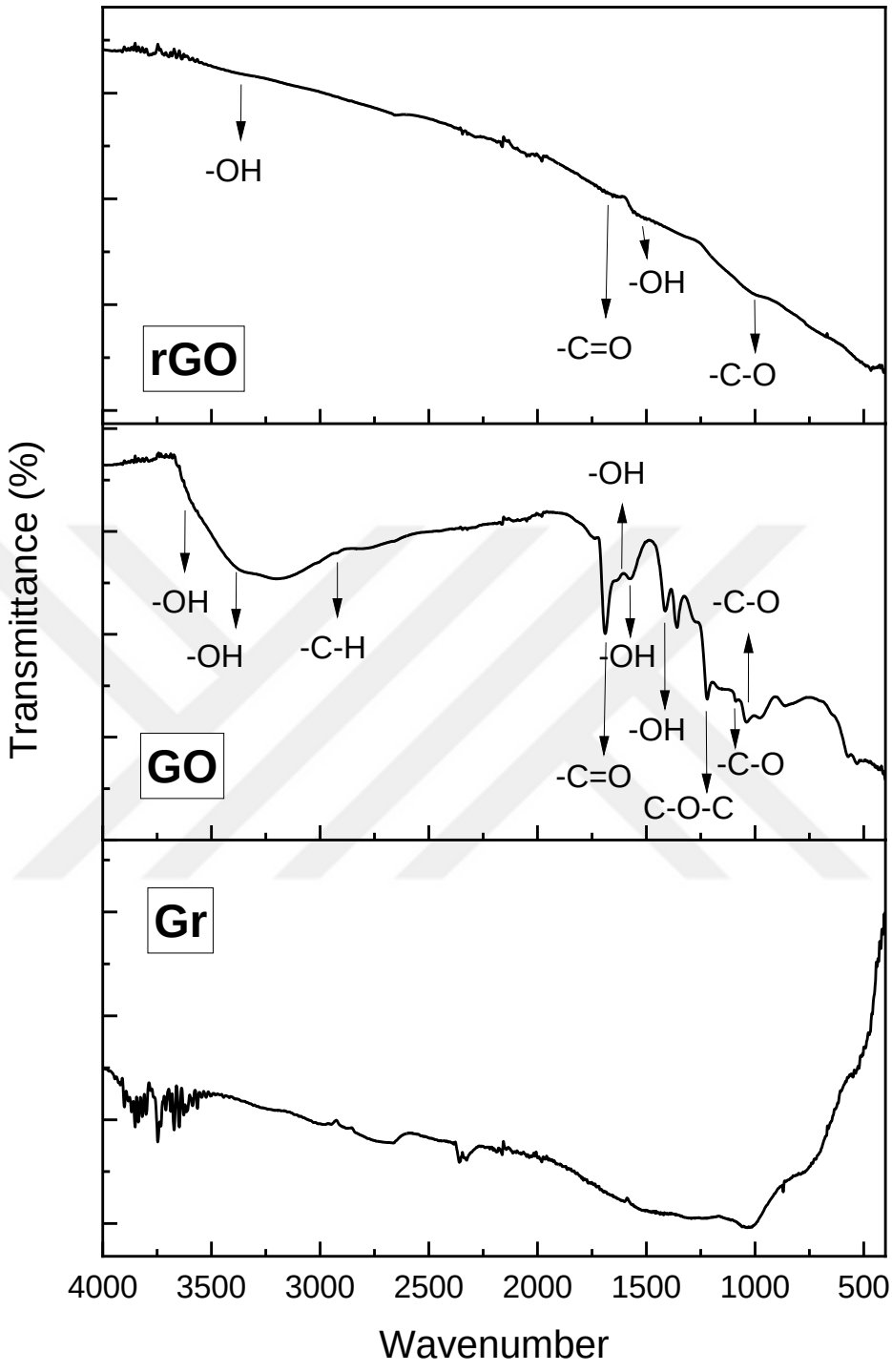

Figure 4.2 FTIR spectrum of Gr, GO, and rGO

Figure 4.2 shows the FTIR spectrum of GO. The peaks belonging to GO and the functional groups incorporated into the graphite structure as a result of the oxidation process are seen (**Table 4.2**). The main characteristics of GO spectra are the stretching bands at 1690 cm^{-1} (Chhabra et al., 2012) and 1600 cm^{-1} (Thakur &

Karak, 2015) attributed to carboxyl groups (C=O), vibration bands at 1280 cm^{-1} (Zahed & Hosseini-Monfared, 2015) atributed to epoxy bonds (C-O-C), and stretching bands for C-O bonds from COOH at 1350 cm^{-1} (Dou et al., 2014), 1080 cm^{-1} (Ban et al., 2012) and 1060 cm^{-1} (Jahanshahi et al., n.d.). The characteristic peaks for OH (hydroxyl) groups appear at 3600 cm^{-1} and 3400 cm^{-1} (the stretching mode) (Obreja et al., 2013; Ţucureanu et al., 2016), and 1620 cm^{-1} and 1547 cm^{-1} (the bending mode) (W. Gao, n.d.; Obreja et al., 2013; Ţucureanu et al., 2016), 1410 cm^{-1} and 1340 cm^{-1} (Kumar et al., 2013; Russo et al., 2013). This analysis shows that the oxidation process caused the destruction of the original extended conjugated π-orbital system in the graphite structure. Moreover, this allowed the CO groups to settle into the graphite carbon skeletal structure (Chang et al., 2013; Obreja et al., 2013; Ţucureanu et al., 2016). In the FTIR spectra of rGO, after the chemical reduction process, although no sharp peaks of CO can be observed, there are peaks of C=O stretching at 1600 cm^{-1}, and C-O stretching at 1060 cm^{-1} (Ban et al., 2012; Obreja et al., 2013; Ţucureanu et al., 2016) . The bands at 3400 cm^{-1} and 1557 cm^{-1} are attributed to the hydroxyl groups. The prominence of the OH peaks decreased significantly, and some of them even disappeared completely (Dou et al., 2014; W. Gao, n.d.; Kumar et al., 2013; Ţucureanu et al., 2016). This is evidence that the reduction process is successful and also shows a result in agreement with the XRD analysis.

Table 4.2. The FTIR peaks of Graphene Oxide (GO)

Wavenumber [cm-1]	***Probable assignment***	***Characteristic vibration mode***
3600	(O–H)	GO, hydroxyl (OH) groups from C–OH group
3400	(O–H)	GO, OH groups from C–OH group or water molecule
1690	(C=O)	General assignments, –COOH group
1620	(H-O-H)	GO, OH groups from water molecule
1600	(C=O)	General assignments, –COOH group
1573	(O–H)	GO, OH group
1410	(O–H or C–OH)	GO, OH group
1350	(C–O)	GO
1340	(O–H)	GO, OH group
1280	(C–O)	GO, epoxy (–C–O–C–) group
1080	(C–O)	GO, carboxyl (–COOH) or alkoxy (–O–) group
1060	(C–O)	GO, carboxyl (–COOH) or alkoxy (–O–) group

4.1.3 Raman Spectroscopy Analysis of Reduced Graphene Oxide

Raman spectroscopy was used in this study because it is a very powerful analysis to study the microstructure of materials (Abid et al., 2018; Jahanshahi et al., n.d.; Zahed & Hosseini-Monfared, 2015). The Raman spectroscopy measurement of synthesized rGO was performed in the METU Center Laboratory in the range between 125-4000 Raman shifts with a 532 nm edge laser. The Raman spectra of rGO usually consist of two very strong optical peaks (*D* and *G*) and one (*2D*) or two (*2D+D*) peaks with relatively weak intensity (**Figure 4.3**) (Chhabra et al., 2012; Gouadec & Colomban, 2007; Jahanshahi et al., n.d.; Obreja et al., 2013; Russo et al., 2013; Sieradzka et al., 2020; Zahed & Hosseini-Monfared, 2015). While the *D band*, located at 1345 cm^{-1} (Table 4.3) in spectrum, is related to the size of the in-plane sp^2 domains, its enlargement denotes the formation of more sp^2 domains (W. Gao, n.d.; Gouadec & Colomban, 2007; Jahanshahi et al., n.d.; Zahed & Hosseini-Monfared, 2015). The *G band* at 1577 cm^{-1} (Table 4.3) also indicates in-plane vibrations of carbon atoms of sp^2 hybridization (Abid et al., 2018; Chang et al., 2013; Gouadec & Colomban, 2007; Sieradzka et al., 2020; Zahed & Hosseini-Monfared, 2015). Moreover, the *2D band* at 2702 cm^{-1} (Table 4.3) is about that calculating the number of layers for rGO using the shape, width, and position of this peak (Abid et al., 2018; Chang et al., 2013; Chong et al., 2015; Gouadec & Colomban, 2007; Krishnamoorthy et al., 2013; Kumar et al., 2013; Sieradzka et al., 2020). In this study, the ratio of D and G peaks intensity (I_D/I_G) indicates a change in the size of the in-plane sp^2 fields after the reduction process. This ration was calculated as "1.11" in this work. In other words, more defects have formed in the rGO structure (Abid et al., 2018; Chang et al., 2013; W. Gao, n.d.; Gouadec & Colomban, 2007; Krishnamoorthy et al., 2013; Sieradzka et al., 2020). These defects in the rGO structure are caused by the chemical agent (L-ascobic acid) used in the reduction process and the ultrasonic treatment used after this process in order to ensure a homogeneous dispersion in DI water (Chang et al., 2013; Kumar et al., 2013; Sieradzka et al., 2020).

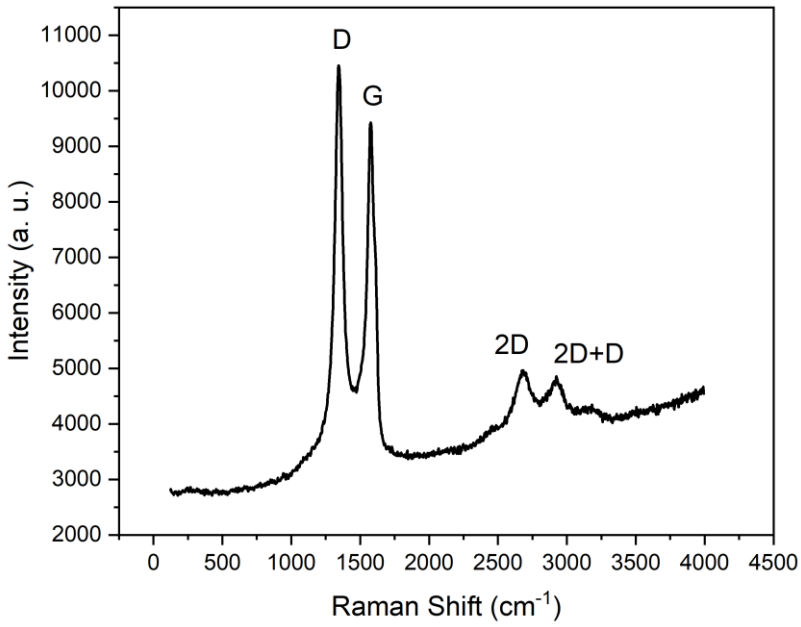

Figure 4.3 The Raman spectrum of Reduced Graphene Oxide.

So as to calculate the number of rGO layers, the ratio of I_{2D}/I_G was used, and it was found to be "0.52". This result shows that the synthesized rGO has a few layers structure (Al-Amin et al., 2016; Ciou et al., 2023; Ordonez et al., 2017). In terms of the number of layers, the calculation result was consistent with the XRD analysis result.

As a consequence, the defects in the structure of rGO and its few layered structures show that oxidation and reduction processes are successfully applied. Such properties of rGO will provide important advantages for biosensor applications. Because its defects will facilitate the attachment of bio-receptors to the structure, there will be no need to use immobilization agents. In addition, the few layers of structure will increase the electrical conductivity of the biosensor (Al-Amin et al., 2016; Cai et al., 2022; Ciou et al., 2023; Novodchuk et al., 2021; Ordonez et al., 2017; Syu et al., 2018; Trung et al., 2014; S. Wang et al., 2022).

Table 4.3. The intensity values and peaks positions of rGO Raman spectrum.

Map Name	*Raman Shift (cm^{-1})*	*Intensity*
D Band	1345	10478
G Band	1577	9429

2D Band	2702	4924
D+D' band	2923	4856

4.1.4 TEM image of Reduced Graphene Oxide

Transmision electron microscopy (TEM) imaging of synthesized rGO was performed in the METU Center Laboratory. The rGO structures were imaged in flake form (Figure 4.4). Owing to the ultrasonic treatment (Deshmukh et al., 2020), the number of the layers cannot be clearly determined in TEM images as the rGO flakes are crumpled, (wrinkled structure) and twisted on themselves (Figure 4.4c, d)(Husnah et al., 2017; Jayachandiran et al., 2018) However, another reason for this is that rGO flakes are transparent (Figure 4.4c). This transparency feature proves that the number of layers of the flakes is few rather than multilayered (Chithaiah et al., 2020; Deshmukh et al., 2020; Husnah et al., 2017; Jayachandiran et al., 2018; Mohan et al., 2015). As a result, TEM images support, albeit relatively, that the synthesized rGO has a few layer of structure, as indicated by the results of Raman and XRD analyses.

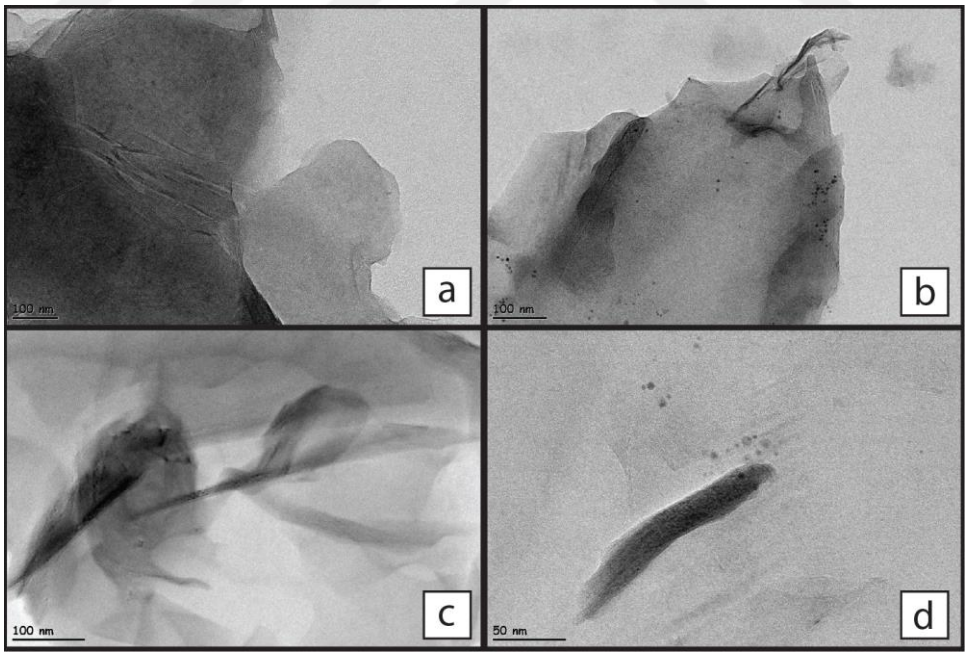

Figure 4.4 The TEM imaging of Reduced Graphene Oxide flakes.

4.2 The Results of Electrical Measurement of GFET based Biosensors

In this part of the study, the electrical measurements of the GFET based biosensor are investigated. The results of the output characteristics and transfer characteristics of the device are compared with similar studies in the literature. The results are described in detail below.

4.2.1 Results of GFET's output characteristics

The graphs in Figure 4.5 show the output characteristic results of the GFET biosensor fabricated with different sizes of the sensory field. The measurement results show that the linearity of the Id-Vds curve shows that the rGO layer between the source and drain electrodes makes good ohmic contact with the electrodes, and at the same time, the current flows continuously between the electrodes. This result proves that the fabricated device works. It is proved that the result obtained is compatible with the studies in the literature (de Moraes & Kubota, 2016a; Fu et al., 2017; Ghany et al., 2017; Yan et al., 2017). Moreover, it was observed that with the increase in the W/L dimensions of the GFET structure, the current flowing between the source and the current increased. This can be explained by the increase in the amount of RGO coated in this way. However, in order for the manufactured devices to be portable, their dimensions must be reduced. This situation constitutes an obstacle to miniaturization (Martins et al., 2021; Matsumoto et al., 2014; X. Wu et al., 2018). Improvements need to be made in terms of production constraints. But as a result, it can be said that the devices produced work. Among the devices, the one with an L length of 2 mm was preferred for further measurements.

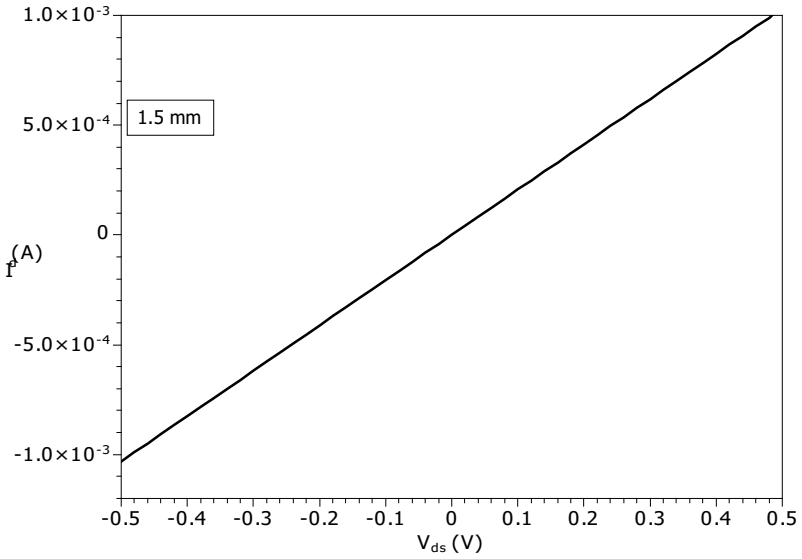
1.0×10⁻³
5.0×10⁻⁴
0
-5.0×10⁻⁴
-1.0×10⁻³
I (A)
1.5 mm
-0.5 -0.4 -0.3 -0.2 -0.1 0 0.1 0.2 0.3 0.4 0.5
V_ds (V)

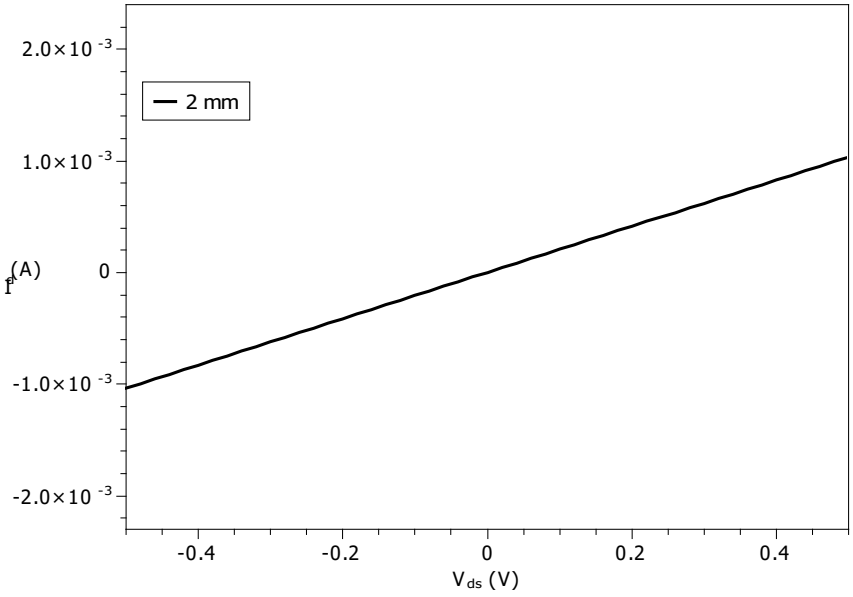
2.0×10⁻³
1.0×10⁻³
0
-1.0×10⁻³
-2.0×10⁻³
I (A)
2 mm
-0.4 -0.2 0 0.2 0.4
V_ds (V)

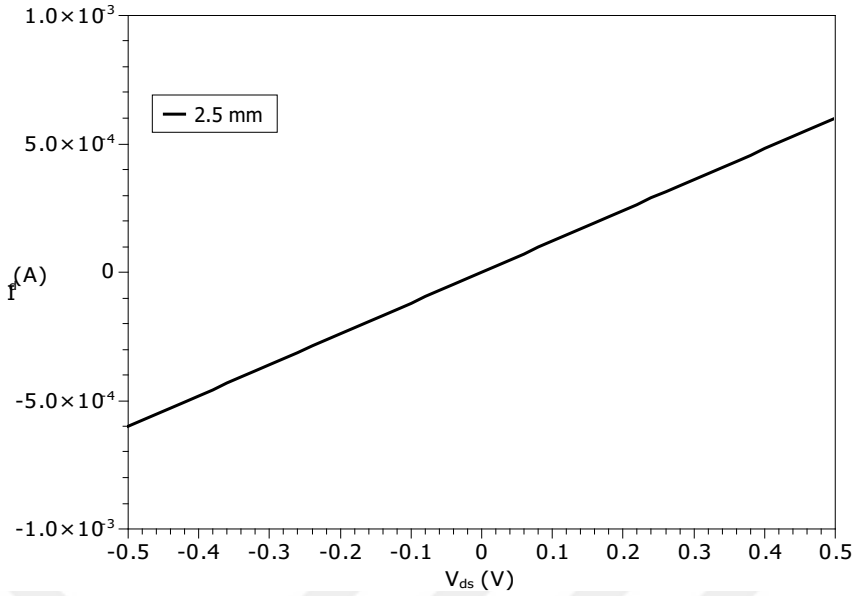

Figure 4.5 The graphs of I_d-V_{ds} characteristic of GFET structure

4.2.2 I-V measurements depending on pH change

In order to determine the transfer characteristics of the GFET transistor, Id-Vgs was first measured by applying a solution (DI water, pH:7) to the ion host. When the graph in Figure 4.6 is analyzed, it is observed that the fabricated GFET shows an ambipolar characteristic. Ambipolar characteristic means that the semiconductor device has the capacity to conduct electrons and holes without changing the channel doping or contact material. Moreover, it can be seen from this graph that the Dirac point voltages of the device are on the positive side. This result means that the rGO layer is p-doped. This means that the hole concentration is higher than the electron concentration. rGO is a p-doped material because it is produced by chemical synthesis.

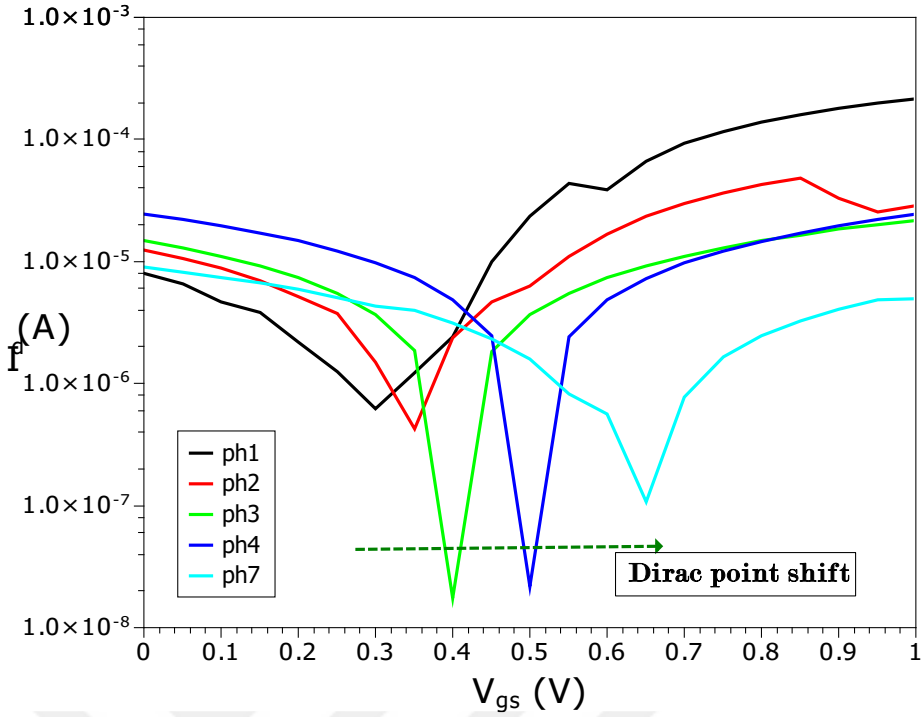

Figure 4.6 The I_d-V_{gs} graphic of GFET with different pH concentration

In addition, in measurements taken with an ionic solution with a pH ranging from 1 to 7, the Dirac point shifts to the right as the pH approaches 7. This can be attributed to the increase of OH ions in the solution and their interaction with the rGO layer. Another piece of information is that the defect structure of the rGO layer allows the chemisorption of OH ions. The fact that the shift in this Dirac point voltage is linear and the R squared value is high suggests that this device is suitable for testing biological analytes.

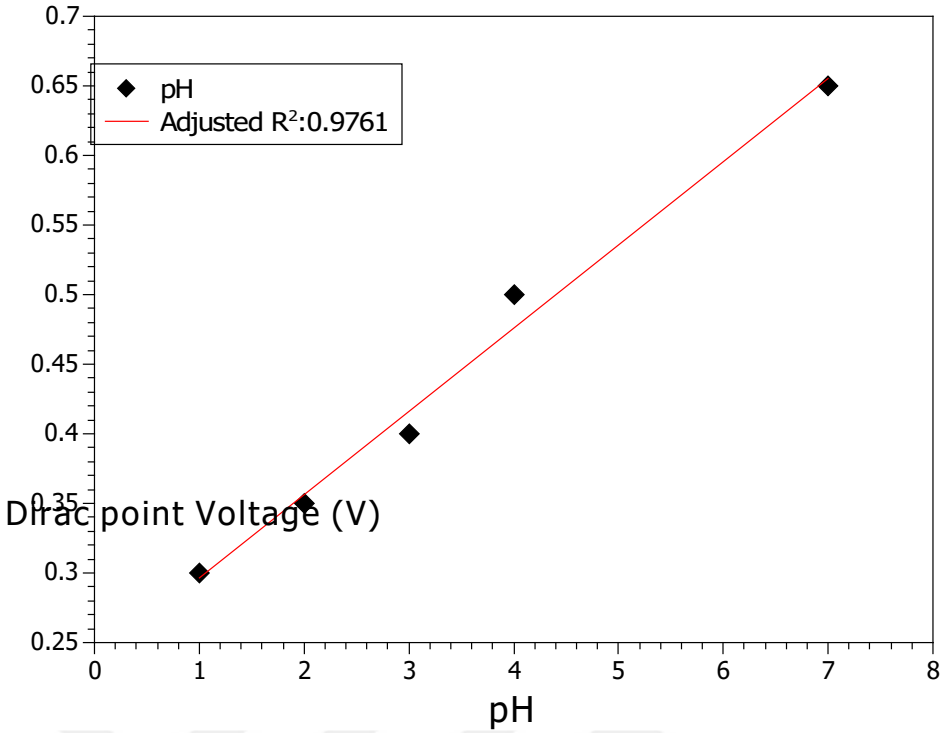

Figure 4.7 The graph of GFETs dirac point voltage depend on pH concentration.

4.2.3 The Id-Vgs measurament of GFET with miR-1268b and miR-6075

The suitability of the GFET biosensor for biological diagnostics was tested by pH experiments. The measurements showed that the device is suitable for biosensor applications. In this phase of the study, the immobilization of biomarkers was tested by an electrical method.

Immobilization studies are performed by first incorporating the counterpart of the material to be detected by a biosensor into the rGO structure. These materials include antibodies, proteins, and nucleic acids. Immobilization techniques are classified into two groups: covalent and non-covalent binding. In covalent binding, the biomolecules of the target of interest are functionalized on the rGO surface via binding materials such as amino groups (-NH2), carboxyl groups (-COOH), or epoxide groups (-O). However, this binding material leads to structural changes in rGO (de Moraes & Kubota, 2016b; Fu et al., 2017; Ivnitski et al., 1999; Martins et al., 2021; Putzbach & Ronkainen, 2013; Tu et al., 2018).

The linker molecules most widely utilized in GFET biosensors are PBASE (1-Pyrene Butyric Acid N-hydroxysuccinimide Ester) and APTES ((3-Aminopropyl) triethoxysilane) (Castellarnau et al., 2008; Kulkarni et al., 2022;

Putzbach & Ronkainen, 2013). For non-covalent binding, physical adsorption is mostly preferable. Physical adsorption of biomolecules interacts with rGO by means such as electrostatic forces, π-π stacking, or van der Waals interactions. In this study, we immobilized anti-miR-1268b and anti-miR-6075 sequence (probe sequence) structures for early diagnosis of lung cancer due to the properties of rGO. In this study, the functionalization of miRNAs was realized on rGO without using any other material. The study by Cai et al. also showed that miRNA sequences can be directly immobilized on rGO sheets (Cai et al., 2022).

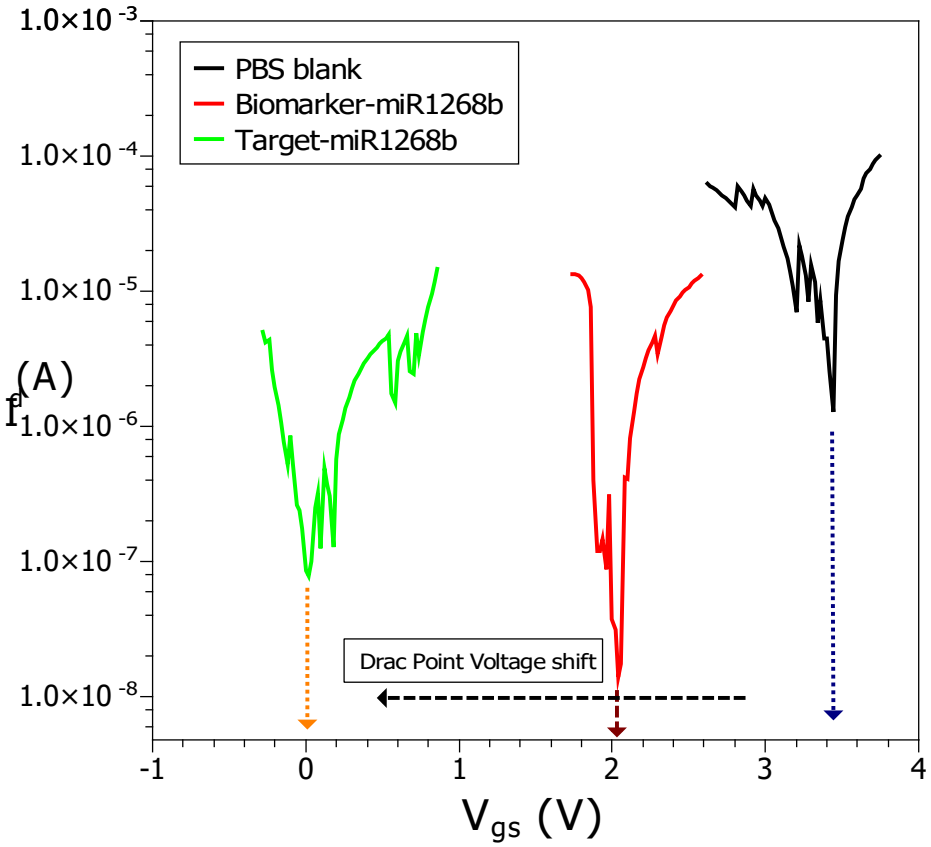

Figure 4.8 The I_d-V_{gs} graph after hybridization between probe sequence and miRNA-1268b sequence.

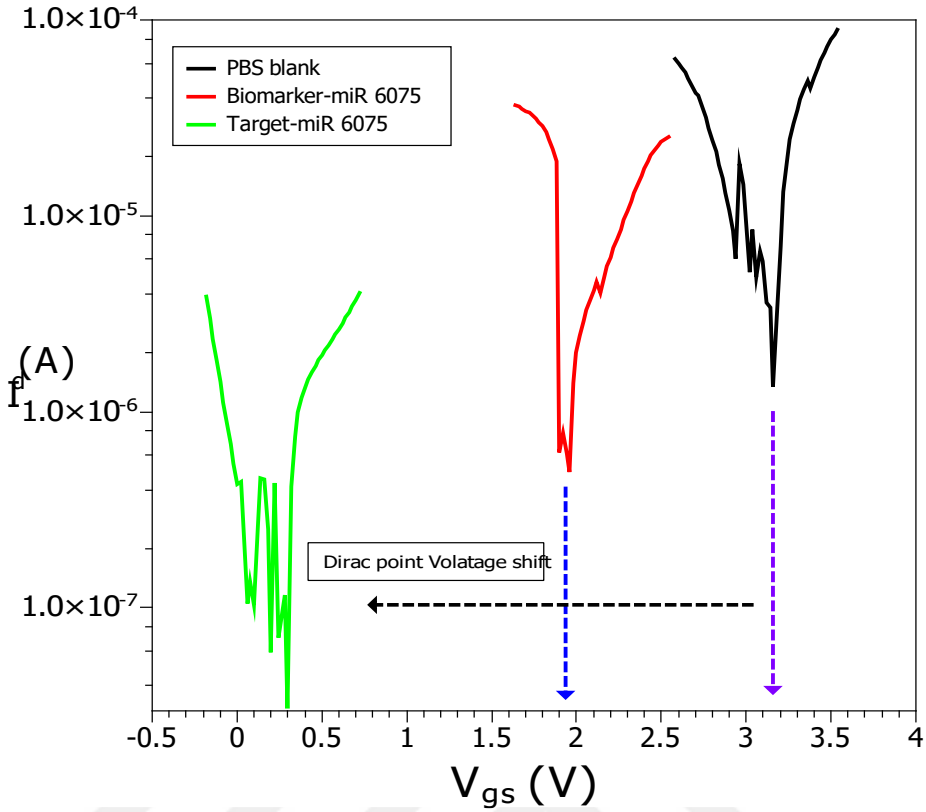

Figure 4.9 The I_d-V_{gs} graph after hybridization between probe sequence and miRNA-6075 sequence.

Initially, a blank measurement with PBS solution was taken with the rGO-FET biosensor device. The Dirac point voltage was determined to be 3.44 V and 3.16 V, respectively (Figures 4.8 and 4.9). Then, the probe sequences of miR-1268b and miR-6075 were immobilized on the rGO surface. After hybridization of the probe sequences and miRNAs, the Id-Vgs transfer characteristics of the GFET biosensor were plotted. As seen in the graph (Figures 4.8 and 4.9), the Dirac point shifts to the left side due to the hybridization between the probes and miRNA sequences. This shift also provides information about the conjugation between the probe sequences and miRNAs. Therefore, while the Dirac point voltages were observed as "2.04 V and 1.96 V" before conjugation, they were determined as "0.30 V and 0.10 V" immediately after conjugation. These voltage shifts initially indicate an electrostatic effect on the rGO structure, while during the measurement, the PBS solution containing miRNA was used to functionalize the rGO. Since the synthesized rGO exhibits p-doped properties (Béraud et al., 2021; Seo et al., 2020; X. Wu et al., 2018), however, the PBS solution brings positive charges to the rGO, causing a shift in the Dirac point voltage (N. Gao et al., 2016; Khatri & Puri, 2022).

Second, it is reported that due to the negative charges on miRNAs, the electron concentration in the rGO detection area increases and a leftward shift is observed (Kybert et al., 2014; Son et al., 2016; Syu et al., 2018). The third is the effect of adding extra capacitance, which we measured in the GFET biosensor device first with PBS and then with biomarkers, probes, and miRNAs conjugation (Kwong Hong Tsang et al., 2019; Lerner et al., 2017; Mansouri Majd & Salimi, 2018; Syu et al., 2018). Every time, we have introduced solutions into the rGO sensing area, which may result in additional capacitance in the GFET biosensor device. Therefore, the n-doping effect by PBS and arrays causes a leftward shift (Kireev et al., 2017; Leyden et al., 2010; Vaziri, 2011).

4.2.4 Specificity and Sensivity of GFET Biosensor

The ability of a reduced graphene oxide (rGO) field effect transistor (FET) biosensor to selectively detect a specific target analyte and discriminate it from other compatible compounds present in a sample is referred to as “specificity” (Mansouri Majd & Salimi, 2018). It is very important for biosensors to assure sensitive and reliable detection. To do so, the non-complementary sequence (miR-99a-5a) was deposited on the rGO, which was functionalized with the probe sequence matching the miRNA-1268b and miR-6075 sequences. As seen in Figure 4.10, the Delta Dirac point voltage showed no change as expected. The cause of this result is the lack of any binding with the probe sequences and the mismatch sequence (Fu et al., 2017; Jacobs et al., 2010), which clarifies that the selected probe sequence is unique only to the miRNA-1268b and miR-6075 sequences (Asakura et al., 2020). These insignificant shifts can be explained by the non-specific binding of the miRNA-1268b and miR-6075 probe sequences and the non-complementary probe sequences. The specificity of a reduced graphene oxide (rGO) field-effect transistor (FET) biosensor expresses its capability to detect and selectively distinguish a specific target analyte from other substances present in a sample. It is an essential characteristic of biosensors to provide accurate and reliable detection.

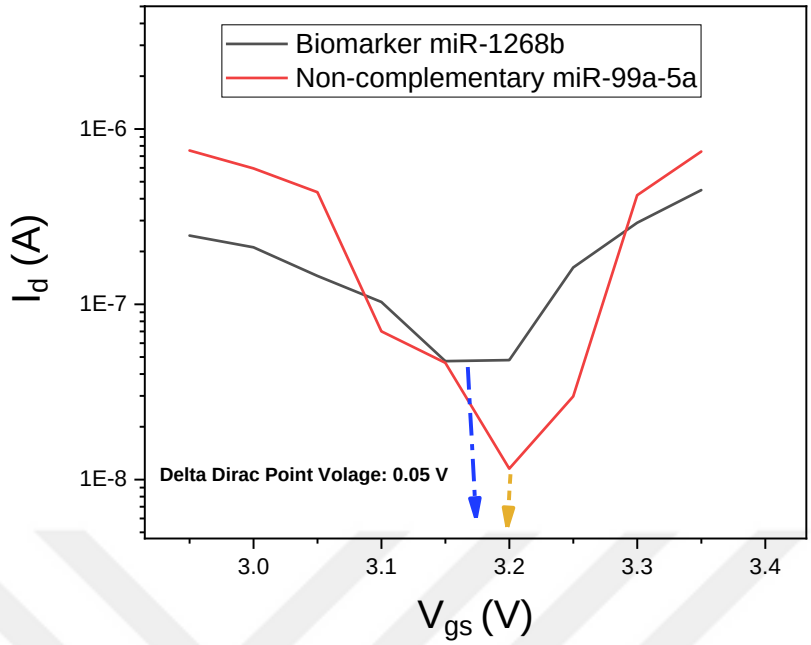

Figure 4.10 The Id-Vgs graph of GFET with non-complementary biomolecules.

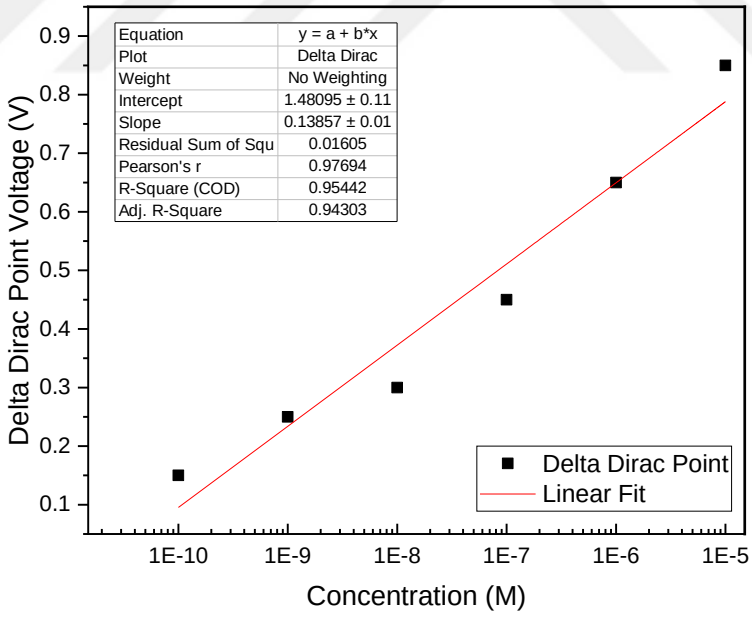

Figure 4.11 The Delta Dirac Point Voltage values of GFET depend on from 100pM to 10µM concentration.

The sensitivity of a GFET biosensor refers to its ability to recognize and measure small changes in the concentration or presence of the target analyte. It is a

critical metric that determines the detection threshold and the biosensor's ability to operate accurately and reliably. To determine the sensitivity of the fabricated GFET device, various concentrations of miRNA-1268b and miR-6075 arrays were prepared. The concentrations of the solution prepared with miRNA arrays were as follows; 10 μM, 1 μM, 100 nM and 100 pM. As can be seen in Figure 4.11, the Delta Dirac point voltage shifts towards lower voltages as the concentration increases. This phenomenon is due to the negative particles in the solutions. The miRNAs at various concentrations interacted effectively with graphene and created an n-doping effect based on reduced graphene oxide-nucleotide interaction. It was also observed that the current values changed during the measurement. The reasons behind the variation of current values are different possible factors, such as impurities in the solutions, temperature and humidity, and defects in the rGO layer. In this study, the lowest detectable limit of detection (LOD) was found to be 100 pM. In addition, it is important to note that a number of variables, such as surface functionalization, temperature, pH, and the complexity of the sample matrix, can affect how sensitive rGO FET biosensors are. Therefore, extensive characterization and tuning are required to achieve the optimum sensitivity for a given application.

5. CONCLUSIONS AND RECOMMENDATIONS

In this thesis, a GFET based biosensor that can detect lung cancer and metastasis at an early stage is aimed at and realized. The study first started with the screening of the FET structure, and a master mask was made from acetate paper. Then the FET structure was fabricated on a Si/SiO_2 substrate using the procedure of conventional semiconductor fabrication technology. Then, the reduced graphene oxide to be used in the substrate region was fabricated from graphite material with reference to the Hummer method. Subsequently, the rGO material was integrated into the FET structure to evolve the FET structure into a GFET structure. Lung cancer-specific miRNAs (miR-1268b and miR-6075) and their complements were obtained from the literature. The miRNAs were used as cancer-specific biomarkers in this study. As a final step, electrical measurements of the GFET biosensor were successfully performed.

When the measurement results of the device were analyzed, it showed a positive response to pH experiments. In other words, a linear result was detected in the I-V graph depending on the changing pH. Again, in the analyte measurements with biomarkers, there were significant shifts in the Dirac points observed in the I-V graph due to the presence of bioanalytes. This shows that the selectivity of the device is good. In the limit of detection measurements, the device responded in the order of 100 pM. In conclusion, a candidate biosensor for early detection of lung cancer has been fabricated in this study. However, in order for the GFET-based biosensor to be a usable device, there are aspects that need to be improved, such as the design and the rGO channel dimensions. Future studies will focus on these issues.

6. REFERENCES

"APA citation system was used in this thesis."

Abdi, D. B., & Kumar, M. J. (2015). Dielectric modulated overlapping gate-on-drain tunnel-FET as a label-free biosensor. *Superlattices and Microstructures*, *86*, 198–202. https://doi.org/10.1016/j.spmi.2015.07.052

Abdolhosseinzadeh, S., Asgharzadeh, H., & Kim, H. S. (2015). Fast and fully-scalable synthesis of reduced graphene oxide. *Scientific Reports*, *5*, 1–7. https://doi.org/10.1038/srep10160

Abid, Sehrawat, P., Islam, S. S., Mishra, P., & Ahmad, S. (2018). Reduced graphene oxide (rGO) based wideband optical sensor and the role of Temperature, Defect States and Quantum Efficiency. *Scientific Reports*, *8*(1). https://doi.org/10.1038/s41598-018-21686-2

Adley, C. C., & Ryan, M. P. (2015). Conductometric biosensors for high throughput screening of pathogens in food. In *High Throughput Screening for Food Safety Assessment: Biosensor Technologies, Hyperspectral Imaging and Practical Applications* (pp. 315–326). Elsevier Inc. https://doi.org/10.1016/B978-0-85709-801-6.00014-9

Afzalian, A., Colinge, J. P., & Flandre, D. (2011). Physics of Gate Modulated Resonant Tunneling (RT)-FETs: Multi-barrier MOSFET for steep slope and high on-current. *Solid-State Electronics*, *59*(1), 50–61. https://doi.org/10.1016/j.sse.2011.01.016

Akter, R., Kyun Rhee, C., & Rahman, M. A. (2013). A stable and sensitive voltammetric immunosensor based on a new non-enzymatic label. *Biosensors and Bioelectronics*, *50*, 118–124. https://doi.org/10.1016/j.bios.2013.06.016

Al-Amin, C., Karabiyik, M., & Pala, N. (2016). Fabrication of Graphene Field-effect Transistor with Field Controlling Electrodes to improve fT. *Microelectronic Engineering*, *164*, 71–74. https://doi.org/10.1016/j.mee.2016.07.011

Alinejadian, N., Kazemi, S. H., Nasirpouri, F., & Odnevall, I. (2023). Electro-deposited nano-Ni/reduced graphene oxide composite film of corrugated surface for high voltammetric sensitivity. *Materials Chemistry and Physics*, *297*. https://doi.org/10.1016/j.matchemphys.2022.127288

Antiochia, R. (2022). Electrochemical biosensors for SARS-CoV-2 detection: Voltametric or impedimetric transduction? In *Bioelectrochemistry* (Vol. 147). Elsevier B.V. https://doi.org/10.1016/j.bioelechem.2022.108190

Asakura, K., Kadota, T., Matsuzaki, J., Yoshida, Y., Yamamoto, Y., Nakagawa, K., Takizawa, S., Aoki, Y., Nakamura, E., Miura, J., Sakamoto, H., Kato, K., Watanabe, S. ichi, & Ochiya, T. (2020). A miRNA-based diagnostic model predicts resectable lung cancer in humans with high accuracy. *Communications Biology*, *3*(1), 2–6. https://doi.org/10.1038/s42003-020-0863-y

Baccar, H., Mejri, M. B., Hafaiedh, I., Ktari, T., Aouni, M., & Abdelghani, A. (2010). Surface plasmon resonance immunosensor for bacteria detection. *Talanta*, *82*(2), 810–814. https://doi.org/10.1016/j.talanta.2010.05.060

Bahadir, E. B., & Sezgintürk, M. K. (2015). Electrochemical biosensors for hormone analyses. In *Biosensors and Bioelectronics* (Vol. 68, pp. 62–71). Elsevier Ltd. https://doi.org/10.1016/j.bios.2014.12.054

Bahri, M., Shi, B., Djebbi, K., Elaguech, M. A., Zhou, D., Ben Ali, M., Tlili, C., & Wang, D. (2021). Toward clean and crackless polymer-assisted transfer of CVD-grown graphene and its recent advances in GFET-based biosensors. In *Materials Today Chemistry* (Vol. 22). Elsevier Ltd. https://doi.org/10.1016/j.mtchem.2021.100578

Ban, F. Y., Majid, S. R., Huang, N. M., & Lim, H. N. (2012). Graphene Oxide and Its Electrochemical Performance. In *Int. J. Electrochem. Sci* (Vol. 7). www.electrochemsci.org

Ben Halima, H., Bellagambi, F. G., Alcacer, A., Pfeiffer, N., Heuberger, A., Hangouët, M., Zine, N., Bausells, J., Elaissari, A., & Errachid, A. (2021). A silicon nitride ISFET based immunosensor for tumor necrosis factor-alpha detection in saliva. A promising tool for heart failure monitoring. *Analytica Chimica Acta*, *1161*. https://doi.org/10.1016/j.aca.2021.338468

Béraud, A., Sauvage, M., Bazán, C. M., Tie, M., Bencherif, A., & Bouilly, D. (2021). Graphene field-effect transistors as bioanalytical sensors: Design, operation and performance. *Analyst*, *146*(2), 403–428. https://doi.org/10.1039/d0an01661f

Bhalla, N., Jolly, P., Formisano, N., & Estrela, P. (2016). Introduction to biosensors. *Essays in Biochemistry*, *60*(1), 1–8. https://doi.org/10.1042/EBC20150001

Blair, E. O., & Corrigan, D. K. (2019). A review of microfabricated electrochemical biosensors for DNA detection. In *Biosensors and Bioelectronics* (Vol. 134, pp. 57–67). Elsevier Ltd. https://doi.org/10.1016/j.bios.2019.03.055

Bollella, P., & Gorton, L. (2018). Enzyme based amperometric biosensors. In *Current Opinion in Electrochemistry* (Vol. 10, pp. 157–173). Elsevier B.V. https://doi.org/10.1016/j.coelec.2018.06.003

Bonanni, A., Loo, A. H., & Pumera, M. (2012). Graphene for impedimetric biosensing. In *TrAC - Trends in Analytical Chemistry* (Vol. 37, pp. 12–21). https://doi.org/10.1016/j.trac.2012.02.011

Borisov, S. M., & Wolfbeis, O. S. (2008). Optical biosensors. In *Chemical Reviews* (Vol. 108, Issue 2, pp. 423–461). https://doi.org/10.1021/cr068105t

Bray, F., Ferlay, J., Soerjomataram, I., Siegel, R. L., Torre, L. A., & Jemal, A. (2018). Global cancer statistics 2018: GLOBOCAN estimates of incidence and mortality worldwide for 36 cancers in 185 countries. *CA: A Cancer Journal for Clinicians*, *68*(6), 394–424. https://doi.org/10.3322/caac.21492

Burghard, M., Klauk, H., & Kern, K. (2009). Carbon-based field-effect transistors for nanoelectronics. In *Advanced Materials* (Vol. 21, Issues 25–26, pp. 2586–2600). https://doi.org/10.1002/adma.200803582

Cai, B., Xia, Z., Wang, J., Wu, S., & Jin, X. (2022). Reduced Graphene Oxide-Based Field Effect Transistor Biosensors for High-Sensitivity miRNA21 Detection. *ACS Applied Nano Materials*, *5*(8), 12035–12044. https://doi.org/10.1021/acsanm.2c03372

Carlsen, K., Jensen, A. B., Jacobsen, E., Krasnik, M., & Johansen, C. (2005). Psychosocial aspects of lung cancer. In *Lung Cancer* (Vol. 47, Issue 3, pp. 293–300). Elsevier Ireland Ltd. https://doi.org/10.1016/j.lungcan.2004.08.002

Carvalho, A. F., Kulyk, B., Fernandes, A. J. S., Fortunato, E., & Costa, F. M. (2022). A Review on the Applications of Graphene in Mechanical Transduction. In *Advanced Materials* (Vol. 34, Issue 8). John Wiley and Sons Inc. https://doi.org/10.1002/adma.202101326

Castellarnau, M., Zine, N., Bausells, J., Madrid, C., Juárez, A., Samitier, J., & Errachid, A. (2007). Integrated cell positioning and cell-based ISFET biosensors. *Sensors and Actuators, B: Chemical*, *120*(2), 615–620. https://doi.org/10.1016/j.snb.2006.01.057

Castellarnau, M., Zine, N., Bausells, J., Madrid, C., Juárez, A., Samitier, J., & Errachid, A. (2008). ISFET-based biosensor to monitor sugar metabolism in bacteria. *Materials Science and Engineering C*, *28*(5–6), 680–685. https://doi.org/10.1016/j.msec.2007.10.074

Catanante, G., Mishra, R. K., Hayat, A., & Marty, J. L. (2016). Sensitive analytical performance of folding based biosensor using methylene blue tagged aptamers. *Talanta*, *153*, 138–144. https://doi.org/10.1016/j.talanta.2016.03.004

Cesewski, E., & Johnson, B. N. (2020). Electrochemical biosensors for pathogen detection. In *Biosensors and Bioelectronics* (Vol. 159). Elsevier Ltd. https://doi.org/10.1016/j.bios.2020.112214

Chandra, P., & Nee, Y. (n.d.). *Next Generation Point- of-care Biomedical Sensors Technologies for Cancer Diagnosis*.

Chang, D. W., Lee, E. K., Park, E. Y., Yu, H., Choi, H. J., Jeon, I. Y., Sohn, G. J., Shin, D., Park, N., Oh, J. H., Dai, L., & Baek, J. B. (2013). Nitrogen-doped graphene nanoplatelets from simple solution edge-functionalization for n-type field-effect transistors. *Journal of the American Chemical Society*, *135*(24), 8981–8988. https://doi.org/10.1021/ja402555n

Charbgoo, F., Soltani, F., Taghdisi, S. M., Abnous, K., & Ramezani, M. (2016). Nanoparticles application in high sensitive aptasensor design. In *TrAC - Trends in Analytical Chemistry* (Vol. 85, pp. 85–97). Elsevier B.V. https://doi.org/10.1016/j.trac.2016.08.008

Chen, H. C., Chen, Y. T., Tsai, R. Y., Chen, M. C., Chen, S. L., Xiao, M. C., Chen, C. L., & Hua, M. Y. (2015). A sensitive and selective magnetic graphene composite-modified polycrystalline-silicon nanowire field-effect transistor for bladder cancer diagnosis. *Biosensors and Bioelectronics*, *66*, 198–207. https://doi.org/10.1016/j.bios.2014.11.019

Chen, Y., Ren, R., Pu, H., Guo, X., Chang, J., Zhou, G., Mao, S., Kron, M., & Chen, J. (2017). Field-Effect Transistor Biosensor for Rapid Detection of Ebola Antigen. *Scientific Reports*, *7*(1), 4–11. https://doi.org/10.1038/s41598-017-11387-7

Chhabra, V., Kaur, R., Kumar, R., Chhabra, V. A., & Deep, A. (2012). *Functionalization of Graphene using Carboxylation process Detection, Quantification and Classification of Insects/Eggs on Crops using Foldscope combined with smartphones. View project CSIR-CSIO View project "International Journal for Science and Emerging Technologies with Latest Trends" 4(1): 13-19 (2012) Functionalization of Graphene using Carboxylation process*. https://www.researchgate.net/publication/301794149

Chithaiah, P., Raju, M. M., Kulkarni, G. U., & Rao, C. N. R. (2020). Simple synthesis of nanosheets of rGO and nitrogenated rGO. *Beilstein Journal of Nanotechnology*, *11*, 68–75. https://doi.org/10.3762/bjnano.11.7

Chiu, N. F., Fan, S. Y., Yang, C. Du, & Huang, T. Y. (2017). Carboxyl-functionalized graphene oxide composites as SPR biosensors with enhanced sensitivity for immunoaffinity detection. *Biosensors and Bioelectronics*, *89*, 370–376. https://doi.org/10.1016/j.bios.2016.06.073

Choi, J., Jeun, M., Yuk, S. S., Park, S., Choi, J., Lee, D., Shin, H., Kim, H., Cho, I. J., Kim, S. K., Lee, S., Song, C. S., & Lee, K. H. (2019). Fully Packaged Portable Thin Film Biosensor for the Direct Detection of Highly Pathogenic Viruses from On-Site Samples. *ACS Nano*, *13*(1), 812–820. https://doi.org/10.1021/acsnano.8b08298

Chong, S. W., Lai, C. W., & Abdul Hamid, S. B. (2015). Green preparation of reduced graphene oxide using a natural reducing agent. *Ceramics International*, *41*(8), 9505–9513. https://doi.org/10.1016/j.ceramint.2015.04.008

Chua, C. K., & Pumera, M. (2014). Chemical reduction of graphene oxide: A synthetic chemistry viewpoint. *Chemical Society Reviews*, *43*(1), 291–312. https://doi.org/10.1039/c3cs60303b

Chung, C., Kim, Y., Shin, D., Ryoo, S., Hong, B. H. E. E., & Min, D. (2012). *Graphene Oxide*.

Ciou, S.-H., Hsieh, A.-H., Lin, Y.-X., Sei, J.-L., Govindasamy, M., Kuo, C.-F., & Huang, C.-H. (2023). Sensitive label-free detection of the biomarker phosphorylated tau−217 protein in Alzheimer's disease using a graphene-based solution-gated field effect transistor. *Biosensors and Bioelectronics*, *228*(February), 115174. https://doi.org/10.1016/j.bios.2023.115174

Colinge, J. P. (2004). Multiple-gate SOI MOSFETs. *Solid-State Electronics*, *48*(6), 897–905. https://doi.org/10.1016/j.sse.2003.12.020

Collins, L. G., Haines, C., Perkel, R., & Enck, R. E. (2007). *Lung Cancer: Diagnosis and Management*. http://familydoctor.org/161.xml.

Congur, G., Eksin, E., & Erdem, A. (2015). Impedimetric Detection of microRNA at Graphene Oxide Modified Sensors. *Electrochimica Acta*, *172*, 20–27. https://doi.org/10.1016/j.electacta.2015.03.210

Congur, G., & Erdem, A. (2019). PAMAM dendrimer modified screen printed electrodes for impedimetric detection of miRNA-34a. *Microchemical Journal*, *148*, 748–758. https://doi.org/10.1016/j.microc.2019.05.040

Cooper, J. A., Melloch, M. R., Singh, R., Agarwal, A., & Palmour, J. W. (2002). Status and Prospects for SiC Power MOSFETs. In *IEEE TRANSACTIONS ON ELECTRON DEVICES* (Vol. 49, Issue 4).

Coulet, P. R. (2005). Enzyme Biosensors. *Biosensors for Food Analysis*, *17*, 28–36. https://doi.org/10.1533/9781845698157.1.28

Cuartero, M., & Bakker, E. (2017). Environmental water analysis with membrane electrodes. In *Current Opinion in Electrochemistry* (Vol. 3, Issue 1, pp. 97–105). Elsevier B.V. https://doi.org/10.1016/j.coelec.2017.06.010

Curulli, A. (2021). Electrochemical biosensors in food safety: Challenges and perspectives. In *Molecules* (Vol. 26, Issue 10). MDPI AG. https://doi.org/10.3390/molecules26102940

Dacey, G. C., & Ross, I. M. (1955). The Field Effect Transistor. *Bell System Technical Journal*, *34*(6), 1149–1189. https://doi.org/10.1002/j.1538-7305.1955.tb03794.x

Del Alamo, J. A., Antoniadis, D. A., Lin, J., Lu, W., Vardi, A., & Zhao, X. (2016). Nanometer-scale III-V MOSFETs. In *IEEE Journal of the Electron Devices Society* (Vol. 4, Issue 5, pp. 205–214). Institute of Electrical and Electronics Engineers Inc. https://doi.org/10.1109/JEDS.2016.2571666

de Moraes, A. C. M., & Kubota, L. T. (2016a). Recent trends in field-effect transistors-based immunosensors. In *Chemosensors* (Vol. 4, Issue 4). MDPI Multidisciplinary Digital Publishing Institute. https://doi.org/10.3390/chemosensors4040020

de Moraes, A. C. M., & Kubota, L. T. (2016b). Recent trends in field-effect transistors-based immunosensors. In *Chemosensors* (Vol. 4, Issue 4). MDPI Multidisciplinary Digital Publishing Institute. https://doi.org/10.3390/chemosensors4040020

Dennard, R. H., Gaensslen, F. H., Yu, H.-N., Rideout, V. L., Bassous, E., & LeBlanc, A. R. (1974). Design of Ion-Implanted MOSFET's with Very Smal Physical Dimensions. *Journal of Solid-State Circuits*, *sc-9*(5), 256–268.

Deshmukh, S. P., Kale, D. P., Kar, S., Shirsath, S. R., Bhanvase, B. A., Saharan, V. K., & Sonawane, S. H. (2020). Ultrasound assisted preparation of rGO/TiO2 nanocomposite for effective photocatalytic degradation of methylene blue under sunlight. *Nano-Structures and Nano-Objects*, *21*. https://doi.org/10.1016/j.nanoso.2019.100407

Diba, F. S., Kim, S., & Lee, H. J. (2015). Amperometric bioaffinity sensing platform for avian influenza virus proteins with aptamer modified gold nanoparticles on carbon chips. *Biosensors and Bioelectronics*, *72*, 355–361. https://doi.org/10.1016/j.bios.2015.05.020

Ding, J., & Qin, W. (2020). Recent advances in potentiometric biosensors. In *TrAC - Trends in Analytical Chemistry* (Vol. 124). Elsevier B.V. https://doi.org/10.1016/j.trac.2019.115803

Dong, X., Shi, Y., Huang, W., Chen, P., & Li, L. J. (2010). Electrical detection of DNA hybridization with single-base specificity using transistors based on CVD-grown graphene sheets. *Advanced Materials*, *22*(14), 1649–1653. https://doi.org/10.1002/adma.200903645

Dou, Y. Y., Luo, M., Liang, S., Zhang, X. L., Ding, X. Y., & Liang, B. (2014). Flexible free-standing graphene-like film electrode for supercapacitors by electrophoretic deposition and electrochemical reduction. *Transactions of Nonferrous Metals Society of China (English Edition)*, *24*(5), 1425–1433. https://doi.org/10.1016/S1003-6326(14)63208-8

Dzyadevych, S., & Jaffrezic-Renault, N. (2014). Conductometric biosensors. In *Biological Identification: DNA Amplification and Sequencing, Optical Sensing, Lab-On-Chip and Portable Systems* (pp. 153–193). Elsevier Ltd. https://doi.org/10.1533/9780857099167.2.153

Eigler, S., Grimm, S., Enzelberger-Heim, M., Müller, P., & Hirscha, A. (2013). Graphene oxide: Efficiency of reducing agents. *Chemical Communications*, *49*(67), 7391–7393. https://doi.org/10.1039/c3cc43612h

Emr, S. A., & Yacynych, A. M. (1995). Use of polymer films in amperometric biosensors. In *Electroanalysis* (Vol. 7, Issue 10, pp. 913–923). https://doi.org/10.1002/elan.1140071002

Erdem, A., Ariksoysal, D. O., Karadeniz, H., Kara, P., Sengonul, A., Sayiner, A. A., & Ozsoz, M. (2005). Electrochemical genomagnetic assay for the detection of hepatitis B virus DNA in polymerase chain reaction amplicons by using disposable sensor technology. *Electrochemistry Communications*, *7*(8), 815–820. https://doi.org/10.1016/j.elecom.2005.05.006

Erdem, A., Eksin, E., & Muti, M. (2014). Chitosan-graphene oxide based aptasensor for the impedimetric detection of lysozyme. *Colloids and Surfaces B: Biointerfaces*, *115*, 205–211. https://doi.org/10.1016/j.colsurfb.2013.11.037

Evtugyn, G., & Hianik, T. (2016). Electrochemical DNA sensors and aptasensors based on electropolymerized materials and polyelectrolyte complexes. In *TrAC - Trends in Analytical Chemistry* (Vol. 79, pp. 168–178). Elsevier B.V. https://doi.org/10.1016/j.trac.2015.11.025

Fathil, M. F. M., Md Arshad, M. K., Ruslinda, A. R., Gopinath, S. C. B., Nuzaihan, M. M. N., Adzhri, R., Hashim, U., & Lam, H. Y. (2017). Substrate-gate coupling in ZnO-FET biosensor for cardiac troponin I detection. *Sensors and Actuators, B: Chemical*, *242*, 1142–1154. https://doi.org/10.1016/j.snb.2016.09.131

Ferain, I., Colinge, C. A., & Colinge, J. P. (2011). Multigate transistors as the future of classical metal-oxide-semiconductor field-effect transistors. In *Nature* (Vol. 479, Issue 7373, pp. 310–316). https://doi.org/10.1038/nature10676

Frew, J. E., Allen, H., & Hill, O. (n.d.). *Electrochemical Biosensors*. https://pubs.acs.org/sharingguidelines

Fu, W., Jiang, L., van Geest, E. P., Lima, L. M. C., & Schneider, G. F. (2017). Sensing at the Surface of Graphene Field-Effect Transistors. In *Advanced Materials* (Vol. 29, Issue 6). Wiley-VCH Verlag. https://doi.org/10.1002/adma.201603610

Gao, N., Gao, T., Yang, X., Dai, X., Zhou, W., Zhang, A., & Lieber, C. M. (2016). Specific detection of biomolecules in physiological solutions using graphene transistor biosensors. *Proceedings of the National Academy of Sciences of the United States of America*, *113*(51), 14633–14638. https://doi.org/10.1073/pnas.1625010114

Gao, W. (n.d.). *Graphite Oxide: Structure, Reduction and Applications*.

Ghany, N. A. A., Elsherif, S. A., & Handal, H. T. (2017). Revolution of Graphene for different applications: State-of-the-art. In *Surfaces and Interfaces* (Vol. 9, pp. 93–106). Elsevier B.V. https://doi.org/10.1016/j.surfin.2017.08.004

Gouadec, G., & Colomban, P. (2007). Raman Spectroscopy of nanomaterials: How spectra relate to disorder, particle size and mechanical properties. In *Progress in Crystal Growth and Characterization of Materials* (Vol. 53, Issue 1, pp. 1–56). https://doi.org/10.1016/j.pcrysgrow.2007.01.001

Grieshaber, D., Mackenzie, R., Vörös, J., & Reimhult, E. (2008). Electrochemical Biosensors-Sensor Principles and Architectures. *Sensors*, *8*, 1400–1458. www.mdpi.org/sensors

Griffiths-Jones, S. (n.d.). miRBase 10 miRBase The MicroRNA Sequence Database. In *From: Methods in Molecular Biology* (Vol. 342). http://microrna.

Griffiths-Jones, S. (2010). MiRBase: MicroRNA sequences and annotation. *Current Protocols in Bioinformatics*, *SUPPL. 29*, 1291–12910. https://doi.org/10.1002/0471250953.bi1209s29

Guan, J.-G., Miao, Y.-Q., & Zhang, Q.-J. (2004). Impedimetric Biosensors. In *JOURNAL OF BIOSCIENCE AND BIOENGINEERING* (Vol. 97, Issue 4).

Gupta, V. K., Yola, M. L., Qureshi, M. S., Solak, A. O., Atar, N., & Üstündağ, Z. (2013). A novel impedimetric biosensor based on graphene oxide/gold nanoplatform for detection of DNA arrays. *Sensors and Actuators, B: Chemical*, *188*, 1201–1211. https://doi.org/10.1016/j.snb.2013.08.034

Gürer, U., Yilmaz, O., Budak, E., & Yilmaz, E. (2022). THE COATING OF REDUCED GRAPHENE OXIDE (rGO): A NOVEL ULTRASONIC-ASSISTED METHOD. *RAP Conference Proceedings*. https://doi.org/10.37392/RapProc.2022.12

Hacıkamiloğlu, E., Gültekin, M., Boztaş, G., Dündar, S., Utku, E. Ş., Kavak Ergün, A., Sevinç, A., Tütüncü, S., Seymen, E., & Türkiye Halk Sağlığı Kurumu. (2017). Türkiye Kanser İstatistikleri. *Türkiye Halk Sağlığı Kurumu*, www.kanser.gov.tr/daire-faaliyetleri/kanser-istati.

Haleem, A., Javaid, M., Singh, R. P., Suman, R., & Rab, S. (2021). Biosensors applications in medical field: A brief review. *Sensors International*, *2*(May), 100100. https://doi.org/10.1016/j.sintl.2021.100100

Ha, M., & Kim, V. N. (2014). Regulation of microRNA biogenesis. In *Nature Reviews Molecular Cell Biology* (Vol. 15, Issue 8, pp. 509–524). Nature Publishing Group. https://doi.org/10.1038/nrm3838

Hashemi, Z. S., Khalili, S., Forouzandeh Moghadam, M., & Sadroddiny, E. (2017). Lung cancer and miRNAs: a possible remedy for anti-metastatic, therapeutic and diagnostic applications. In *Expert Review of Respiratory Medicine* (Vol. 11, Issue 2, pp. 147–157). Taylor and Francis Ltd. https://doi.org/10.1080/17476348.2017.1279403

Haun, J. B., Yoon, T. J., Lee, H., & Weissleder, R. (2010). Magnetic nanoparticle biosensors. In *Wiley Interdisciplinary Reviews: Nanomedicine and Nanobiotechnology* (Vol. 2, Issue 3, pp. 291–304). https://doi.org/10.1002/wnan.84

Hayat, A., Catanante, G., & Marty, J. L. (2014). Current trends in nanomaterial-based amperometric biosensors. In *Sensors (Switzerland)* (Vol. 14, Issue 12, pp. 23439–23461). MDPI AG. https://doi.org/10.3390/s141223439

Hayes, R. (n.d.). Field-Effect (FET) transistors. *Spring*, 61–74.

He, Q., Wu, S., Yin, Z., & Zhang, H. (2012). Graphene-based electronic sensors. *Chemical Science*, *3*(6), 1764–1772. https://doi.org/10.1039/c2sc20205k

Ho, J. A. A., Chang, H. C., Shih, N. Y., Wu, L. C., Chang, Y. F., Chen, C. C., & Chou, C. (2010). Diagnostic detection of human lung cancer-associated antigen using a gold nanoparticle-based electrochemical immunosensor. *Analytical Chemistry*, *82*(14), 5944–5950. https://doi.org/10.1021/ac1001959

Husnah, M., Fakhri, H. A., Rohman, F., Aimon, A. H., & Iskandar, F. (2017). A modified Marcano method for improving electrical properties of reduced graphene oxide (rGO). *Materials Research Express*, *4*(6). https://doi.org/10.1088/2053-1591/aa707f

Hwang, M. T., Heiranian, M., Kim, Y., You, S., Leem, J., Taqieddin, A., Faramarzi, V., Jing, Y., Park, I., van der Zande, A. M., Nam, S., Aluru, N. R., & Bashir, R. (2020). Ultrasensitive detection of

nucleic acids using deformed graphene channel field effect biosensors. *Nature Communications*, *11*(1). https://doi.org/10.1038/s41467-020-15330-9

Hwang, M. T., Preston, B. L., Joon, L., Duyoung, C., Alexander, H. M., Gennadi, G., & Ratnesh, L. (2016). Highly specific SNP detection using 2D graphene electronics and DNA strand displacement. *Proceedings of the National Academy of Sciences of the United States of America*, *113*(26), 7088–7093. https://doi.org/10.1073/pnas.1603753113

Introduction, A. (1997). *An Introduction to Transistors*. 1–5.

Islam, M. A. (2020). *Gate-All-Around Nanowire MOSFET for DNA Sequencing*.

Ivnitski, D., Abdel-Hamid, I., Atanasov, P., & Wilkins, E. (1999). Biosensors for detection of pathogenic bacteria. In *Biosensors & Bioelectronics* (Vol. 14). www.elsevier.com

Jacobs, C. B., Peairs, M. J., & Venton, B. J. (2010). Review: Carbon nanotube based electrochemical sensors for biomolecules. In *Analytica Chimica Acta* (Vol. 662, Issue 2, pp. 105–127). https://doi.org/10.1016/j.aca.2010.01.009

Jahanshahi, M., Jabari, R., Rashidi, A. M., & Ghoreyshi, A. A. (n.d.). *Synthesis and Characterization of Thermally-Reduced Graphene*. https://doi.org/10.5829/idosi.ijee.2013.04.01.09

Jahromi, A. K., Shieh, H., Low, K., Tasnim, N., Najjaran, H., & Hoorfar, M. (2022). Experimental comparison of direct and indirect aptamer-based biochemical functionalization of electrolyte-gated graphene field-effect transistors for biosensing applications. *Analytica Chimica Acta*, *1222*. https://doi.org/10.1016/j.aca.2022.340177

Jansson, M. D., & Lund, A. H. (2012). MicroRNA and cancer. In *Molecular Oncology* (Vol. 6, Issue 6, pp. 590–610). John Wiley and Sons Ltd. https://doi.org/10.1016/j.molonc.2012.09.006

Jayachandiran, J., Yesuraj, J., Arivanandhan, M., Raja, A., Suthanthiraraj, S. A., Jayavel, R., & Nedumaran, D. (2018). Synthesis and Electrochemical Studies of rGO/ZnO Nanocomposite for Supercapacitor Application. *Journal of Inorganic and Organometallic Polymers and Materials*, *28*(5), 2046–2055. https://doi.org/10.1007/s10904-018-0873-0

Jayanthi, V. S. P. K. S. A., Das, A. B., & Saxena, U. (2017). Recent advances in biosensor development for the detection of cancer biomarkers. In *Biosensors and Bioelectronics* (Vol. 91, pp. 15–23). Elsevier Ltd. https://doi.org/10.1016/j.bios.2016.12.014

Jiang, K., Fei, T., Jiang, F., Wang, G., & Zhang, T. (2014). A dew sensor based on modified carbon black and polyvinyl alcohol composites. *Sensors and Actuators, B: Chemical*, *192*, 658–663. https://doi.org/10.1016/j.snb.2013.11.004

Jin, X., Zhang, H., Li, Y. T., Xiao, M. M., Zhang, Z. L., Pang, D. W., Wong, G., Zhang, Z. Y., & Zhang, G. J. (2019). A field effect transistor modified with reduced graphene oxide for immunodetection of Ebola virus. *Microchimica Acta*, *186*(4). https://doi.org/10.1007/s00604-019-3256-5

Joshi, G. K., Deitz-Mcelyea, S., Johnson, M., Mali, S., Korc, M., & Sardar, R. (2014). Highly specific plasmonic biosensors for ultrasensitive MicroRNA detection in plasma from pancreatic cancer patients. *Nano Letters*, *14*(12), 6955–6963. https://doi.org/10.1021/nl503220s

Kant Upadhyay, R., Soin, N., Bhattacharya, G., Saha, S., Barman, A., & Sinha Roy, S. (n.d.). *Grape extract assisted green synthesis of reduced graphene oxide for water treatment application*.

Karimi-Maleh, H., Orooji, Y., Karimi, F., Alizadeh, M., Baghayeri, M., Rouhi, J., Tajik, S., Beitollahi, H., Agarwal, S., Gupta, V. K., Rajendran, S., Ayati, A., Fu, L., Sanati, A. L., Tanhaei, B., Sen, F., shabani-nooshabadi, M., Asrami, P. N., & Al-Othman, A. (2021). A critical review on the use of potentiometric based biosensors for biomarkers detection. In *Biosensors and Bioelectronics* (Vol. 184). Elsevier Ltd. https://doi.org/10.1016/j.bios.2021.113252

Karunakaran, C., Rajkumar, R., & Bhargava, K. (2015). Introduction to Biosensors. In *Biosensors and Bioelectronics* (pp. 1–68). Elsevier Inc. https://doi.org/10.1016/B978-0-12-803100-1.00001-3

Khanmohammadi, A., Aghaie, A., Vahedi, E., Qazvini, A., Ghanei, M., Afkhami, A., Hajian, A., & Bagheri, H. (2020). Electrochemical biosensors for the detection of lung cancer biomarkers: A review. *Talanta*, *206*(July 2019), 120251. https://doi.org/10.1016/j.talanta.2019.120251

Khatayevich, D., Page, T., Gresswell, C., Hayamizu, Y., Grady, W., & Sarikaya, M. (2014). Selective detection of target proteins by peptide-enabled graphene biosensor. *Small*, *10*(8), 1505–1513. https://doi.org/10.1002/smll.201302188

Khatri, R., & Puri, N. K. (2022). Electrochemical biosensor utilizing dual-mode output for detection of lung cancer biomarker based on reduced graphene oxide-modified reduced-molybdenum disulfide multi-layered nanosheets. *Journal of Materials Research*, *37*(8), 1451–1463. https://doi.org/10.1557/s43578-022-00546-w

Kim, A., Ah, C. S., Park, C. W., Yang, J. H., Kim, T., Ahn, C. G., Park, S. H., & Sung, G. Y. (2010). Direct label-free electrical immunodetection in human serum using a flow-through-apparatus approach with integrated field-effect transistors. *Biosensors and Bioelectronics*, *25*(7), 1767–1773. https://doi.org/10.1016/j.bios.2009.12.026

Kim, H. E., Schuck, A., Lee, J. H., & Kim, Y. S. (2019). Solution-gated graphene field effect transistor for TP53 DNA sensor with coplanar electrode array. *Sensors and Actuators, B: Chemical*, *291*, 96–101. https://doi.org/10.1016/j.snb.2019.03.080

Kim, H., Park, S., Jeong, I. G., Song, S. H., Jeong, Y., Kim, C. S., & Lee, K. H. (2021). Noninvasive Precision Screening of Prostate Cancer by Urinary Multimarker Sensor and Artificial Intelligence Analysis. *ACS Nano*, *15*(3), 4054–4065. https://doi.org/10.1021/acsnano.0c06946

Kim, J. W., Jang, Y. ha, Ku, G. M., Kim, S., Lee, E., Cho, K., Lim, K. il, & Lee, W. H. (2018). Liquid coplanar-gate organic/graphene hybrid electronics for label-free detection of single and double-stranded DNA molecules. *Organic Electronics*, *62*, 163–167. https://doi.org/10.1016/j.orgel.2018.07.032

Kim, J. Y., Ahn, J. H., Choi, S. J., Im, M., Kim, S., Duarte, J. P., Kim, C. H., Park, T. J., Lee, S. Y., & Choi, Y. K. (2012). An underlap channel-embedded field-effect transistor for biosensor application in watery and dry environment. *IEEE Transactions on Nanotechnology*, *11*(2), 390–394. https://doi.org/10.1109/TNANO.2011.2175006

Kim, J. Y., Choi, M. J., & Jang, H. W. (2021). Ferroelectric field effect transistors: Progress and perspective. *APL Materials*, *9*(2). https://doi.org/10.1063/5.0035515

Kim, S., Kwon, D. W., Kim, S., Lee, R., Kim, T. H., Mo, H. S., Kim, D. H., & Park, B. G. (2018). Analysis of current drift on p-channel pH-Sensitive SiNW ISFET by capacitance measurement. *Current Applied Physics*, *18*, S68–S74. https://doi.org/10.1016/j.cap.2017.11.021

Kirchhain, A., Bonini, A., Vivaldi, F., Poma, N., & Di Francesco, F. (2020). Latest developments in non-faradic impedimetric biosensors: Towards clinical applications. In *TrAC - Trends in Analytical Chemistry* (Vol. 133). Elsevier B.V. https://doi.org/10.1016/j.trac.2020.116073

Kireev, D., Brambach, M., Seyock, S., Maybeck, V., Fu, W., Wolfrum, B., & Offenhaüsser, A. (2017). Graphene transistors for interfacing with cells: Towards a deeper understanding of liquid gating and sensitivity. *Scientific Reports*, *7*(1), 1–12. https://doi.org/10.1038/s41598-017-06906-5

Kour, R., Arya, S., Young, S.-J., Gupta, V., Bandhoria, P., & Khosla, A. (2020). Review—Recent Advances in Carbon Nanomaterials as Electrochemical Biosensors. *Journal of The Electrochemical Society*, *167*(3), 037555. https://doi.org/10.1149/1945-7111/ab6bc4

Kovalska, E., Lesongeur, P., Hogan, B. T., & Baldycheva, A. (2019). Multi-layer graphene as a selective detector for future lung cancer biosensing platforms. *Nanoscale*, *11*(5), 2476–2483. https://doi.org/10.1039/c8nr08405j

Krishnamoorthy, K., Veerapandian, M., Yun, K., & Kim, S. J. (2013). The chemical and structural analysis of graphene oxide with different degrees of oxidation. *Carbon*, *53*, 38–49. https://doi.org/10.1016/j.carbon.2012.10.013

Kulkarni, M. B., Ayachit, N. H., & Aminabhavi, T. M. (2022). Biosensors and Microfluidic Biosensors: From Fabrication to Application. In *Biosensors* (Vol. 12, Issue 7). MDPI. https://doi.org/10.3390/bios12070543

Kumar, P., Kumar Singh, A., Hussain, S., Nam Hui, K., San Hui, K., Eom, J., Jung, J., & Singh, J. (2013). Graphene: Synthesis, Properties and Application in Transparent Electronic Devices. *Reviews in Advanced Sciences and Engineering*, *2*(4), 238–258. https://doi.org/10.1166/rase.2013.1043

Kurosawa, S., Park, J. W., Aizawa, H., Wakida, S. I., Tao, H., & Ishihara, K. (2006). Quartz crystal microbalance immunosensors for environmental monitoring. *Biosensors and Bioelectronics*, *22*(4 SPEC. ISS.), 473–481. https://doi.org/10.1016/j.bios.2006.06.030

Kwong, D., & Tsang, H. (n.d.). *Chemically Functionalised Graphene Biosensor for the Label-free Sensing of Exosomes Declaration Statement of Originality*.

Kwong Hong Tsang, D., Lieberthal, T. J., Watts, C., Dunlop, I. E., Ramadan, S., del Rio Hernandez, A. E., & Klein, N. (2019). Chemically Functionalised Graphene FET Biosensor for the Label-free Sensing of Exosomes. *Scientific Reports*, *9*(1). https://doi.org/10.1038/s41598-019-50412-9

Kybert, N. J., Han, G. H., Lerner, M. B., Dattoli, E. N., Esfandiar, A., & Charlie Johnson, A. T. (2014). Scalable arrays of chemical vapor sensors based on DNA-decorated graphene. *Nano Research*, *7*(1), 95–103. https://doi.org/10.1007/s12274-013-0376-9

Lagarde, F., & Jaffrezic-Renault, N. (2011). New Trends in Biosensors for Water Monitoring. *Environmental Biosensors*. https://doi.org/10.5772/19945

Lakard, B. (2020). Electrochemical biosensors based on conducting polymers: A review. In *Applied Sciences (Switzerland)* (Vol. 10, Issue 18). MDPI AG. https://doi.org/10.3390/APP10186614

Lamberti, P., la Mura, M., Pasadas, F., Jiménez, D., & Tucci, V. (2021). Tolerance analysis of a GFET transistor for aerospace and aeronautical application. *IOP Conference Series: Materials Science and Engineering*, *1024*(1). https://doi.org/10.1088/1757-899X/1024/1/012005

Leech, D. (1994). Affinity biosensors. *Chemical Society Reviews*, *23*(3), 205–213. https://doi.org/10.1039/CS9942300205

Lerner, M. B., Pan, D., Gao, Y., Locascio, L. E., Lee, K. Y., Nokes, J., Afsahi, S., Lerner, J. D., Walker, A., Collins, P. G., Oegema, K., Barron, F., & Goldsmith, B. R. (2017). Large scale commercial fabrication of high quality graphene-based assays for biomolecule detection. *Sensors and Actuators, B: Chemical*, *239*, 1261–1267. https://doi.org/10.1016/j.snb.2016.09.137

Lesiak, B., Trykowski, G., Tóth, J., Biniak, S., Kövér, L., Rangam, N., Stobinski, L., & Malolepszy, A. (2021). Chemical and structural properties of reduced graphene oxide—dependence on the reducing agent. *Journal of Materials Science*, *56*(5), 3738–3754. https://doi.org/10.1007/s10853-020-05461-1

Leung, A., Shankar, P. M., & Mutharasan, R. (2007). A review of fiber-optic biosensors. In *Sensors and Actuators, B: Chemical* (Vol. 125, Issue 2, pp. 688–703). https://doi.org/10.1016/j.snb.2007.03.010

Leyden, M. R., Schuman, C., Sharf, T., Kevek, J., Remcho, V. T., & Minot, E. D. (2010). Fabrication and characterization of carbon nanotube field-effect transistor biosensors. *Organic Semiconductors in Sensors and Bioelectronics III*, *7779*, 77790H. https://doi.org/10.1117/12.861329

Liang, Y., Liang, X., Zhang, Z., Li, W., Huo, X., & Peng, L. (2015). High mobility flexible graphene field-effect transistors and ambipolar radio-frequency circuits. *Nanoscale*, *7*(25), 10954–10962. https://doi.org/10.1039/c5nr02292d

Ligler, F. S. (2009). Perspective on optical biosensors and integrated sensor systems. *Analytical Chemistry*, *81*(2), 519–526. https://doi.org/10.1021/ac8016289

Li, M., Yang, X., Ren, J., Qu, K., & Qu, X. (2012). Using graphene oxide high near-infrared absorbance for photothermal treatment of Alzheimer's disease. *Advanced Materials*, *24*(13), 1722–1728. https://doi.org/10.1002/adma.201104864

Lin, J., & Ju, H. (2005). Electrochemical and chemiluminescent immunosensors for tumor markers. *Biosensors and Bioelectronics*, *20*(8 SPEC. ISS.), 1461–1470. https://doi.org/10.1016/j.bios.2004.05.008

Li, P., Zhang, B., & Cui, T. (2015). Towards intrinsic graphene biosensor: A label-free, suspended single crystalline graphene sensor for multiplex lung cancer tumor markers detection. *Biosensors and Bioelectronics*, *72*, 168–174. https://doi.org/10.1016/j.bios.2015.05.007

Liu, J., Chen, C., & Zhao, Y. (2019). Progress and Prospects of Graphdiyne-Based Materials in Biomedical Applications. *Advanced Materials*, *31*(42), 1–9. https://doi.org/10.1002/adma.201804386

Lu, J., Tan, T., Zhu, L., Dong, H., & Xian, R. (2020). Hypomethylation Causes MIR21 Overexpression in Tumors. *Molecular Therapy - Oncolytics*, *18*, 47–57. https://doi.org/10.1016/j.omto.2020.05.011

Lundstrom, M. (2008). A Review of MOSFET Fundamentals. *Nanotechnology*, 1–52.

Lundstrom, M., & Ren, Z. (2002). Essential Physics of Carrier Transport in Nanoscale MOSFETs. In *IEEE TRANSACTIONS ON ELECTRON DEVICES* (Vol. 49, Issue 1).

Lu, T. X., & Rothenberg, M. E. (2018). MicroRNA. *Journal of Allergy and Clinical Immunology*, *141*(4), 1202–1207. https://doi.org/10.1016/j.jaci.2017.08.034

Mack, R. D., Michail, S., Wei, S., Mcdougall, L., Hollingsworth, M. A., Delneste, Y., Donnet-Hughes, A., Schiffrin, E. J., Knorr, D., Heldman, D. R., Lund, D. B., Tamine, A. Y., Marshall, V. M. E., Law, B. A., Dellaglio, F., Torriani, S., Vlaeminck, G., Cornet, R., Hunger, W., … Bourgeois, C. M. ; P. (1999). Refined Carbohydrate Foods and Disease. In *Antonie van Leeuwenhoek Int. J. Gen. Mol. Microbiol* (Vol. 39). Academic Press 47 Schweizer.

MaClellan, S. A., Macaulay, C., Lam, S., & Garnis, C. (2014). Pre-profiling factors influencing serum microRNA levels. *BMC Clinical Pathology*, *14*(1), 1–11. https://doi.org/10.1186/1472-6890-14-27

Mansouri Majd, S., & Salimi, A. (2018). Ultrasensitive flexible FET-type aptasensor for CA 125 cancer marker detection based on carboxylated multiwalled carbon nanotubes immobilized onto reduced graphene oxide film. In *Analytica Chimica Acta* (Vol. 1000). Elsevier B.V. https://doi.org/10.1016/j.aca.2017.11.008

Marrani, A. G., Coico, A. C., Giacco, D., Zanoni, R., Scaramuzzo, F. A., Schrebler, R., Dini, D., Bonomo, M., & Dalchiele, E. A. (2018). Integration of graphene onto silicon through electrochemical reduction of graphene oxide layers in non-aqueous medium. *Applied Surface Science*, *445*, 404–414. https://doi.org/10.1016/j.apsusc.2018.03.147

Marrinucci, D., Bethel, K., Bruce, R. H., Curry, D. N., Hsieh, B., Humphrey, M., Krivacic, R. T., Kroener, J., Kroener, L., Ladanyi, A., Lazarus, N. H., Nieva, J., & Kuhn, P. (2007). Case study of the morphologic variation of circulating tumor cells. *Human Pathology*, *38*(3), 514–519. https://doi.org/10.1016/j.humpath.2006.08.027

Martin, A., & Patra, P. (2014). Graphene Biosensor for Early Detection of Cancer Utilizing Antigen Concentrations in Saliva. *ASEE 2014 Zone 1 Conference*. http://www.asee.org/documents/zones/zone1/2014/Student/PDFs/59.pdf

Martins, E. de F., Pinotti, L. F., Silva, C. de C. C., & Rocha, A. R. (2021). Addressing the theoretical and experimental aspects of low-dimensional-materials-based fet immunosensors: A review. In *Chemosensors* (Vol. 9, Issue 7). MDPI AG. https://doi.org/10.3390/chemosensors9070162

Masud, M. K., Umer, M., Hossain, M. S. A., Yamauchi, Y., Nguyen, N. T., & Shiddiky, M. J. A. (2019). Nanoarchitecture Frameworks for Electrochemical miRNA Detection. In *Trends in Biochemical Sciences* (Vol. 44, Issue 5, pp. 433–452). Elsevier Ltd. https://doi.org/10.1016/j.tibs.2018.11.012

Matsumoto, K., Maehashi, K., Ohno, Y., & Inoue, K. (2014). Recent advances in functional graphene biosensors. *Journal of Physics D: Applied Physics*, *47*(9). https://doi.org/10.1088/0022-3727/47/9/094005

Mehrotra, P. (2016). Biosensors and their applications - A review. *Journal of Oral Biology and Craniofacial Research*, *6*(2), 153–159. https://doi.org/10.1016/j.jobcr.2015.12.002

Minna, J. D., Roth, J. A., & Gazdar, A. F. (2002). *Focus on lung cancer* (Vol. 1).

Mirzaii Babolghani, F., & Mohammadi-Manesh, E. (2019). Simulation and experimental study of FET biosensor to detect polycyclic aromatic hydrocarbons. *Applied Surface Science*, *488*(May), 662–670. https://doi.org/10.1016/j.apsusc.2019.05.202

Mohamed, A. A., Noguchi, H., Tsukiiwa, M., Chen, C., Heath, R. S., Mubarak, M. Q. E., Komikawa, T., Tanaka, M., Okochi, M., de Visser, S. P., Hayamizu, Y., & Blanford, C. F. (2022). A GFET Nitrile Sensor Using a Graphene-Binding Fusion Protein. *Advanced Functional Materials*, *32*(46). https://doi.org/10.1002/adfm.202207669

Mohan, P., Yang, J., Jena, A., & Suk Shin, H. (2015). VS2/rGO hybrid nanosheets prepared by annealing of VS4/rGO. *Journal of Solid State Chemistry*, *224*, 82–87. https://doi.org/10.1016/j.jssc.2014.06.031

Mohr, A. M., & Mott, J. L. (2015). Overview of microRNA biology. In *Seminars in Liver Disease* (Vol. 35, Issue 1, pp. 3–11). Thieme Medical Publishers, Inc. https://doi.org/10.1055/s-0034-1397344

Molassiotis, A., Uyterlinde, W., Hollen, P. J., Sarna, L., Palmer, P., & Krishnasamy, M. (2015). Supportive care in lung cancer: Milestones over the past 40 years. *Journal of Thoracic Oncology*, *10*(1), 10–18. https://doi.org/10.1097/JTO.0000000000000407

Moldovan, C., Iosub, R., Radu, C., Codreanu, N., Ion, M., Codreanu, C., Firtat, B., Necula, D., Ion, A., Ion, I., Harvey, T., & Summersgill, P. (2008). Enzymatic biosensor for insecticides detection. *Proceedings of the International Semiconductor Conference, CAS*, *1*, 147–150. https://doi.org/10.1109/SMICND.2008.4703353

Morales, M. A., & Halpern, J. M. (2018). Guide to Selecting a Biorecognition Element for Biosensors. *Bioconjugate Chemistry*, *29*(10), 3231–3239. https://doi.org/10.1021/acs.bioconjchem.8b00592

Moselund, K. E., Bouvet, D., Pott, V., Meinen, C., Kayal, M., & Ionescu, A. M. (2008). Punch-through impact ionization MOSFET (PIMOS): From device principle to applications. *Solid-State Electronics*, *52*(9), 1336–1344. https://doi.org/10.1016/j.sse.2008.04.021

Nabaei, V., Chandrawati, R., & Heidari, H. (2018). Magnetic biosensors: Modelling and simulation. In *Biosensors and Bioelectronics* (Vol. 103, pp. 69–86). Elsevier Ltd. https://doi.org/10.1016/j.bios.2017.12.023

Negahdary, M., & Angnes, L. (2022). Application of electrochemical biosensors for the detection of microRNAs (miRNAs) related to cancer. In *Coordination Chemistry Reviews* (Vol. 464). Elsevier B.V. https://doi.org/10.1016/j.ccr.2022.214565

Nishizawa, J.-I., Terasaki, T., & Shibata, J. (1975). Field-effect_transistor_versus_analog_transistor_static_induction_transistor. *IEEE Transaction on Electron Devices*, *ED-22*(4), 185–197.

Nooreldeen, R., & Bach, H. (2021). Current and future development in lung cancer diagnosis. In *International Journal of Molecular Sciences* (Vol. 22, Issue 16). MDPI AG. https://doi.org/10.3390/ijms22168661

Novodchuk, I., Bajcsy, M., & Yavuz, M. (2021). Graphene-based field effect transistor biosensors for breast cancer detection: A review on biosensing strategies. *Carbon*, *172*, 431–453. https://doi.org/10.1016/j.carbon.2020.10.048

Obreja, A. C., Cristea, D., Gavrila, R., Schiopu, V., Dinescu, A., Danila, M., & Comanescu, F. (2013). Isocyanate functionalized graphene/P3HT based nanocomposites. *Applied Surface Science*, *276*, 458–467. https://doi.org/10.1016/j.apsusc.2013.03.117

Oprea, D., Sanz, C. G., Barsan, M. M., & Enache, T. A. (2022). PC-12 Cell Line as a Neuronal Cell Model for Biosensing Applications. In *Biosensors* (Vol. 12, Issue 7). MDPI. https://doi.org/10.3390/bios12070500

Ordonez, R. C., Hayashi, C. K., Torres, C. M., Melcher, J. L., Kamin, N., Severa, G., & Garmire, D. (2017). Rapid Fabrication of Graphene Field-Effect Transistors with Liquid-metal Interconnects and Electrolytic Gate Dielectric Made of Honey. *Scientific Reports*, *7*(1), 1–9. https://doi.org/10.1038/s41598-017-10043-4

Özbek, O., Isildak, Ö., & Isildak, I. (2021a). A potentiometric biosensor for the determination of valproic acid: Human blood–based study of an anti–epileptic drug. *Biochemical Engineering Journal*, *176*. https://doi.org/10.1016/j.bej.2021.108181

Özbek, O., Isildak, Ö., & Isildak, I. (2021b). A potentiometric biosensor for the determination of valproic acid: Human blood–based study of an anti–epileptic drug. *Biochemical Engineering Journal*, *176*. https://doi.org/10.1016/j.bej.2021.108181

Pandey, C. M., & Malhotra, B. D. (2019). Biosensors: Fundamentals and applications. In *Biosensors: Fundamentals and Applications*. https://doi.org/10.1515/9783110641080

Parker, C. O., Lanyon, Y. H., Manning, M., Arrigan, D. W. M., & Tothill, I. E. (2009). Electrochemical immunochip sensor for aflatoxin M1 detection. *Analytical Chemistry*, *81*(13), 5291–5298. https://doi.org/10.1021/ac900511e

Park, J., Koo, K., Noh, N., Chang, J. H., Cheong, J. Y., Dae, K. S., Park, J. S., Ji, S., Kim, I. D., & Yuk, J. M. (2021). Graphene Liquid Cell Electron Microscopy: Progress, Applications, and Perspectives. *ACS Nano*, *15*(1), 288–308. https://doi.org/10.1021/acsnano.0c10229

Pei-Wen, Y., Che-Wei, H., Yu-Jie, H., Min-Cheng, C., Hsin-Hao, L., Shey-Shi, L., & Chih-Ting, L. (2014). A device design of an integrated CMOS poly-silicon biosensor-on-chip to enhance performance of biomolecular analytes in serum samples. *Biosensors and Bioelectronics*, *61*, 112–118. https://doi.org/10.1016/j.bios.2014.05.010

Phiri, J., Gane, P., & Maloney, T. C. (2017). General overview of graphene: Production, properties and application in polymer composites. In *Materials Science and Engineering B: Solid-State Materials for Advanced Technology* (Vol. 215, pp. 9–28). Elsevier Ltd. https://doi.org/10.1016/j.mseb.2016.10.004

Poghossian, A. S. (1997). Method of fabrication of ISFET-based biosensors on an Si-SiO 2-Si structure. In *Sensors and Actuators B* (Vol. 44).

Pohanka, M., & Skládal, P. (2008). Electrochemical biosensors - Principles and applications. In *Journal of Applied Biomedicine* (Vol. 6, Issue 2, pp. 57–64). University of South Bohemia in Ceske Budejovice Faculty of Health and Social Sciences. https://doi.org/10.32725/jab.2008.008

Prew, B. A. (1975). Physics of Semiconductor Devices. In *Physics Bulletin* (Vol. 26, Issue 9). https://doi.org/10.1088/0031-9112/26/9/031

Putzbach, W., & Ronkainen, N. J. (2013). Immobilization techniques in the fabrication of nanomaterial-based electrochemical biosensors: A review. In *Sensors (Switzerland)* (Vol. 13, Issue 4, pp. 4811–4840). MDPI AG. https://doi.org/10.3390/s130404811

Ramanathan, K., & Danielsson, B. (2001). Principles and applications of thermal biosensors. In *Biosensors & Bioelectronics* (Vol. 16). www.elsevier.com

Randviir, E. P., Brownson, D. A. C., & Banks, C. E. (2014). A decade of graphene research: Production, applications and outlook. In *Materials Today* (Vol. 17, Issue 9, pp. 426–432). Elsevier B.V. https://doi.org/10.1016/j.mattod.2014.06.001

Rocha-Santos, T. A. P. (2014). Sensors and biosensors based on magnetic nanoparticles. In *TrAC - Trends in Analytical Chemistry* (Vol. 62, pp. 28–36). Elsevier B.V. https://doi.org/10.1016/j.trac.2014.06.016

Rodrigues, T., Curti, F., Leroux, Y. R., Barras, A., Pagneux, Q., Happy, H., Kleber, C., Boukherroub, R., Hasler, R., Volpi, S., Careri, M., Corradini, R., Szunerits, S., & Knoll, W. (2023). Discovery of a Peptide Nucleic Acid (PNA) aptamer for cardiac troponin I: Substituting DNA with neutral PNA maintains picomolar affinity and improves performances for electronic sensing with graphene field-effect transistors (gFET). *Nano Today*, *50*, 101840. https://doi.org/10.1016/j.nantod.2023.101840

Rogers, K. R. (2000). Principles of affinity-based biosensors. *Applied Biochemistry and Biotechnology - Part B Molecular Biotechnology*, *14*(2), 109–129. https://doi.org/10.1385/mb:14:2:109

Russo, P., Hu, A., & Compagnini, G. (2013). Synthesis, properties and potential applications of porous graphene: A review. In *Nano-Micro Letters* (Vol. 5, Issue 4, pp. 260–273). Open Access House of Science and Technology. https://doi.org/10.5101/nml.v5i4.p260-273

Ryon, S., #1, S., Li, Y.-C., Jang, H., Khoshakhlagh, P., Akbari, M., Nasajpour, A., Zhang, Y. S., Tamayol, A., & Khademhosseini, A. (2016). Graphene-based materials for tissue engineering Graphical Abstract HHS Public Access. *Adv Drug Deliv Rev*, *105*, 255–274. https://doi.org/10.1016/j.addr.2016.03.007.Graphene-based

Sasipongpana, S., Rayanasukha, Y., Prichanont, S., Thanachayanont, C., Porntheeraphat, S., Houngkamhang, N., & Sasipongpana, S. (2017). Extended-gate field effect transistor (EGFET) for carbaryl pesticide detection based on enzyme inhibition assay. In *Materials Today: Proceedings* (Vol. 4). www.sciencedirect.comwww.materialstoday.com/proceedings

Schabath, M. B., & Cote, M. L. (2019). Cancer progress and priorities: Lung cancer. *Cancer Epidemiology Biomarkers and Prevention*, *28*(10), 1563–1579. https://doi.org/10.1158/1055-9965.EPI-19-0221

Schmekel, B., Winquist, F., & Vikström, A. (2014). Analysis of breath samples for lung cancer survival. *Analytica Chimica Acta*, *840*, 82–86. https://doi.org/10.1016/j.aca.2014.05.034

Schuck, A., Kim, H. E., Jung, K. M., Hasenkamp, W., & Kim, Y. S. (2020). Monitoring the hemostasis process through the electrical characteristics of a graphene-based field-effect transistor. *Biosensors and Bioelectronics*, *157*, 112167. https://doi.org/10.1016/j.bios.2020.112167

Seo, G., Lee, G., Kim, M. J., Baek, S. H., Choi, M., Ku, K. B., Lee, C. S., Jun, S., Park, D., Kim, H. G., Kim, S. J., Lee, J. O., Kim, B. T., Park, E. C., & Kim, S. Il. (2020). Rapid Detection of COVID-19 Causative Virus (SARS-CoV-2) in Human Nasopharyngeal Swab Specimens Using Field-Effect Transistor-Based Biosensor. *ACS Nano*, *14*(4), 5135–5142. https://doi.org/10.1021/acsnano.0c02823

Sezgintürk, M. K. (2020). Introduction to commercial biosensors. *Commercial Biosensors and Their Applications: Clinical, Food, and Beyond*, 1–28. https://doi.org/10.1016/B978-0-12-818592-6.00001-3

Shabaninejad, Z., Yousefi, F., Movahedpour, A., Ghasemi, Y., Dokanehiifard, S., Rezaei, S., Aryan, R., Savardashtaki, A., & Mirzaei, H. (2019). Electrochemical-based biosensors for microRNA detection: Nanotechnology comes into view. In *Analytical Biochemistry* (Vol. 581). Academic Press Inc. https://doi.org/10.1016/j.ab.2019.113349

Sheliakina, M., Arkhypova, V., Soldatkin, O., Saiapina, O., Akata, B., & Dzyadevych, S. (2014). Urease-based ISFET biosensor for arginine determination. *Talanta*, *121*, 18–23. https://doi.org/10.1016/j.talanta.2013.12.042

Shengtao, Z., Anyan, G., Huanfang, G., & Xiangqian, C. (2011). International Journal of Industrial Chemistry Characterization of Exfoliated Graphite Prepared with the Method of Secondary Intervening. *Int. J. Ind. Chem*, *2*(2), 123–130. www.ijichem.org

Shockleyt, W. (1948). Surface states and rectification at metal semiconductor contact. In *Phys. Rev* (Vol. 74, Issue 8).

Shul'gao, A. A., Soldatkin, A. P., El'skaya, A. V, Dzyadevich, S. V, Patskovsky, S. V, & Strikha, V. I. (1994). Thin-film conductometric biosensors for glucose and urea determination*. In *Biosensors & Bioelectronics* (Vol. 9).

Siegel, R. L., Miller, K. D., & Jemal, A. (2019). Cancer statistics, 2019. *CA: A Cancer Journal for Clinicians*, *69*(1), 7–34. https://doi.org/10.3322/caac.21551

Sieradzka, M., Ślusarczyk, C., Fryczkowski, R., & Janicki, J. (2020). Insight into the effect of graphite grain sizes on the morphology, structure and electrical properties of reduced graphene oxide. *Journal of Materials Research and Technology*, *9*(4), 7059–7067. https://doi.org/10.1016/j.jmrt.2020.05.026

Singh, A., Sharma, A., Ahmed, A., Sundramoorthy, A. K., Furukawa, H., Arya, S., & Khosla, A. (2021). Recent advances in electrochemical biosensors: Applications, challenges, and future scope. In *Biosensors* (Vol. 11, Issue 9). MDPI. https://doi.org/10.3390/bios11090336

Sivarajasekar, N., Dharshni, Ra., & Dharshini, Rd. (2019). THERMAL BIOSENSORS AND THEIR APPLICATIONS Reverse micelles View project Biosorption of cationic dyes View project THERMAL BIOSENSORS AND THEIR APPLICATIONS. *American International Journal of Research in Science*, 50. http://www.iasir.net

Soldano, C., Mahmood, A., & Dujardin, E. (2010). Production, properties and potential of graphene. In *Carbon* (Vol. 48, Issue 8, pp. 2127–2150). https://doi.org/10.1016/j.carbon.2010.01.058

Song, S., Wang, L., Li, J., Fan, C., & Zhao, J. (2008). Aptamer-based biosensors. *TrAC - Trends in Analytical Chemistry*, *27*(2), 108–117. https://doi.org/10.1016/j.trac.2007.12.004

Son, M., Kim, D., Kang, J., Lim, J. H., Lee, S. H., Ko, H. J., Hong, S., & Park, T. H. (2016). Bioelectronic nose using odorant binding protein-derived peptide and carbon nanotube field-effect transistor for the assessment of salmonella contamination in food. *Analytical Chemistry*, *88*(23), 11283–11287. https://doi.org/10.1021/acs.analchem.6b03284

Strehlitz, B., Nikolaus, N., & Stoltenburg, R. (2008). Protein detection with aptamer biosensors. In *Sensors* (Vol. 8, Issue 7, pp. 4296–4307). https://doi.org/10.3390/s8074296

Sung, H., Ferlay, J., Siegel, R. L., Laversanne, M., Soerjomataram, I., Jemal, A., & Bray, F. (2021). Global Cancer Statistics 2020: GLOBOCAN Estimates of Incidence and Mortality Worldwide for 36 Cancers in 185 Countries. *CA: A Cancer Journal for Clinicians*, *71*(3), 209–249. https://doi.org/10.3322/caac.21660

Surekha, G., Krishnaiah, K. V., Ravi, N., & Padma Suvarna, R. (2020). FTIR, Raman and XRD analysis of graphene oxide films prepared by modified Hummers method. *Journal of Physics: Conference Series*, *1495*(1). https://doi.org/10.1088/1742-6596/1495/1/012012

Susman, E. (2005). Metastatic Pancreatic Cancer. *Oncology Times*, *27*(8), 58–59. https://doi.org/10.1097/01.cot.0000289977.50307.4c

Syu, Y.-C., Hsu, W.-E., & Lin, C.-T. (2018). Review—Field-Effect Transistor Biosensing: Devices and Clinical Applications. *ECS Journal of Solid State Science and Technology*, *7*(7), Q3196–Q3207. https://doi.org/10.1149/2.0291807jss

Tanoue, L. T., Tanner, N. T., Gould, M. K., & Silvestri, G. A. (2015). Lung cancer screening. *American Journal of Respiratory and Critical Care Medicine*, *191*(1), 19–33. https://doi.org/10.1164/rccm.201410-1777CI

Thakur, S., & Karak, N. (2015). Alternative methods and nature-based reagents for the reduction of graphene oxide: A review. *Carbon*, *94*(June), 224–242. https://doi.org/10.1016/j.carbon.2015.06.030

Thévenot, D. R., Toth, K., Durst, R. A., & Wilson, G. S. (2001). Electrochemical biosensors: Recommended definitions and classification. In *Analytical Letters* (Vol. 34, Issue 5, pp. 635–659). https://doi.org/10.1081/AL-100103209

Torrisi, L., Salvato, G., Cutroneo, M., Librizzi, F., Torrisi, A., & Silipigni, L. (2022). Source-drain electrical conduction and radiation detection in graphene-based field effect transistor (GFET). *Journal of Instrumentation*, *17*(2). https://doi.org/10.1088/1748-0221/17/02/P02008

Trung, T. Q., Tien, N. T., Kim, D., Jang, M., Yoon, O. J., & Lee, N. E. (2014). A flexible reduced graphene oxide field-effect transistor for ultrasensitive strain sensing. *Advanced Functional Materials*, *24*(1), 117–124. https://doi.org/10.1002/adfm.201301845

Ţucureanu, V., Matei, A., & Avram, A. M. (2016). FTIR Spectroscopy for Carbon Family Study. In *Critical Reviews in Analytical Chemistry* (Vol. 46, Issue 6, pp. 502–520). Taylor and Francis Ltd. https://doi.org/10.1080/10408347.2016.1157013

Tu, J., Gan, Y., Liang, T., Hu, Q., Wang, Q., Ren, T., Sun, Q., Wan, H., & Wang, P. (2018). Graphene FET array biosensor based on ssDNA aptamer for ultrasensitive Hg2+ detection in environmental pollutants. *Frontiers in Chemistry*, *6*(AUG). https://doi.org/10.3389/fchem.2018.00333

Turner, A. P. F. (2013). Biosensors: Sense and sensibility. *Chemical Society Reviews*, *42*(8), 3184–3196. https://doi.org/10.1039/c3cs35528d

Valera, E., Ramón-Azcón, J., Rodríguez, Á., Castañer, L. M., Sánchez, F. J., & Marco, M. P. (2007). Impedimetric immunosensor for atrazine detection using interdigitated µ-electrodes (IDµE's). *Sensors and Actuators, B: Chemical*, *125*(2), 526–537. https://doi.org/10.1016/j.snb.2007.02.048

Vasilescu, A., & Marty, J. L. (2016). Electrochemical aptasensors for the assessment of food quality and safety. In *TrAC - Trends in Analytical Chemistry* (Vol. 79, pp. 60–70). Elsevier B.V. https://doi.org/10.1016/j.trac.2015.11.024

Vaziri, S. (2011). Fabrication and Characterization of Graphene Field Effect Transistors. *Thesis*, 1–42.

Vishnoi, A., & Rani, S. (2017). MiRNA biogenesis and regulation of diseases: An overview. In *Methods in Molecular Biology* (Vol. 1509, pp. 1–10). Humana Press Inc. https://doi.org/10.1007/978-1-4939-6524-3_1

Wadowska, K., Bil-Lula, I., Trembecki, Ł., & Śliwińska-Mossoń, M. (2020). Genetic markers in lung cancer diagnosis: A review. In *International Journal of Molecular Sciences* (Vol. 21, Issue 13, pp. 1–24). MDPI AG. https://doi.org/10.3390/ijms21134569

Wang, J. (2005). Carbon-nanotube based electrochemical biosensors: A review. *Electroanalysis*, *17*(1), 7–14. https://doi.org/10.1002/elan.200403113

Wang, J., Liang, R., & Qin, W. (2020). Molecularly imprinted polymer-based potentiometric sensors. In *TrAC - Trends in Analytical Chemistry* (Vol. 130). Elsevier B.V. https://doi.org/10.1016/j.trac.2020.115980

Wang, S., Qi, X., Hao, D., Moro, R., Ma, Y., & Ma, L. (2022). Review—Recent Advances in Graphene-Based Field-Effect-Transistor Biosensors: A Review on Biosensor Designing Strategy. *Journal of The Electrochemical Society*, *169*(2), 027509. https://doi.org/10.1149/1945-7111/ac4f24

Wang, S., Zhang, Y., An, W., Wei, Y., Liu, N., Chen, Y., & Shuang, S. (2015). Magnetic relaxation switch immunosensor for the rapid detection of the foodborne pathogen Salmonella enterica in milk samples. *Food Control*, *55*, 43–48. https://doi.org/10.1016/j.foodcont.2015.02.031

Wang, T., Zhou, Y., Lei, C., Luo, J., Xie, S., & Pu, H. (2017). Magnetic impedance biosensor: A review. In *Biosensors and Bioelectronics* (Vol. 90, pp. 418–435). Elsevier Ltd. https://doi.org/10.1016/j.bios.2016.10.031

Wang, Y., Gao, X., Wei, F., Zhang, X., Yu, J., Zhao, H., Sun, Q., Yan, F., Yan, C., Li, H., & Ren, X. (2014). Diagnostic and prognostic value of circulating miR-21 for cancer: A systematic review and meta-analysis. *Gene*, *533*(1), 389–397. https://doi.org/10.1016/j.gene.2013.09.038

Wei, Q., Li, R., Du, B., Wu, D., Han, Y., Cai, Y., Zhao, Y., Xin, X., Li, H., & Yang, M. (2011). Multifunctional mesoporous silica nanoparticles as sensitive labels for immunoassay of human chorionic gonadotropin. *Sensors and Actuators, B: Chemical*, *153*(1), 256–260. https://doi.org/10.1016/j.snb.2010.09.073

Wu, K. L., Tsai, Y. M., Lien, C. T., Kuo, P. L., & Hung, J. Y. (2019). The roles of microRNA in lung cancer. *International Journal of Molecular Sciences*, *20*(7), 1–25. https://doi.org/10.3390/ijms20071611

Wu, X., Mu, F., Wang, Y., & Zhao, H. (2018). Graphene and graphene-based nanomaterials for DNA detection: A review. *Molecules*, *23*(8). https://doi.org/10.3390/molecules23082050

Xia, K., Zhang, Y., Cao, S., Wu, Y., Guo, W., Yuan, W., & Zhang, S. (2015). MiR-411 regulated ITCH expression and promoted cell proliferation in human hepatocellular carcinoma cells. *Biomedicine and Pharmacotherapy*, *70*(C), 158–163. https://doi.org/10.1016/j.biopha.2015.01.001

Xianyu, Y., Wang, Q., & Chen, Y. (2018). Magnetic particles-enabled biosensors for point-of-care testing. In *TrAC - Trends in Analytical Chemistry* (Vol. 106, pp. 213–224). Elsevier B.V. https://doi.org/10.1016/j.trac.2018.07.010

Xie, B., Ramanathan, K., & Danielsson, B. (n.d.). *Mini / micro thermal biosensors and other related devices for biochemical / clinical analysis and monitoring*.

Xu, S., Jiang, S., Zhang, C., Yue, W., Zou, Y., Wang, G., Liu, H., Zhang, X., Li, M., Zhu, Z., & Wang, J. (2018). Ultrasensitive label-free detection of DNA hybridization by sapphire-based graphene field-effect transistor biosensor. *Applied Surface Science*, *427*, 1114–1119. https://doi.org/10.1016/j.apsusc.2017.09.113

Yang, G., Xiao, Z., Tang, C., Deng, Y., Huang, H., & He, Z. (2019). Recent advances in biosensor for detection of lung cancer biomarkers. *Biosensors and Bioelectronics*, *141*(May), 111416. https://doi.org/10.1016/j.bios.2019.111416

Yang, M., Javadi, A., Li, H., & Gong, S. (2010). Ultrasensitive immunosensor for the detection of cancer biomarker based on graphene sheet. *Biosensors and Bioelectronics*, *26*(2), 560–565. https://doi.org/10.1016/j.bios.2010.07.040

Yan, H., Xu, Y., Lu, Y., & Xing, W. (2017). *Reduced Graphene Oxide-Based Solid-Phase Extraction for the Enrichment and Detection of microRNA*. https://doi.org/10.1021/acs.analchem.7b03138

Ying, L., Du, L., Zou, R., Shi, L., Zhang, N., Jin, J., Xu, C., Zhang, F., Zhu, C., Wu, J., Chen, K., Huang, M., Wu, Y., Zhang, Y., Zheng, W., Pan, X., Chen, B., Lin, A., Tam, J. K. C., … Su, D. (2020). Development of a serum miRNA panel for detection of early stage non-small cell lung cancer. *Proceedings of the National Academy of Sciences of the United States of America*, *117*(40), 25036–25042. https://doi.org/10.1073/pnas.2006212117

Yin, T., & Qin, W. (2013). Applications of nanomaterials in potentiometric sensors. In *TrAC - Trends in Analytical Chemistry* (Vol. 51, pp. 79–86). Elsevier B.V. https://doi.org/10.1016/j.trac.2013.06.009

Yoon, J. Y., & Kim, B. (2012). Lab-on-a-chip pathogen sensors for food safety. *Sensors (Switzerland)*, *12*(8), 10713–10741. https://doi.org/10.3390/s120810713

Zahed, B., & Hosseini-Monfared, H. (2015). A comparative study of silver-graphene oxide nanocomposites as a recyclable catalyst for the aerobic oxidation of benzyl alcohol: Support effect. *Applied Surface Science*, *328*, 536–547. https://doi.org/10.1016/j.apsusc.2014.12.078

Zare, P., Aleemardani, M., Seifalian, A., Bagher, Z., & Seifalian, A. M. (2021). Graphene oxide: Opportunities and challenges in biomedicine. *Nanomaterials*, *11*(5), 1–18. https://doi.org/10.3390/nano11051083

Zeng, J., Duarte, P. A., Ma, Y., Savchenko, O., Shoute, L., Khaniani, Y., Babiuk, S., Zhuo, R., Abdelrasoul, G. N., Charlton, C., Kanji, J. N., Babiuk, L., Edward, C., & Chen, J. (2022). An impedimetric biosensor for COVID-19 serology test and modification of sensor performance via dielectrophoresis force. *Biosensors and Bioelectronics*, *213*. https://doi.org/10.1016/j.bios.2022.114476

Zeng, X., Zhang, X., & Zou, Q. (2016). Integrative approaches for predicting microRNA function and prioritizing disease-related microRNA using biological interaction networks. *Briefings in Bioinformatics*, *17*(2), 193–203. https://doi.org/10.1093/bib/bbv033

Zeng, Y., Bao, J., Zhao, Y., Huo, D., Chen, M., Qi, Y., Yang, M., Fa, H., & Hou, C. (2018). A sandwich-type electrochemical immunoassay for ultrasensitive detection of non-small cell lung cancer biomarker CYFRA21-1. *Bioelectrochemistry*, *120*, 183–189. https://doi.org/10.1016/j.bioelechem.2017.11.003

Zhan, B., Li, C., Yang, J., Jenkins, G., Huang, W., & Dong, X. (2014). Graphene field-effect transistor and its application for electronic sensing. *Small*, *10*(20), 4042–4065. https://doi.org/10.1002/smll.201400463

Zhang, Q., Li, X., Qian, C., Dou, L., Cui, F., & Chen, X. (2018). Label-free electrochemical immunoassay for neuron specific enolase based on 3D macroporous reduced graphene oxide/polyaniline film. *Analytical Biochemistry*, *540–541*(October 2017), 1–8. https://doi.org/10.1016/j.ab.2017.10.009

Zhang, S. (2020). Review of Modern Field Effect Transistor Technologies for Scaling. *Journal of Physics: Conference Series*, *1617*(1). https://doi.org/10.1088/1742-6596/1617/1/012054

Zhong, Y. L., Tian, Z., Simon, G. P., & Li, D. (2015). Scalable production of graphene via wet chemistry: Progress and challenges. In *Materials Today* (Vol. 18, Issue 2, pp. 73–78). Elsevier B.V. https://doi.org/10.1016/j.mattod.2014.08.019

Zhong, Y., Zhen, Z., & Zhu, H. (2017). Graphene: Fundamental research and potential applications. In *FlatChem* (Vol. 4, pp. 20–32). Elsevier B.V. https://doi.org/10.1016/j.flatc.2017.06.008

Zhylyak, G. A., Dzyadevich, S. V, Korpan, Y. I., Soldatkin, A. P., & El'skaya, A. V. (1995). B Application of urease conductometric biosensor for heavy-metal ion determination. In *Sensors and Actuators B* (Vol. 24).

Zolper, J. C. (n.d.). *A REVIEW OF JUNCTION FIELD EFFECT TRANSISTORS FOR HIGH-TEMPERATURE AND HIGH-POWER ELECTRONICS*.

Zunic, B., & Peter, S. (2018). *World ' s largest Science , Technology & Medicine Open Access book publisher*. *2016*, 267–322.